TECHNISCHE UNIVERSITÄT MÜNCHEN

Institut für Humangenetik

Klinikum rechts der Isar

Helmholtz Zentrum München

(Direktor: Univ.-Prof. Dr. Th. A. Meitinger)

Analysis of two Candidate Genes for Neurodegeneration with Brain Iron Accumulation (NBIA)

Stephan Matthias Cuno

Vollständiger Abdruck der von der Fakultät für Medizin der Technischen Universität München zur Erlangung des akademischen Grades eines

Doktors der Medizin

genehmigten Dissertation.

Vorsitzender:		Univ.-Prof. Dr. E. J. Rummeny
Prüfer der Dissertation:	1.	Univ.-Prof. Dr. Th. A. Meitinger
	2.	Univ.-Prof. Dr. J. Schlegel

Die Dissertation wurde am 31.08.2015 bei der Technischen Universität München eingereicht und durch die Fakultät für Medizin am 15.06.2016 angenommen.

Parts of this thesis have been published:

Haack, T.B., Hogarth, P., Kruer, M.C., Gregory, A., Wieland, T., Schwarzmayr, T., Graf, E., Sanford, L., Meyer, E., Kara, E., Cuno, S.M., Harik, S.I., Dandu, V.H., Nardocci, N., Zorzi, G., Dunaway, T., Tarnopolsky, M., Skinner, S., Frucht, S., Hanspal, E., Schrander-Stumpel, C., Héron, D., Mignot, C., Garavaglia, B., Bhatia, K., Hardy, J., Strom, T.M., Boddaert, N., Houlden, H.H., Kurian, M.A., Meitinger, T., Prokisch, H., Hayflick, S.J. (2012): Exome Sequencing Reveals De Novo WDR45 Mutations Causing a Phenotypically Distinct, X-Linked Dominant Form of NBIA. In Am. J. Hum. Genet. 91 (6), pp. 1144-1149.

Hayflick, S.J., Kruer, M.C., Gregory, A., Haack, T.B., Kurian, M.A., Houlden, H.H., Anderson, J., Boddaert, N., Sanford, L., Harik, S.I., Dandu, V.H., Nardocci, N., Zorzi, G., Dunaway, T., Tarnopolsky, M., Skinner, S., Holden, K.R., Frucht, S., Hanspal, E., Schrander-Stumpel, C., Mignot, C., Héron, D., Saunders, D.E., Kaminska, M., Lin, J.-P., Lascelles, K., Cuno, S.M., Meyer, E., Garavaglia, B., Bhatia, K., Silva, R. de, Crisp, S., Lunt, P., Carey, M., Hardy, J., Meitinger, T., Prokisch, H., Hogarth, P. (2013): β-Propeller protein-associated neurodegeneration: a new X-linked dominant disorder with brain iron accumulation. In Brain 136 (Pt 6), pp. 1708-1717.

Table of Contents

List of Abbreviations

°C	degree Celsius
µg	microgram
µl	microliter
AD	autosomal dominant
AE	acrodermatitis enteropathica
AR	autosomal recessive
bp	base pair
BPAN	beta-propeller protein-associated neurodegeneration
CAG	cytosine adenine guanine
cAMP	cyclic adenosine monophosphate
CJD	Creutzfeldt-Jakob disease
CoA	coenzyme A
COASY	coenzyme A synthase
CoPAN	COASY protein-associated neurodegeneration
COR	C-terminal of Ras
dATP	deoxyadenosine triphosphate
dbIHG	exome database in the Institute of Human Genetics, Neuherberg, Germany
dbSNP	online database for single nucleotide polymorphisms
dCTP	deoxycytidine triphosphate
ddNTP	dideoxynucleoside triphosphate
dGTP	deoxyguanosine triphosphate
DNA	deoxyribonucleic acid
dNTP	deoxynucleoside triphosphate
dTTP	deoxythymidine triphosphate
EDS	Ehlers-Danlos syndrome
EDTA	ethylenediaminetetraacetic acid
ER	endoplasmic reticulum
et al.	et alii/et aliae
ExAC	Exome Aggregation Consortium
FA2H	fatty acid 2-hydroxylase
FAHN	fatty acid 2-hydroxylase-associated neurodegeneration
FLAIR	fluid-attenuated inversion-recovery

FTL	ferritin light chain
g	gram
GER	Germany
GH	growth hormone
GHRHR	growth hormone releasing hormone receptor
GPCR	G-protein coupled receptor
GTPase	guanosine triphosphate phosphohydrolase
hetero	heterozygous
homo	homozygous
HpaII	haemophilus parainfluenzae II
HPLC	high performance liquid chromatography
IGF-1	insulin-like growth factor 1
IRT	iron regulated transporter
kbp	kilobase pair
KO	knockout
KRS	Kufor-Rakeb syndrome
LRRK2	leucine-rich repeat kinase 2
MAF	minor allele frequency
MAPKKK	mitogen-activated protein kinase kinase kinase
MECP2	methyl-CpG-binding protein 2
mg	milligram
min	minute
ml	milliliter
MPAN	mitochondrial membrane protein-associated neurodegeneration
MR	magnetic resonance
MRI	magnetic resonance imaging
mut	mutation
n.a.	not available
NBIA	neurodegeneration with brain iron accumulation
NBMA	neurodegeneration with brain manganese accumulation
NCBI	National Center for Biotechnology Information
Neg	negative control
ng	nanogram
PANK2	pantothenate kinase 2

PARK	Parkinson's disease
PCR	polymerase chain reaction
PD	Parkinson's disease
PKAN	pantothenate kinase-associated neurodegeneration
PLAN	phospholipase A2-associated neurodegeneration
pmol	picomol
PrP^{C}	cellular prion protein
PrP^{Sc}	scrapie prion protein
Ras	rat sarcoma
RefSeq	reference sequence
RNA	ribonucleic acid
Roc	ras of complex
rpm	revolutions per minute
s	second
SCD-EDS	spondylocheiro dysplastic form of the Ehlers-Danlos syndrome
SENDA	static encephalopathy of childhood with neurodegeneration in adulthood
SLC39	solute carrier 39
SNP	single nucleotide polymorphism
Taq	thermus aquaticus
TBE	tris(hydroxymethyl)aminomethane, boric acid, EDTA
TE	tris(hydroxymethyl)aminomethane, EDTA
TIRCON	Treat Iron-Related Childhood-Onset Neurodegeneration
TSE	turbo-spin-echo
U	unit
UCSC	University of California Santa Cruz
UK	United Kingdom
USA	United States of America
WDR45	WD40 repeat 45 (W – tryptophan, D – aspartic acid)
WIPI	WD40 repeat interacting with phosphoinositides
WSS	Woodhouse-Sakati syndrome
WT	wild type
XD	X-linked dominant
ZIP	ZRT, IRT-like protein
ZRT	zinc regulated transporter

1 Introduction

1.1 NBIA

Neurodegeneration with brain iron accumulation or NBIA is a group of diseases that share a progressive neurodegenerative disease process and an accumulation of iron in the brain which usually involves the basal ganglia (Gregory and Hayflick 2005). NBIA has an estimated prevalence of 1-3:1,000,000 (Kalman et al. 2012). NBIA was historically named Hallervorden-Spatz syndrome. Hallervorden (1882-1965) and Spatz (1888-1969) were two German neuropathologists who first described the disease in 1922 (Hallervorden and Spatz 1922; Zhou et al. 2001). Because of their research activities in active euthanasia of mentally ill individuals during World War II (Shevell 1992), the name Hallervorden-Spatz syndrome was replaced with 'neurodegeneration with brain iron accumulation' or NBIA (Hayflick 2003).

In 2012, Kalman et al. listed nine NBIA types (Kalman et al. 2012). Together with the most recently described NBIA type which is COASY protein-associated neurodegeneration (CoPAN) (Dusi et al. 2014), there are currently 10 NBIA forms. Pantothenate kinase-associated neurodegeneration (PKAN), phospholipase A2-associated neurodegeneration (PLAN) and mitochondrial membrane protein-associated neurodegeneration (MPAN) are among the most common NBIA types (Haack et al. 2012). Other forms are aceruloplasminemia and neuroferritinopathy, both of which have a direct link to iron storage or metabolism, fatty acid 2-hydroxylase-associated neurodegeneration (FAHN), Kufor-Rakeb syndrome (KRS) and Woodhouse-Sakati syndrome (WSS) (Kalman et al. 2012). Beta-propeller protein-associated neurodegeneration (BPAN) is a recently discovered subtype (Haack et al. 2012). PLA2G6 and ATP13A2, the genes associated with PLAN and KRS, respectively, are assigned to a PARK locus (Paisan-Ruiz et al. 2009; Morgan et al. 2006; Hampshire et al. 2001; Ramirez et al. 2006). WDR45, the gene associated with BPAN has been proposed as a PARK gene as well (Haack et al. 2012). Table 1 provides a summary of NBIA subtypes which have been published between 1995 and 2014.

Despite advances in NBIA research in the last two decades, still about 30% of individuals with NBIA have no genetic diagnosis (Dusi et al. 2014). Until today, no causal therapy has been reported for NBIA.

Efforts to improve symptoms with iron chelating therapy have been made. The most thorough therapeutic study in NBIA is the TIRCON study (Treat Iron-Related Childhood-Onset Neurodegeneration) (Kalman et al. 2012). Kalman et al. reported about the recently founded international registry for NBIA. It is an EU-FP7-funded project that was initiated in the context of TIRCON. The registry may allow a better integration and combination of resources and knowledge of NBIA (Kalman et al. 2012). Kwiatkowski et al. reported about an individual with autosomal dominant idiopathic NBIA which they treated with deferiprone. They observed moderate improvements both in clinical symptoms and in MRI (magnetic resonance imaging) findings over the course of 2.5 years in that particular case (Kwiatkowski et al. 2012).

In 2014, Cossu et al. reported about six individuals with NBIA that were treated with deferiprone for three to four years. They measured clinical outcome with clinical scores and blinded video rating. T2*-weighted MR images were done to assess changes in pallidal iron content. Five of six affected subjects had a genetically confirmed diagnosis of PKAN and one had idiopathic NBIA. Out of the six individuals, three showed clinical stabilization or improvement, two showed no change or mildly worsening and one showed a definite clinical worsening. MR images indicated a decrease in iron content in the globus pallidus in four of six subjects (see Figure 1) (Cossu et al. 2014).

Studies from Kwiatkowski et al. and Cossu et al. indicate that individuals with NBIA may benefit from treatment with deferiprone (Kwiatkowski et al. 2012; Cossu et al. 2014). However, no randomized, placebo-controlled clinical studies have been reported so far.

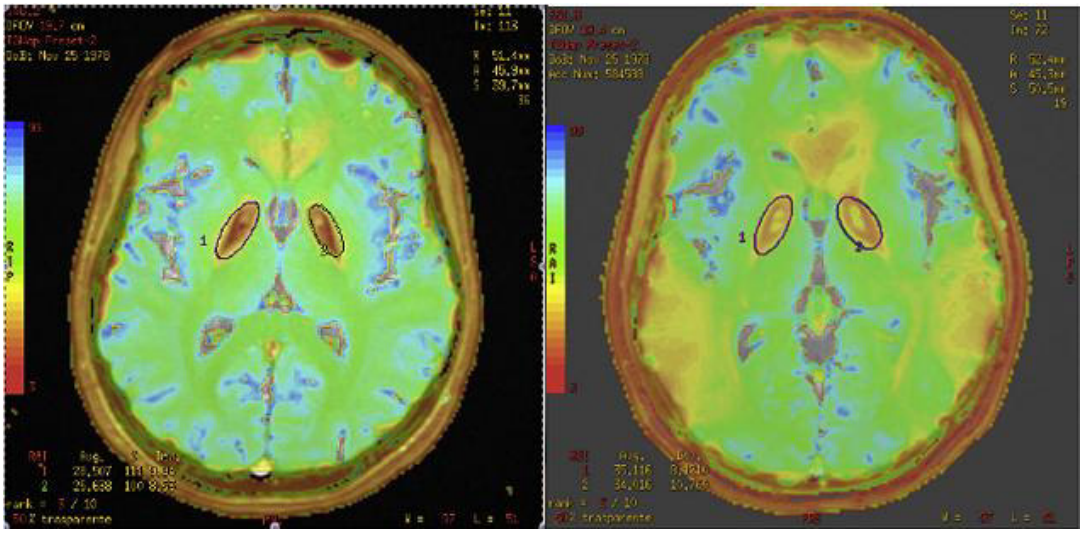

Figure 1 – Axial T2*-weighted MRI of an individual with PKAN treated with deferiprone

These MR images show T2*-weighted multiparametric color MR images of an individual with PKAN. The affected subject was treated with deferiprone for four years. The left MR image is at the time of treatment onset, the right image is after four years. The two circles indicate the position of the globus pallidus. The reduction of parameters reflecting pallidal iron content can be seen (Cossu et al. 2014, p. 653). With kind permission from Parkinsonism and Related Disorders, Elsevier.

Table 1 – NBIA subtypes

Disease	Gene	Chromo-some	Mode of inheritance	Protein	Literature
PKAN	PANK2	20	AR	pantothenate kinase 2	(Zhou et al. 2001)
PLAN	PLA2G6	22	AR	Ca^{2+} -independent phospholipase A2	(Morgan et al. 2006)
MPAN	C19ORF12	19	AR	orphan	(Hartig et al. 2011)
Acerulo-plasminemia	CP	3	AR	ceruloplasmin	(Yoshida et al. 1995; Harris et al. 1995)
Neuroferritino-pathy	FTL	19	AD	ferritin light chain	(Curtis et al. 2001)
FAHN	FA2H	16	AR	fatty acid 2-hydroxylase	(Edvardson et al. 2008)
Kufor-Rakeb syndrome	ATP13A2	1	AR	P-type ATPase ATP13A2	(Ramirez et al. 2006)
WSS	C2ORF37	2	AR	orphan	(Alazami et al. 2008)
CoPAN	COASY	17	AR	coenzyme A synthase	(Dusi et al. 2014)
BPAN	WDR45	X	XD	WD40 repeat protein 45	(Haack et al. 2012)

1.2 NBIA subtypes

1.2.1 Pantothenate kinase-associated neurodegeneration (PKAN)

Pantothenate kinase-associated neurodegeneration (PKAN) is the major subtype of NBIA (Hayflick et al. 2003; Kalman et al. 2012). The responsible gene pantothenate kinase 2 (PANK2) which is located on chromosome 20p13 was identified in 2001 (Zhou et al. 2001). Thus, it is among the first three NBIA types that have been matched to a gene. Ceruloplasmin mutations were identified in individuals with aceruloplasminemia already in 1995 (Harris et al. 1995; McNeill et al. 2008b). Ferritin light chain or FTL mutations were identified in neuroferritinopathy in 2001 (Zhou et al. 2001; Curtis et al. 2001).

1.2.1.1 Genetics and biochemistry

As with most NBIA subtypes, PKAN has an autosomal recessive mode of inheritance (Zhou et al. 2001; Hayflick et al. 2003). According to Zhou et al., the gene PANK2 encodes for pantothenate kinase 2 (PANK2), an enzyme which phosphorylates pantothenate (vitamin B5). In the human there are four isoforms of pantothenate kinase: PANK1, PANK2, PANK3 and PANK4 (Zhou et al. 2001). The phosphorylation of pantothenate (vitamin B5) is the first and rate-limiting step of coenzyme A biosynthesis in both bacteria and eukaryotes (Jackowski and Rock 1981; Rock et al. 2000). PANK2 has been shown to be located and active in mitochondria (Hörtnagel et al. 2003; Kotzbauer et al. 2005).

1.2.1.2 Clinical presentation

Hayflick et al. investigated the clinical characteristics of pantothenate kinase-associated neurodegeneration in a large cohort of NBIA (formerly Hallervorden-Spatz syndrome). They investigated 123 patients from 98 families with NBIA. They noticed clinical differences in individuals with PKAN and subsequently classified PKAN into classic and atypical PKAN. With classic PKAN, age of onset was 3 years of age on average (ranging from 0.5 to 12 years). With atypical PKAN, age of onset was 14 years of age on average (ranging from 1 to 28 years) and thus much older than with classic PKAN. Difficulties with gait and posture were the most common presenting symptoms with the cohort of classic PKAN. It was found in nearly 80 percent of individuals affected. With classic disease, extrapyramidal symptoms

such as dystonia were salient features. Corticospinal tract involvement and cognitive decline were other features that were recognized in parts of the cohort. Symptoms of retinopathy or electroretinographic evidence of retinopathy were identified in nearly half of the individuals with classic PKAN. In contrast to that, retinopathy was rare with atypical PKAN. With atypical disease, speech difficulties at an early stage of the disease were characteristic and were the most common presenting symptom. Extrapyramidal symptoms and corticospinal tract involvement were encountered frequently in the course of the disease. Psychiatric symptoms were more common than with classic PKAN. Whereas most individuals with classic PKAN were unable to ambulate within 15 years after onset of the disease, most individuals with atypical disease were able to ambulate into adulthood and had a slower progression of disease (Hayflick et al. 2003).

1.2.1.3 Imaging

Sethi et al., Angelini et al. and Hayflick et al. described MRI features in pantothenate kinase-associated neurodegeneration. Characteristic imaging pattern on MRI investigations can be very helpful in finding the diagnosis of PKAN. One distinguished sign that can be seen on T2-weighted MRI, is the so-called ‘eye-of-the-tiger sign’. This radiologic sign is marked by central hyperintensity with a surrounding rim of marked hypointensity in the globus pallidus. This resembles an eye of a tiger (see Figure 2). The finding of an eye-of-the-tiger sign had already been reported in individuals with NBIA before the genetic association with PANK2 was identified (Sethi et al. 1988; Angelini et al. 1992; Hayflick et al. 2003).

The finding of an eye-of-the-tiger sign in an individual presenting with neurologic symptoms is highly suspicious for PKAN (Hayflick et al. 2003). Although the eye-of-the-tiger sign is very typical for PKAN, it is not pathognomonic. It has been reported as a rare finding in neuroferritinopathy (McNeill et al. 2008a) and MPAN (Hartig et al. 2011). In other neurologic diseases such as multiple system atrophy, eye-of-the-tiger like MR images have been suggested as well (Chang et al. 2009). Furthermore, the sign has also been reported to vanish during the course of the disease in an individual with PKAN (Baumeister et al. 2005).

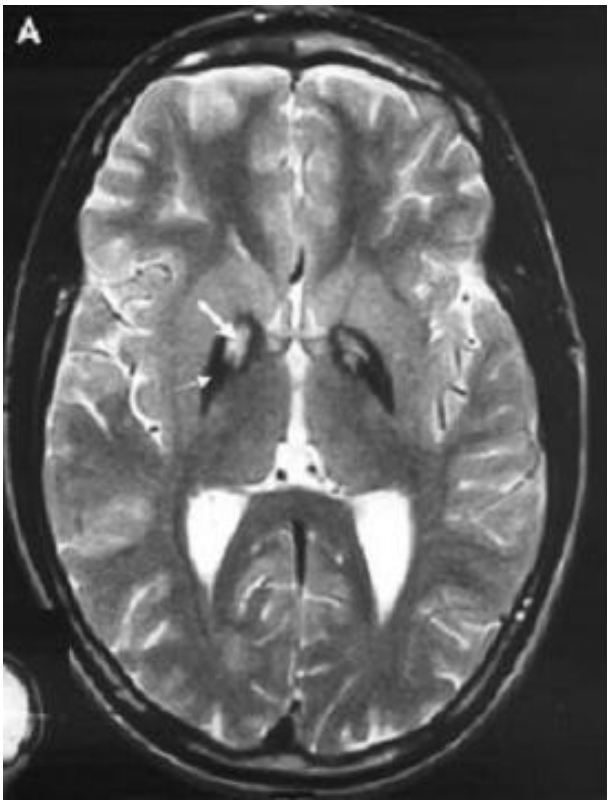

Figure 2 – Axial T2-weighted MRI showing an eye-of-the-tiger sign in PKAN

The axial T2-weighted MR imaging of an individual with mutations in PANK2 displays an eye-of-the-tiger sign. The thin arrow indicates the pallidal hypointensity. The thick arrow points to a focal hyperintensity within the pallidal hypointensity. The combination of both resembles an eye of a tiger (Hartig et al. 2006, p. 253). With kind permission from Annals of Neurology, John Wiley and Sons.

1.2.2 Phospholipase A2-associated neurodegeneration (PLAN)

Phospholipase A2-associated neurodegeneration (PLAN) is the subtype of NBIA that is associated with mutations in the gene phospholipase A2 Group 6 (PLA2G6). The gene was matched to PLAN in 2006 (Morgan et al. 2006; Kurian et al. 2008). It is one of the three major genes associated with NBIA (Haack et al. 2012). The gene PLA2G6 is located on chromosome 22 (Morgan et al. 2006). PLA2G6 encodes a calcium-independent phospholipase (Morgan et al. 2006). Phospholipase A2 enzymes catalyze the release of free fatty acids from phospholipids (Ackermann et al. 1994). Because of the parkinsonian features in individuals with PLA2G6-related dystonia-parkinsonism, PLA2G6 has been proposed as a PARK locus (Paisan-Ruiz et al. 2009).

Clinically, PLAN can be classified into three categories. The first and classic form is infantile neuroaxonal dystrophy (INAD), the second is atypical neuroaxonal dystrophy (NAD) and the third is PLA2G6-related dystonia-parkinsonism (Gregory et al. 2008; Paisan-Ruiz et al. 2009). In their review, Kurian et al. refer to these three forms as infantile onset PLAN, childhood onset PLAN and adult onset PLAN, respectively (Kurian et al. 2011).

1.2.2.1 Infantile neuroaxonal dystrophy (INAD)

Aicardi and Castelein reported clinical signs and symptoms of eight individuals with a clinical diagnosis of INAD and compared these with 42 other case reports of INAD in the literature at that time. Onset of disease was between six months and two years in all 50 cases. They describe progressive motor deterioration with pyramidal tract signs and marked hypotonia, ocular involvement as well as mental deterioration (Aicardi and Castelein 1979). Carrilho et al. and Kurian et al. described clinical signs and symptoms in cohorts of individuals with mutations identified in PLA2G6. Hypotonia, spastic tetraparesis and dystonia are very frequent symptoms. Likewise ocular involvement with nystagmus, strabismus and optic atrophy eventually leading to blindness are present in most individuals with INAD (Carrilho et al. 2008; Kurian et al. 2008). Carrilho et al. reported that most individuals never learn to walk. Furthermore, progressive marked cognitive deficits are observed in the course of the disease (Carrilho et al. 2008). In INAD, high voltage fast rhythms are often detectable on EEG (Aicardi and Castelein 1979). Most individuals with INAD show an overall rapid decline. Those individuals included in the studies from Kurian et al. and Gregory et al., that

had already died, had an average age at death of about 10 years of age (Kurian et al. 2008; Gregory et al. 2008).

1.2.2.2 Atypical Neuroaxonal dystrophy

Gregory et al. did mutation screenings on individuals with classic INAD and individuals with idiopathic NBIA. They identified PLA2G6 mutations in 80% of individuals with clinical characteristics of classic INAD. These individuals formed a relatively homogeneous group. However, Gregory et al. also found PLA2G6 mutations in about 20% of individuals with idiopathic NBIA. The latter group comprising six individuals differed significantly from individuals with classic INAD. Gregory et al. proposed to categorize them as atypical NAD (Gregory et al. 2008).

Gregory et al. reports that individuals with atypical NAD have an average onset of disease of about four years of age (range 1.5 to 6.5). Motor dysfunctions such as gait abnormalities or ataxia are major presenting symptoms. Speech delay and reduced social interaction are common symptoms as well and can precede motor dysfunctions. Progressive motor dysfunctions involving dystonia, tetraparesis and dysarthria as well as psychiatric disturbances mark the course of the disease. In addition to a later onset of disease, atypical NAD progresses more slowly than classic INAD. In contrast to classic INAD, truncal hypotonia, strabismus and fast EEG were not observed in the six individuals with atypical NAD studied by Gregory et al. (Gregory et al. 2008).

1.2.2.3 PLA2G6-related dystonia-parkinsonism

PLA2G6-related dystonia-parkinsonism is the third recognized entity of PLAN. It comprises a heterogeneous subgroup of only few individuals diagnosed worldwide. Most individuals described have an onset of disease in their early adulthood (Paisan-Ruiz et al. 2009; Sina et al. 2009). One individual has even been reported that was 37 years old at onset of disease (Shi et al. 2011). Paisan-Ruiz et al. and Sina et al. reported that symptoms of parkinsonism dominate and include bradykinesia, rigidity, facial hypomimia and tremor. Marked dystonia is observed as well (Paisan-Ruiz et al. 2009; Sina et al. 2009). In the clinical course, rapid cognitive decline leading to dementia commonly becomes evident (Paisan-Ruiz et al. 2009; Sina et al. 2009). Different psychiatric symptoms such as depression, delusion, paranoia and personality

changes have been described in case reports in the literature (Paisan-Ruiz et al. 2009; Yoshino et al. 2010; Bower et al. 2011). According to Paisan-Ruiz et al. and Sina et al., motor dysfunctions respond to levodopa treatment quite well. However, drug-induced early dyskinesias compromise the long-term benefit of the treatment (Paisan-Ruiz et al. 2009; Sina et al. 2009).

1.2.2.4 MR Imaging in PLAN

According to Gregory et al., cerebellar atrophy is very frequently seen in individuals with classic INAD and atypical NAD. With both classic INAD and atypical NAD hypointensities on T2-weighted MR images may be present in the globus pallidus and less often in the substantia nigra as well (Gregory et al. 2008). Cerebellar atrophy and T2-weighted hypointensities in the globus pallidus have also been described for PLA2G6-related dystonia-parkinsonism (Bower et al. 2011).

1.2.3 Mitochondrial membrane protein-associated neurodegeneration (MPAN)

In 2011, Hartig et al. identified mutations in the gene C19ORF12 in a cohort of individuals with NBIA from Poland (Hartig et al. 2011). Hartig et al. expressed a fused C19ORF12-GFP protein in fibroblasts and subsequently showed that this fusion protein localizes to mitochondria. Hence, they proposed the name ‘mitochondrial membrane protein-associated neurodegeneration’ or ‘MPAN’ for the NBIA subtype associated with mutations in C19ORF12 (Hartig et al. 2011). The gene name C19ORF12 stands for Chromosome 19 open reading frame 12, indicating its chromosomal position on 19q12 (Horvath et al. 2012). Like most NBIA subtypes, MPAN is an autosomal recessive disorder (Hartig et al. 2011). In the Polish cohort investigated by Hartig et al., 18 of 24 affected individuals shared the same homozygous mutation. This is an 11 base pairs (bp) deletion that leads to a premature stop codon {c.[204_214del], p.[Gly69Argfs*10]}. Haplotype analysis suggested a founder effect with a common founder at least 50 to 100 generations ago (Hartig et al. 2011). Following the discovery of MPAN, Panteghini et al. investigated an Italian cohort of 105 individuals with idiopathic NBIA and identified three individuals with MPAN (Panteghini et al. 2012). The frequency of MPAN cannot be assessed exactly at the moment, however, Haack et al. assessed it to be among the three major NBIA types (Haack et al. 2012).

MPAN has a later onset of disease and a slower progression than classic PKAN (Hartig et al. 2011; Hayflick et al. 2003). In the 24 Polish individuals investigated in the study by Hartig et al., the onset of disease ranged between 4 and 21 years and was on average 10 years. One additional individual with MPAN examined in the study had a diagnosis of Parkinson's disease and was already 25, when first symptoms began (Hartig et al. 2011). According to Hartig et al., one or more extrapyramidal symptoms like oromandibular dystonia, generalized dystonia or parkinsonism are present in most individuals with MPAN. Likewise, pyramidal signs and symptoms such as hyperreflexia, positive Babinski sign and spasticity are common. Dysarthria is a frequent feature (Hartig et al. 2011). Psychiatric symptoms, including disinhibited or impulsive behavior, compulsive behavior, depression, emotional lability and paranoid hallucinations were reported in individuals with MPAN as well (Hartig et al. 2011; Deschauer et al. 2012). Cognitive dysfunctions may occur in later stages of the disease (Panteghini et al. 2012). Optic atrophy, a well-known feature of PLAN (Kurian et al. 2008) occurs very frequently in MPAN, as well, although visual impairment seems to be less devastating (Hartig et al. 2011). Motor axonal neuropathy may be present on electrophysiologic examination (Hartig et al. 2011).

Clinical presentation can vary. MPAN was reported to mimic juvenile amyotrophic lateral sclerosis with prominent concurrent upper and lower motor neuron symptoms (Deschauer et al. 2012). As mentioned above, one individual with MPAN, investigated by Hartig et al., had a diagnosis of Parkinson's disease. His akinesia was treated effectively with levodopa for several years but eventually, strong fluctuations of the individual's symptoms developed (Hartig et al. 2011). MR images in MPAN (see Figure 3) show hypointensities on T2-weighted images in the globus pallidus and substantia nigra bilaterally (Hartig et al. 2011). Hartig et al. reported about one individual with MPAN in their study who had an eye-of-the-tiger sign on MR imaging (Hartig et al. 2011). However, this radiographic sign is an MRI finding that is actually typical for PKAN (Hayflick et al. 2003).

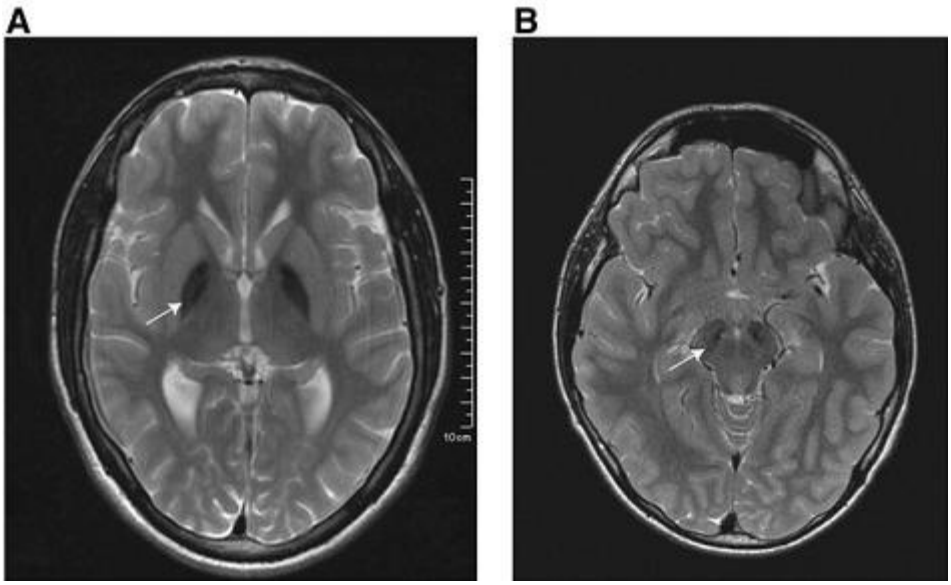

Figure 3 – Axial T2-weighted MRI of individuals with MPAN

Axial T2-weighted MR images of subjects with MPAN are displayed. Bilateral hypointensities of the globus pallidus (A, arrow) and bilateral hypointensities of the substantia nigra (B, arrow) are shown on T2-weighted MR images (Hartig et al. 2011, p. 547). With kind permission from American Journal of Human Genetics, Elsevier.

Neuropathological investigations in one individual of the Polish cohort, studied by Hartig et al., showed iron-containing deposits. These accumulations were mainly localized in the globus pallidus and substantia nigra. Alpha-synuclein positive Lewy bodies and tau-positive neuronal inclusions were detected in various brain regions (Hartig et al. 2011).

1.2.4 Aceruloplasminemia

In March 1995, almost simultaneously, two research groups identified independently the molecular basis for aceruloplasminemia, an autosomal recessive form of NBIA (Yoshida et al. 1995; Harris et al. 1995). Yoshida et al. detected a homozygous 5 base pair deletion in the ceruloplasmin gene (Yoshida et al. 1995) whereas Harris et al. found a homozygous 5 base pair insertion in the same gene (Harris et al. 1995). Both mutations were identified in Japanese individuals (Yoshida et al. 1995; Harris et al. 1995). Most mutations have been found in the ceruloplasmin gene since that time, have been recognized in individuals of Japanese origin (McNeill et al. 2008b). The ceruloplasmin gene is located on chromosome 3 (Yang et al. 1986).

Holmberg and Laurell identified ceruloplasmin to be a copper binding blue plasma protein (Holmberg and Laurell 1948). Holmberg and Laurell also noticed that it is an enzyme with oxidase activity (Holmberg and Laurell 1951). In addition to the transportation of copper, ceruloplasmin was shown to be a ferrioxidase that is important in iron metabolism (Osaki et al. 1966).

In 2008, McNeill et al. investigated 33 cases of aceruloplasminemia with CP gene mutations in the literature. They paid particular attention to the neurologic presentation of individuals with CP gene mutations. The average age at the time of neurological diagnosis was 51 years. However, there was a wide range from 16 to 72 years. 28 individuals had homozygote ceruloplasmin mutations, and 5 had heterozygote mutations in the ceruloplasmin gene. Heterozygotes were more likely to have mild disease (McNeill et al. 2008b). According to McNeill et al., neurologic features such as ataxia, dysarthria and cognitive impairment are common in individuals with aceruloplasminemia. Retinal degeneration is a particularly frequent feature, affecting about 75% of individuals. Some individuals develop chorea or parkinsonism. Aceruloplasminemia is a multi-organ disease. Individuals with aceruloplasminemia are prone to develop diabetes mellitus. Anemia may develop as well (McNeill et al. 2008b).

According to McNeill et al., T2-weighted images on MRI show hypointensities in most areas of the brain in homozygous cases of aceruloplasminemia. Brain regions affected include subcortical structures (basal ganglia nuclei, thalamus, and dentate nucleus) as well as cerebral and cerebellar cortices (McNeill et al. 2008b).

Iron and copper levels in blood are helpful in finding the correct diagnosis. In homozygous individuals reviewed by McNeill et al., serum iron and copper levels were very low, ferritin levels were elevated 3 to 40 times the upper limit of normal and serum ceruloplasmin was undetectable. In heterozygous cases, serum copper and ceruloplasmin were about half the normal value and serum iron and ferritin were normal (McNeill et al. 2008b). Chelation therapy has been reported in single cases to provide some clinical improvement (Miyajima et al. 1997; Haemers et al. 2004; Kuhn et al. 2007; Skidmore et al. 2008).

1.2.5 Neuroferritinopathy

In 2001, Curtis et al. identified mutations in the ferritin light chain gene in individuals with a disease they called neuroferritinopathy (Curtis et al. 2001). In contrast to other NBIA disorders, this is so far the only one with autosomal dominant inheritance (Curtis et al. 2001; Keogh et al. 2012). The gene FTL is located on chromosome 19q13. It encodes for the ferritin light polypeptide (Curtis et al. 2001). Hereditary ferritinopathy is another name for neuroferritinopathy relating to the fact that histopathological changes have been found in organs other than the brain as well (Vidal et al. 2004). Since the discovery of a 460InsA mutation in 2001, at least seven different pathogenic mutations have been published (Keogh et al. 2012). Due to a founder effect in the Cumbrian region of England, 460InsA is the most common mutation in neuroferritinopathy (Chinnery et al. 2007). Neuroferritinopathy is an adult-onset form of NBIA. Symptoms are similar to Huntington's disease, which is autosomal dominant as well (Chinnery et al. 2007).

Chinnery et al. investigated 40 symptomatic individuals with the 460InsA mutation to depict the clinical features. Symptoms included dystonia, chorea, orolingual dyskinesias, dysarthria, dysphagia and psychiatric disturbances. The mean age at the onset of disease was about 40 years but was ranging widely from 13 to 63 years. Focal onset chorea and focal leg or arm dystonia were the two most common presenting symptoms (Chinnery et al. 2007). Thirty-eight of the 40 individuals were followed up. The initially presenting symptom usually predominated in the clinical course. Commonly observed features were dystonia (83%), chorea (70%), oromandibular dyskinesia (65%), a characteristic dysarthria (63%), action-specific dystonia (63%), dysphagia (40%) and bradykinesia (35%) (Chinnery et al. 2007). Psychiatric disturbances were noted frequently involving disinhibition and emotional lability. Early cognitive deficits may occur but are usually subtle (Chinnery et al. 2007).

In neuroferritinopathy, MR images of the brain (see Figure 4) typically show T2*-weighted hypointensities in the dentate nucleus (95%), the substantia nigra (81%), the cerebral cortex (71%), the basal ganglia nuclei involving the globus pallidus (38%) and the putamen (28%), and in the thalamus (19%) (McNeill et al. 2008a). McNeill et al. and Kruer et al. reported about areas of hyperintensity that may be seen within hypointensities. These hyperintensities are likely fluid-filled cystic cavitations (McNeill et al. 2008a; Kruer et al. 2012). Very rarely, an eye-of-the-tiger sign which PKAN is typical for (Hayflick et al. 2003) can be seen in neuroferritinopathy (McNeill et al. 2008a).

MRI findings are particular important in neuroferritinopathy as they may precede clinical symptoms (Keogh et al. 2012). Keogh et al. investigated asymptomatic first-degree relatives of known 460InsA mutation carriers. Those, who were identified to have the same genetic mutation, showed evidence of MRI changes prior to clinical deterioration (Keogh et al. 2012).

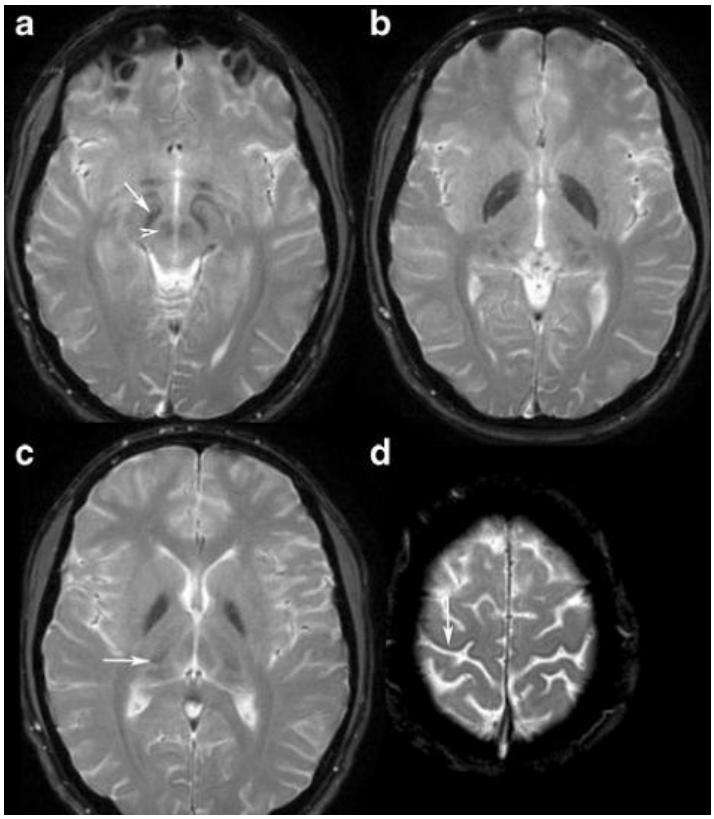

Figure 4 – Axial T2*-weighted MRI of an individual with neuroferritinopathy
T2* weighted MRI showing hypointensities in different areas of the brain. (a, arrow) indicates the substantia nigra. (a, arrowhead) points to the red nucleus. (b) and (c) show the globus pallidus. (c, arrow) indicates the thalamus. (d, arrow) indicates the cerebral cortex (Keogh et al. 2012, p. 95). With kind permission from Neurogenetics, Springer Science and Business Media.

In neuroferritinopathy, serum iron levels are usually within normal range, however, serum ferritin levels are decreased in some individuals (Curtis et al. 2001; Chinnery et al. 2007). Attempts by Chinnery et al. to induce clinical improvement by venesection or chelation therapy in a small group of patients were not successful (Chinnery et al. 2007).

1.2.6 Fatty acid 2-hydroxylase-associated neurodegeneration (FAHN)

In 2008, Edvardson et al. detected mutations in the fatty acid 2-hydroxylase (FA2H) gene in individuals with SPG35 – a form of hereditary spastic paraplegia (Edvardson et al. 2008; Dick et al. 2010). The phenotypic spectrum of mutations in the FA2H gene is broad (Edvardson et al. 2008; Kruer et al. 2010; Garone et al. 2011). Kruer et al. found mutations in FA2H in individuals with idiopathic NBIA. They proposed the name FAHN (fatty acid 2-hydroxylase-associated neurodegeneration) for this subtype of NBIA (Kruer et al. 2010).

Alderson et al. identified the gene FA2H (fatty acid 2-hydroxylase) on chromosome 16. FA2H encodes fatty acid 2-hydroxylase, a membrane-bound protein that catalyzes the hydroxylation of free fatty acids (Alderson et al. 2004). In the ensuing metabolic pathway, free 2-hydroxy fatty acids are incorporated into ceramide, which is a subcomponent of the myelin sheath (Eckhardt et al. 2005). A mouse model of FAHN with a FA2H knockout, developed by Zöller et al., suggests a role of FA2H in the long-term maintenance of myelin structures. FA2H knockout mice develop late-onset myelin sheath and axon degeneration (Zöller et al. 2008).

Edvardson et al., Kruer et al. and Garone et al. describe a wide phenotypic spectrum. Onset of disease is in childhood. Typical symptoms are spasticity and gait disturbances. Individuals with FAHN may develop ataxia, dystonia and dysarthria. Non-motor dysfunctions such as cognitive deficits and seizures may occur. Ophthalmologic disease may develop including optic nerve atrophy and nystagmus (Edvardson et al. 2008; Kruer et al. 2010; Garone et al. 2011).

Kruer et al., Edvardson et al. and Dick et al. described MRI features in Fatty acid 2-hydroxylase-associated neurodegeneration. MRI findings involve hypointensities on T2-weighted MR images in the globus pallidus. Furthermore, subcortical and periventricular white matter hyperintensities can be observed on T2-weighted images. Other MRI findings involve mild cerebral atrophy, marked pontocerebellar atrophy and thinning of the corpus callosum (Kruer et al. 2010; Edvardson et al. 2008; Dick et al. 2010).

1.2.7 Kufor-Rakeb syndrome (KRS)

Ramirez et al. identified Kufor-Rakeb syndrome (KRS) to be a rare autosomal recessive disease that is associated with mutations in the gene ATP13A2. The connection between mutations in this gene and Kufor-Rakeb syndrome was detected in 2006 in a Chilean pedigree (Ramirez et al. 2006). The name of the disease originates from the village Kufor-Rakeb in Jordan, where the firstly described family came from (Najim al-Din et al. 1994; Behrens et al. 2010). The gene ATP13A2 is located on chromosome 1 (Ramirez et al. 2006). ATP13A2 encodes a type 5 P-type ATPase which is mainly expressed in neurons (Ramirez et al. 2006). The loss of the ATPase has been shown to lead to a lysosomal dysfunction (Dehay et al. 2012; Usenovic et al. 2012).

In 2010, Schneider et al. noticed MRI findings in an individual with KRS similar to what can be seen in other NBIA disorders. They observed T2*-weighted hypointensities in the putamen and caudate nucleus which could be explained by iron accumulation. They consequently suggested grouping KRS under the umbrella of NBIA (Schneider et al. 2010). Other important MRI findings include generalized brain atrophy, particularly in later stages of the disease (Najim al-Din et al. 1994).

Najim al-Din et al. described the first family with Kufor-Rakeb syndrome with five affected siblings. They noticed parkinsonian symptoms, pyramidal symptoms, dementia and supranuclear upgaze paresis (Najim al-Din et al. 1994). Behrens et al. and Eiberg et al. contributed to define the signs and symptoms of KRS. The clinical hallmarks of KRS are early-onset parkinsonism, pyramidal signs and dementia. Parkinsonian features may include bradykinesia, hypomimia, cogwheel rigidity and tremor. Pyramidal signs may involve spasticity, paresis, hyperreflexia and extensor plantar response (Behrens et al. 2010; Eiberg et al. 2012). Behrens et al. also reported about sleeping difficulties and visual and auditory hallucinations (Behrens et al. 2010). Behrens et al. described an onset of disease between 10 to 13 years of age (Behrens et al. 2010) whereas Eiberg et al. noticed a wider range with individuals having an onset of disease at 10 to 29 years of age (Eiberg et al. 2012). ATP13A2 is listed as Park gene PARK9 reflecting the overlap with other forms of early-onset parkinsonism (Ramirez et al. 2006). Levodopa therapy, which is well-known to help with Parkinson's disease, also leads to improvement of extrapyridamal dysfunctions in KRS (Najim al-Din et al. 1994).

1.2.8 Woodhouse-Sakati syndrome (WSS)

In 1983, Woodhouse and Sakati described a distinct syndrome consisting of neurologic symptoms, diabetes mellitus, hypogonadism, alopecia and electrocardiogram abnormalities in two consanguineous Saudi Arabian families (Woodhouse and Sakati 1983). It was 25 years later that Alazami et al. identified the molecular basis of the disease. In 2008, they identified mutations in the gene C2ORF37 in one of the original Saudi Arabian families and other families with Woodhouse-Sakati syndrome (WSS). The gene C2ORF37 is located on chromosome 2q and encodes a nucleolar protein which is little investigated so far (Alazami et al. 2008). WSS is an autosomal recessive disease (Alazami et al. 2008). Like other NBIA disorders, it is listed in the international registry for neurodegeneration with brain iron accumulation (Kalman et al. 2012).

WSS is a rare multisystemic disease (Woodhouse and Sakati 1983). Woodhouse and Sakati first described clinical signs and symptoms of the disease. The investigated individuals showed mental retardation, deafness, hypogonadism with low estrogen or testosterone levels, diabetes mellitus, alopecia, facial dysmorphy and electrocardiogram abnormalities (Woodhouse and Sakati 1983). With a higher number of individuals that have been identified, the phenotypic spectrum has broadened. In particular, more neurologic features have been identified (Al-Semari and Bohlega 2007). In addition to mental retardation and deafness, Al-Semari and Bohlega noticed extrapyramidal symptoms such as focal or generalized dystonia and dysarthria that appear in the course of the disease. The appearance of the first neurologic symptoms was noted in the second and early third decade of life (Al-Semari and Bohlega 2007).

According to Al-Semari et al., MR images of individuals with WSS show widespread diffuse white matter hyperintensities on T2-weighted images. Furthermore, T2-weighted hypointensities have been detected in the globus pallidus, substantia nigra and red nucleus (Al-Semari and Bohlega 2007). Individuals with WSS usually have low serum IGF-1 (insulin-like growth factor 1) which can be diagnostically helpful (Al-Semari and Bohlega 2007).

1.2.9 COASY protein-associated neurodegeneration (CoPAN)

In 2014, Dusi et al. reported on a new gene associated with NBIA. They performed whole exome sequencing in an individual with idiopathic NBIA. They detected a homozygous missense mutation in the gene coenzyme A synthase (COASY). In subsequent screenings in various cohorts of idiopathic NBIA a second individual with compound heterozygote mutations in COASY was identified (Dusi et al. 2014).

According to Dusi et al., both individuals showed a similar phenotype. They presented with gait difficulties in the first years of life. They developed spastic-dystonic paraparesis and tetraparesis. Individuals later showed parkinsonian-like features, cognitive deficits and obsessive-compulsive behavior. Both individuals lost ability to ambulate independently, one by the age of 15 years, the other by the age of 20 years (Dusi et al. 2014).

T2-weighted MR images in the two affected individuals showed bilateral hypointense globi pallidi. In one individual, general hypointensity of the globi pallidi was accompanied by a central region of hyperintensity similar to the eye-of-the-tiger sign (Dusi et al. 2014). Mutations in COASY are the second gene defect associated with both CoA synthesis and neurodegeneration with brain iron accumulation (Dusi et al. 2014). In 2001, Zhou et al. identified mutations in PANK2, another enzyme that is involved in coenzyme A synthesis (Zhou et al. 2001). Dusi et al. proposed ‘COASY protein-associated neurodegeneration’ or ‘CoPAN’ as the term for this new NBIA type (Dusi et al. 2014).

1.3 NBIA candidate genes

1.3.1 SLC39A14 and the SLC39 family

The group of solute carriers 39 (SLC39) comprises 14 genes (SLC39A1 - SLC39A14) that encode 14 ZIP transporters (ZIP1 - ZIP14). ZIP stands for 'ZRT, IRT-like protein' (Grotz et al. 1998; Taylor 2000; Girijashanker et al. 2008). ZRT is the abbreviation of 'zinc regulated transporter' (Zhao and Eide 1996) and IRT the abbreviation of 'iron regulated transporter' (Eide et al. 1996). The ZIP transporters are a group of metal ion transporters most of which have the capacity to transport zinc (Taylor 2000; Girijashanker et al. 2008). Computational analyses suggest that about 10% of human proteins have zinc-binding sequences which makes zinc an important trace element in the human proteome (Andreini et al. 2006). However, some ZIP transporters have the capability to transport other metals than zinc as well (Pinilla-Tenas et al. 2011; Wang et al. 2012).

1.3.1.1 SLC39A14 encoding ZIP14

SLC39A14 is the gene coding for the protein ZIP14 which has been demonstrated to function as a transmembrane metal ion transporter (Taylor et al. 2005; Liuzzi et al. 2006). According to Girijashanker et al., SLC39A14 contains eight coding exons, namely exons 2 to 9. Exon 1 has not been shown to be coding in humans. There are two different exons 4 (4a and 4b) (Girijashanker et al. 2008). According to data from genome browser, there are also two different exons 9 (9a and 9b) (https://www.genome.ucsc.edu) (University of California Santa Cruz 2012).

Nine of the 14 ZIP proteins (ZIP 4 - 8, 10, 12 - 14) belong to the LIV-1 subfamily of ZIP transporters (Taylor 2000; Jenkitkasemwong et al. 2012). Members of this subfamily are different to other ZIP transporters, namely that they have a special signature sequence ((H/E)EXPHEXGD) in common (Taylor 2000; Taylor et al. 2005). This sequence is located in transmembrane domain V (Taylor et al. 2005) and resembles a zinc-binding motif known from zinc metalloproteases (HEXXH) (Jongeneel et al. 1989; Taylor 2000). Figure 5 demonstrates the transmembranous and subcellular localization of ZIP transporters.

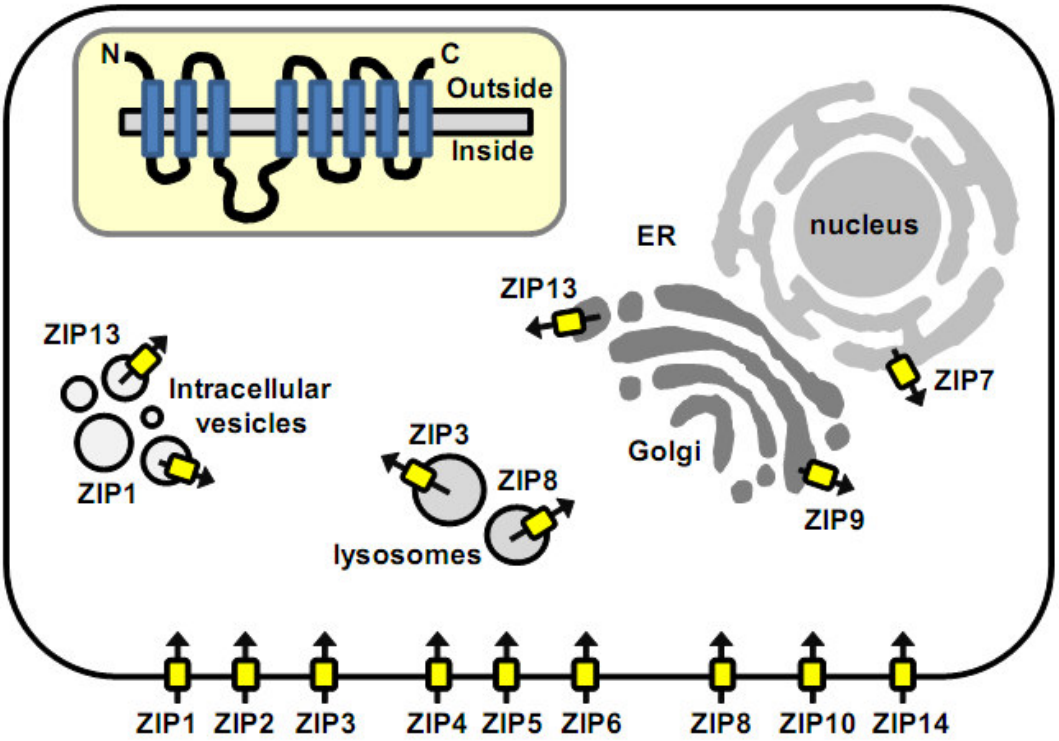

Figure 5 – Subcellular localization of ZIP transporters and transmembranous topology

The graphic demonstrates the subcellular localization of human ZIP transporters in a simplified cell containing a nucleus, endoplasmic reticulum (ER), Golgi apparatus, lysosomes and intracellular vesicles. Arrows indicate the typical directions of metal ion transport for each ZIP transporter. The yellow-shaded inset demonstrates the predicted transmembranous topology of a ZIP transporter (Jeong and Eide 2013, p. 615). With kind permission from Molecular Aspects of Medicine, Elsevier.

Phylogenetically, SLC39A14 and SLC39A8 are most closely related within the SLC39A (ZIP) family (see Figure 6) (Girijashanker et al. 2008). In both SLC39A14 and SLC39A8, the first histidine of the HEXPHEXGD amino acid sequence is exchanged by a glutamic acid, thus conferring a unique EEXPHEXGD sequence to these two genes (Begum et al. 2002; Taylor et al. 2005).

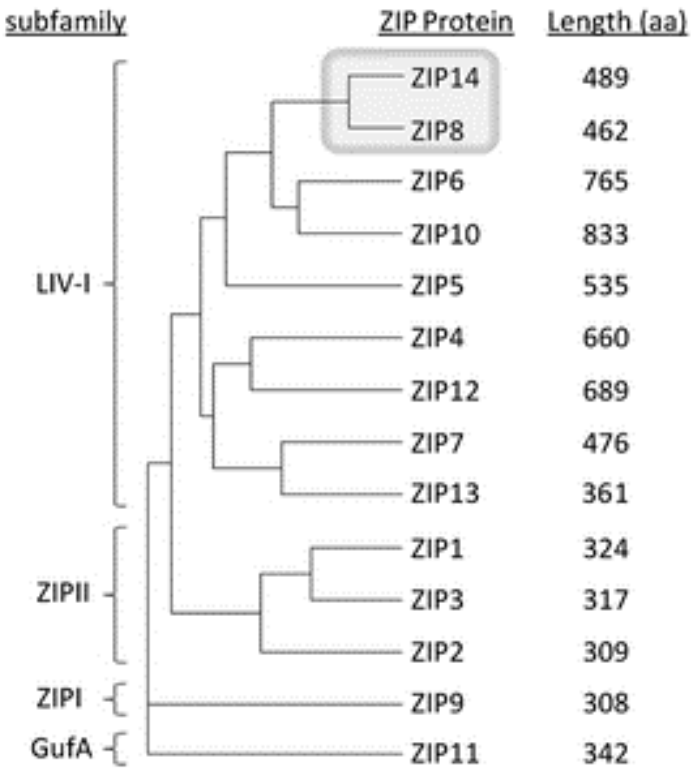

Figure 6 – Phylogenetic relationships of the 14 ZIP transporters

The simplified dendrogram displays the phylogenetic relationships of the 14 murine ZIP transporters. The LIV-1 subfamily of ZIP transporters is shown and the particular phylogenetic similarity of ZIP14 and ZIP8 is demonstrated. Amino acid lengths are provided (Jenkitkasemwong et al. 2012, p. 644). With kind permission from Biometals, Springer Science and Business Media.

Pinilla-Tenas et al. used RNA-injected Xenopus oocytes to investigate murine ZIP14 properties. They showed that murine ZIP14 can transport several divalent metal ions, namely iron (Fe^{2+}), zinc (Zn^{2+}) and manganese (Mn^{2+}), which are essential trace elements as well as cadmium (Cd^{2+}), which is a toxic metal. They found that murine ZIP14 can transport free iron and is specific for ferrous iron (Fe^{2+}). Ferric iron (Fe^{3+}), which is trivalent is not transported (Pinilla-Tenas et al. 2011). Wang et al. demonstrated that ZIP8 is able to transport iron, zinc, manganese and cadmium as well. In addition, ZIP8 has been shown to transport cobalt (Wang et al. 2012).

According to Taylor et al., the human ZIP14 is expressed ubiquitously in tissues. The tissue expression levels investigated by Taylor et al. showed highest values for liver, pancreas, thyroid gland and heart. ZIP14 is also expressed in the brain, although to a lower degree (Taylor et al. 2005).

1.3.2 WD40 repeat protein WDR45

WDR45 is a protein belonging to a large group of proteins called WD40 repeat proteins (Proikas-Cezanne et al. 2004; Behrends et al. 2010). The letters 'WD' stand for the amino acids tryptophan and aspartic acid, respectively. WD repeat is a synonym for WD40 repeat (Neer et al. 1994).

WD40 repeat proteins are proteins with a characteristic structural pattern (Neer et al. 1994). Fong et al. identified the first WD40 repeat protein. They investigated transducin, the beta subunit of a G protein and noticed a pattern of contiguous homologous segments (Fong et al. 1986). In 1994, Neer et al. systematically searched databases for WD40 repeat proteins and suggested common criteria for WD40 repeat proteins. WD40 repeat proteins are built up of four to eight repeats. Each repeat has a region of variable length (6 to 94 amino acids) and a core of a more constant length (23 to 41 amino acids, mostly around 40 amino acids). The core is flanked by GH (glycine-histidine) and WD (tryptophan-aspartic acid) or equivalent amino acids (Neer et al. 1994).

1.3.2.1 WIPI family

WDR45 is also called WIPI-4. WIPI stands for 'WD repeat interacting with phosphoinositides'. Together with WIPI-1, WIPI-2 and WIPI-3, WDR45 belongs to the WIPI WD40 repeat protein family, a highly conserved subset of WD40 repeat proteins (Proikas-Cezanne et al. 2004). According to Proikas-Cezanne et al., the four WIPI genes phylogenetically originated from two ancestor genes. These ancestor genes split into four genes in vertebrates. Thus, the four WIPI genes can be subdivided into two groups, one containing WIPI-1 and WIPI-2, and the other containing WIPI-3 and WIPI-4. There are representatives for each group with plants, fungi and animals. Genes of the WIPI-3 and WIPI-4 group have also been found in some protozoans (Proikas-Cezanne et al. 2004).

1.3.2.2 Three-dimensional structure of WD40 repeat proteins

Wall et al. investigated the three-dimensional structure of the heterotrimeric G proteins which consist of an $alpha_{i1}$ subunit, a $beta_1$ subunit and a $gamma_2$ subunit. The WD40 repeat domain is part of the $beta_1$ subunit (Wall et al. 1995). It is the first WD40 repeat protein whose structure was investigated thoroughly and thus serves as a model for other WD40 repeat proteins (Li and Roberts 2001).

Figure 7 – Structure of the G protein heterotrimer with the WD40 repeat domain
The architecture of the G protein heterotrimer is displayed with the WD40 repeat domain in the center. The $alpha_{i1}$ subunit is colored blue, the $beta_1$ subunit green, and the $gamma_2$ subunit yellow. A switch region of the $alpha_{i1}$ subunit and several residues are displayed in red. The three N mark the amino termini of the subunits. The seven blades of the beta-propeller are numbered with 1 to 7 around the periphery of the propeller. The four strands of blade 1 are labeled with A to D. The D-strands of each blade are rendered in blue and connect the WD40 cores with each other (Wall et al. 1995, p. 1049). With kind permission from Cell, Elsevier.

According to Wall et al., one repeat unit contains four strands. A four-stranded anti-parallel sheet forms a blade. Several blades together are arranged in a radial manner in a way that they form a propeller leaving a tunnel in the center (see Figure 7). Due to the predominant beta sheet form, the protein is called a beta-propeller and in the case of the heterotrimeric G protein, it is a seven-bladed beta-propeller (Wall et al. 1995). The members of the WIPI protein family also contain seven blades. Thus, they form seven-bladed beta-propellers as well (Proikas-Cezanne et al. 2004).

2 Aims of the Investigation

The purpose of this work was a genetic investigation of the two candidate genes (SLC39A14 and WDR45) in cohorts of patients with idiopathic NBIA.

Prior to this study, one family with three affected individuals and one family with two affected individuals had been identified to harbor homozygote mutations in SLC39A14 by collaborating foreign research groups. An autosomal recessive mode of inheritance was assumed, because all five individuals of these two families had homozygote mutations in this gene (personal communication[1]). Only scarce clinical data were available. Therefore, in the present investigation, individuals with symptoms of NBIA but without genetic diagnosis (idiopathic NBIA) were screened for mutations in SLC39A14. The main question for SLC39A14 was whether it is indeed an NBIA-associated gene. Additional mutations in SLC39A14 would support this hypothesis and increase the knowledge of the phenotypic spectrum of the disease.

In the case of WDR45, samples and clinical datasets of 13 sporadic index patients had been investigated prior to this study. These patients constituted a distinct clinical subgroup within a large cohort of individuals with NBIA. Whole exome sequencing had identified WDR45 mutations in all these 13 patients (Haack et al. 2012). The aim was to screen for further WDR45 gene mutations in five preselected individuals which had been diagnosed with idiopathic NBIA and had clinical characteristics similar to the index patients. This was done to gain more clinical phenotype data in individuals with WDR45 mutations. All but one of the 13 sporadic index subjects mentioned above were females. X-inactivation studies were planned to elucidate X-inactivation patterns in females with WDR45 gene mutations.

[1] Kurian, M.A., Neurosciences Unit, Institute of Child Health, University College London, London, UK, 03/2012.

3 Materials and Methods

3.1 Materials

In the following, the general laboratory devices, technical devices, chemicals, reagents, software tools and online databases as well as the corresponding manufacturers or website addresses are listed.

3.1.1 General laboratory devices

Autoclave 5075 ELV	Systec, Wettenberg, GER
Centrifuge 4k15	Sigma-Aldrich, St. Louis, USA
Centrifuge/vortex FVL-2400 Combi Spin	Peqlab, Erlangen, GER
Freezer comfort at - 21 °C	Liebherr, Ochsenhausen, GER
Freezer premium at - 21 °C	Liebherr, Ochsenhausen, GER
Heating oven	Memmert, Büchenbach, GER
Ice machine AF30	Scotsman, Vernon Hills, USA
Magnetic mixer	IKA Labortechnik, Staufen im Breisgau, GER
Microwave Severin MW 7803	Severin, Sundern, GER
Power supply PAC 300	Bio-Rad Laboratories, Hercules, USA
Refrigerator profi line at 5 °C	Liebherr, Ochsenhausen, GER
Thermo shaker	Haep Labor Consult, Bovenden, GER
Thermostable adhesive seals	Thermo Fisher Scientific, Waltham, USA

3.1.2 Technical devices

Camera E.A.S.Y 440K	Herolab, Wiesloch, GER
Electrophoresis chamber	Bio-Rad Laboratories, Hercules, USA
NanoDrop 1000 Spectrophotometer	Thermo Fisher Scientific, Waltham, USA
PTC-225 thermal cycler	Bio-Rad Laboratories, Hercules, USA
Sequencer ABI 3730 DNA Analyzer	Applied Biosystems, Foster City, USA
UVT-40 M Transilluminator	Herolab, Wiesloch, GER

Vacuum pump	Merck Millipore, Billerica, USA

3.1.3 Chemicals and reagents

1 kbp DNA Ladder	Thermo Fisher Scientific, Waltham, USA
100 bp Plus DNA Ladder	Thermo Fisher Scientific, Waltham, USA
6-carboxyfluorescein-labeled primers	Metabion international AG, Martinsried, GER
Big Dye Buffer	Applied Biosystems, Foster City, USA
Big Dye Terminator	Applied Biosystems, Foster City, USA
Boric acid	Roth, Karlsruhe, GER
DNA Agarose	Biozym Scientific, Hessisch Oldendorf, GER
dNTP Set (dATP+dCTP+dGTP+dTTP)	Thermo Fisher Scientific, Waltham, USA
EDTA	Sigma-Aldrich, St. Louis, USA
Ethanol absolute	Merck, Whitehouse Station, USA
Formamide	Applied Biosystems, Foster City, USA
Herculase II fusion polymerase	Agilent Technologies, Santa Clara, USA
Herculase II reaction buffer (5x)	Agilent Technologies, Santa Clara, USA
HpaII restriction enzyme	New England Biolabs, Ipswich, USA
HPLC water	VWR International, Radnor, USA
Liz500 Standard	Applied Biosystems, Foster City, USA
Loading Dye	Thermo Fisher Scientific, Waltham, USA
Magnesium chloride	Qiagen, Hilden, GER
NEBuffer1 (1x)	New England Biolabs, Ipswich, USA
PCR Purification Plate Nucleofast	Macherey-Nagel, Düren, GER
Primers	Metabion international AG, Martinsried, GER
Q-Solution (5x)	Qiagen, Hilden, GER
DNA Stain G	Serva, Electrophoresis, Heidelberg, GER
Taq-DNA-Polymerase (5 U/µl)	Qiagen, Hilden, GER
Taq PCR buffer (10x)	Qiagen, Hilden, GER
Tris(hydroxymethyl)aminomethane	Roth, Karlsruhe, GER

3.1.4 Software

GeneStudio Contig Editor software	GeneStudio Incorporated, Suwanee, USA
GeneMapper software	Applied Biosystems, Foster City, USA
Microsoft Excel 2007	Microsoft, Redmond, USA
NanoDrop ND-1000 software	Thermo Fisher Scientific, Waltham, USA

3.1.5 In-house databases

Exome database (dbIHG)	Institute of Human Genetics, Neuherberg, GER
Primer database	Institute of Human Genetics, Neuherberg, GER

3.1.6 Online databases

UCSC Genome Browser	https://www.genome.ucsc.edu
NCBI SNP database (dbSNP)	http://www.ncbi.nlm.nih.gov/SNP
Exome Aggregation Consortium Browser	http://exac.broadinstitute.org
MutationTaster	http://www.mutationtaster.org

3.2 Methods

The following flowchart in Figure 8 summarizes the methods that were used in chronologic order in order to obtain and evaluate sequence data. Each section is explained in more detail in the following subheadings. If not otherwise indicated these methods were used for both SLC39A14 and WDR45.

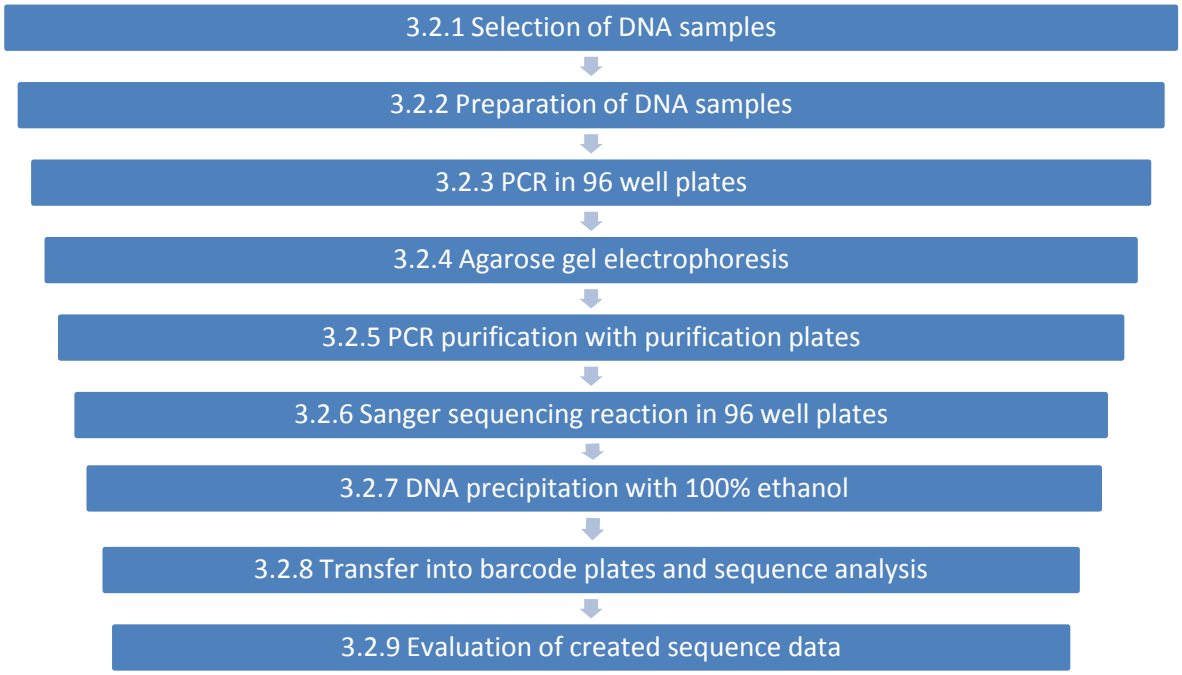

Figure 8 – Overview of applied methods

3.2.1 Selection of DNA samples

3.2.1.1 DNA samples for SLC39A14 mutation screening

A total of 285 DNA samples from individuals with idiopathic NBIA were included to screen for mutations in SLC39A14. Two times 95 DNA samples came from the local collection of DNA samples. Numerous clinicians from both hospitals and practices have been sending DNA samples from patients with idiopathic NBIA to the Institute of Human Genetics, Helmholtz Zentrum München in Neuherberg, Germany for many years. The DNA either arrives as already prepared DNA sample or is prepared from blood by technicians. Furthermore, collaborating researchers from the Istituto Neurologico Carlo Besta, Italy, sent 95 additional samples particular for the purpose to be included in the screening for mutations in SLC39A14. All 285 individuals had in common that they were from individuals suspected to have NBIA. The 285 DNA samples were distributed to three 96-well plates. Tables 2 to 4 show the three plates with 95 DNA samples and one negative control for each plate.

3.2.1.2 DNA samples for WDR45 mutation screening

Five individuals with idiopathic NBIA (DNA sample numbers 49841, 67011, 59421, 55722, 55723) and one asymptomatic relative (55724) belonged to a clinically defined subgroup of NBIA where WDR45 mutations were suspected. The five affected subjects and the asymptomatic relative were investigated for mutations in WDR45. Detailed clinical information was available in the local dataset (Institute of Human Genetics, Helmholtz Zentrum München in Neuherberg, Germany). For individual 49841, additional information was obtained by phone from the individual's mother.

Table 2 – SLC39A14_Plate 1

	1	2	3	4	5	6	7	8	9	10	11	12
A	18731	19316	19783	21690	22027	23297	27014	29545	30660	31755	34105	38226
B	19132	19349	20285	21719	22028	23594	27284	29963	30765	31996	34635	40950
C	19278	19406	20957	22021	22685	24060	27285	30525	30847	32098	34661	41428
D	19279	19438	21128	22022	22696	24176	27946	30526	30904	32475	35938	47994
E	19300	19456	21162	22023	23077	24383	28288	30527	31193	32499	35848	48976
F	19301	19569	21262	22024	23120	25329	28336	30528	31194	32649	35980	49443
G	19307	19608	21301	22025	23127	26256	28653	30529	31196	33144	36199	51711
H	19308	19659	21330	22026	23128	26542	29147	30530	31499	33538	37448	Neg

Table 3 – SLC39A14_Plate 2

	1	2	3	4	5	6	7	8	9	10	11	12
A	41284	44689	45441	49308	54996	57191	60252	62694	45528	45548	45560	45574
B	41633	44705	45442	49390	55006	57252	61462	62906	45532	45549	45561	45575
C	43834	44706	45503	49841	55010	58036	61467	63003	45534	45553	45563	45576
D	43836	44743	46131	51428	55034	58622	61864	63450	45537	45554	45567	45577
E	43976	44948	46156	51917	55038	59535	61865	45522	45541	45555	45568	45578
F	44340	44977	46877	53586	56393	59536	61866	45523	45545	45556	45569	45579
G	44603	45190	46973	54078	56568	59584	61994	45524	45546	45557	45572	45580
H	44674	45367	48936	54081	56682	59586	62552	45527	45547	45559	45573	Neg

Table 4 – SLC39A14_Plate 3

	1	2	3	4	5	6	7	8	9	10	11	12
A	A1225	DYT838	HA114	HA146	HA161	HA179	HA196	HA230	HA257	HA287	HA61	MT4106
B	BDM135	DYT848	HA118	HA147	HA164	HA181	HA204	HA235	HA258	HA288	HA83	MT4442
C	BDM260	DYT859	HA137	HA153	HA165	HA182	HA205	HA247	HA259	HA289	HA96	MT4814
D	BDM357	DYT911	HA138	HA155	HA166	HA183	HA209	HA248	HA260	HA291	IND28	MT4866
E	BDM367	H1878	HA139	HA156	HA167	HA185	HA213	HA249	HA261	HA292	MT2900	MT5038
F	DRPLA5	H1879	HA140	HA158	HA168	HA186	HA218	HA250	HA277	HA57	MT3368	MT5073
G	DYT1168	HA112	HA141	HA159	HA170	HA192	HA220	HA252	HA280	HA59	MT3605	PK1582
H	DYT731	HA113	HA142	HA160	HA172	HA193	HA221	HA254	HA283	HA60	MT4032	Neg

3.2.2 Preparation of DNA samples

A part of the DNA samples were already completely prepared for the application of polymerase chain reaction (PCR). The majority of DNA samples needed either concentration measurement, dilution to a concentration of 50 ng/µl or both.

Nanodrop 1000 spectrophotometer was used to measure DNA concentration where necessary. This device is a spectrophotometer which is capable to measure by means of photometry a variety of substances, among them DNA and RNA. The device is connected to a personal computer with a Nanodrop 1000 software program. After the software had been started, 2 µl HPLC water was applied for one to two minutes to clean the fiber optic. Then, 1.6 µl TE buffer was applied to receive a blank value. To assure accuracy controls, samples with DNA of known concentration (53 and 103 ng/µl) were tested. Measurement of DNA concentration with a volume of 1.0 to 1.6 µl followed. The fiber optic was cleaned between samples and particularly when finishing DNA measurements. Aliquots with a concentration of 50 ng/µl were prepared for about half of the DNA samples where aliquots were not already available.

3.2.3 PCR in 96-well plates

To gain sequence data in this mutation screening, polymerase chain reaction (PCR) was an important tool. A PCR needs DNA templates, primers, thermostable polymerase such as Taq DNA polymerase, dNTPs and PCR buffer. In a cyclic reaction, double strand DNA is first separated into single strand DNA at 95 °C (denaturation). Secondly, primers bind to single strand DNA at a lower temperature (annealing). Thirdly, DNA polymerase synthesizes a complementary DNA strand in 5'→3' direction (extension). The repetition of this cycle allows the production of many site-specific DNA copies.

When the experiments with SLC39A14 and WDR45 described in this study were initiated, primers, PCR conditions and PCR protocols for both genes had already been established in the laboratory (see Table 15 in Supplementary materials). Protocols 1 and 2 (see Table 5) were applied for SLC39A14 and protocol 3 (see Table 5) was applied for WDR45. Each protocol specifies how much volume is used per single PCR reaction, that is, per well. Two different PCR conditions were used for SLC39A14, predominantly PCR cycler condition 1 was used (see Table 6). If PCR cycler condition 1 was not successful, PCR cycler condition 2 (see Table

7) was applied. PCR cycler condition 3 was used for WDR45 (see Table 8). PCRs were done in 96-well plates. In the case of SLC39A14, 95 DNA samples and one negative control per plate were used with a different primer pair for each plate. In the case of WDR45, exons were arranged on one plate.

Table 5 – PCR protocols 1, 2 and 3: volumes for single PCR reaction

		SLC39A14		WDR45
PCR component	**Concentration**	**Protocol 1 (volume in µl)**	**Protocol 2 (volume in µl)**	**Protocol 3 (volume in µl)**
HPLC water	-	10,64	10.72	10.72
Q-Solution (5x)	-	4	4	4
PCR buffer (10x)	-	2	2	2
dNTP mixture[2]	Each dNTP 2 pmol/µl	2	2	2
Forward primer	10 pmol/µl	0.8	0.4	0.8
Reverse primer	10 pmol/µl	0.8	0.4	0.8
Taq polymerase	5 U/µl	0.08	0.08	0.08
DNA	50 ng/µl	0.4	0.4 - 0.5	0.5

Table 6 – PCR cycler condition 1: SLC39A14

Step	**Process**	**Temperature**	**Time**
1	Denaturation	95 °C	5 min
2	Denaturation	95 °C	30 s
3	Annealing	65 °C minus 0.5 °C per cycle	30 s
4	Extension	72 °C	1 min (sample repeats: 45 s)
5	Go to Step 2: 21 times		
6	Denaturation	95 °C	30 s
7	Annealing	54 °C	30 s
8	Extension	72 °C	1 min (sample repeats: 45 s)
9	Go to Step 6: 24 times		
10	Extension	72 °C	10 min
11	Cooling Down	20 °C	1 min

[2] dNTPs: equal concentrations of dATP, dCTP, dGTP and dTTP.

Table 7 – PCR cycler condition 2: SLC39A14

Step	Process	Temperature	Time
1	Denaturation	95 °C	5 min
2	Denaturation	95 °C	45 s
3	Annealing	60 °C	45 s
4	Extension	72 °C	1 min
5	Go to Step 2: 35 times		
6	Extension	72 °C	5 min
7	Cooling Down	20 °C	1 min

Table 8 – PCR cycler condition 3: WDR45

Step	Process	Temperature	Time
1	Denaturation	95 °C	5 min
2	Denaturation	95 °C	30 s
3	Annealing	55 °C	30 s
4	Extension	72 °C	1 min
5	Go to Step 2: 39 times		
6	Extension	72 °C	10 min
7	Cooling Down	20 °C	1 min

3.2.4 Agarose gel electrophoresis

To predict if PCRs were successful, agarose gel electrophoresis was applied. A subset of PCRs of each PCR plate was checked, usually eight wells from a 96-well plate including the negative control. The following steps were performed:

First, TBE (10x) buffer had to be prepared. TBE (10x) buffer was made of 102 g Tris(hydroxymethyl)aminomethane, 55 g boric acid and 7.5 g EDTA mixed in 2000 ml deionized water. TBE (10x) buffer was subsequently diluted 1:10 to TBE (1x). Six g agarose were put into 400 ml TBE (1x) buffer and brought to boil in a microwave. Once boiled, 16 µl Serva DNA Stain G was added. The so gained 1.5% liquid agarose gel was put into a gel cassette with a comb for 30 minutes. The solidified gel was put into a gel chamber. Six µl mixtures consisting of 3 µl PCR product and 3 µl Loading Dye (6x or 2x) were prepared. Six µl of either 100 bp or 1 kbp DNA Ladder was used as a marker. Each 6 µl sample was

pipetted into a well and gel electrophoresis was started. 120 V, 400 mA and a time of 20 minutes were chosen as electrophoresis parameters. After 20 minutes the gel was put on a UV transilluminator. A picture was taken and printed. With the bands depicted on the printout, it was possible to predict PCR success.

3.2.5 PCR purification with purification plates

Purification of PCR products is important to selectively retain DNA remote of other PCR components such as primers. This was done after gel electrophoresis showed proper bands. The purification plate has special semi-permeable membranes which allow the selective retention of DNA. Cleaning of PCR products comprised the following four steps. First, PCR products were transferred into a 96-well PCR purification plate. Second, HPLC water was added to receive a total volume of around 100 µl per well. Third, the purification plate was connected to a vacuum filtration system. Forth, with a vacuum pump, a pressure difference of 15 - 20 mmHg was built up. Within eight to ten minutes, water, primers and other lower-molecular components were removed leaving purified DNA in the plate. Fifth, 16 to 20 µl HPLC water was added per well. The DNA was dissolved in the water and then transferred into a new 96-well plate.

3.2.6 Sanger sequencing reaction in 96-well plates

The purified DNA is then used for Sanger sequencing. The Sanger sequencing method, also called chain terminator sequencing, was introduced in 1977 (Sanger et al. 1977). Sanger sequencing is a modified PCR. DNA templates, primers, DNA polymerase enzyme such as Taq DNA polymerase, dNTPs, a low concentration of dye-labeled terminating ddNTPs and a buffer are needed. Normal dNTPs have a free 3'-OH-group whereas ddNTPs do not. The sequencing PCR starts like a normal PCR. Once a ddNTP is incorporated into the newly produced strand, the elongation is halted. The insertion of dNTPs and ddNTPs occurs randomly and is only dependent on the concentration of each NTP. Thus, strands with different size and four different dye-labeled ends are produced.

In the following section, the reaction mixture used for the sequencing reaction is described. A mixture of 0.5 µl Big Dye Terminator, 1.5 µl Big Dye Buffer and 1 µl HPLC water was

prepared. The Big Dye Terminator contains Taq DNA polymerase, dNTPs and ddNTPs. One µl of either forward primer or reverse primer (10 pmol/µl) was added to separate reactions. Then, 1 µl of the purified PCR product was added to each reaction. If agarose gel electrophoresis showed sufficient but less prominent bands, up to 2 µl of the purified PCR product was used. Reaction plates were sealed with thermostable adhesive seals. Reaction plates were centrifuged at about 500 rpm for several seconds. Plates were put into thermal cyclers and the sequencing reaction program (see Table 9) was started.

Table 9 – Sequencing reaction

Step	Process	Temperature	Time
1	Denaturation	96 °C	1 min
2	Denaturation	96 °C	10 s
3	Annealing	50 °C	5 s
4	Extension	60 °C	4 min
5	Go to Step 2: 25 times		
6	Cooling Down	20 °C	1 min

3.2.7 DNA precipitation with 100% ethanol

After the sequencing reaction, DNA needed to be purified again. To do this, ethanol precipitation was applied. Both DNA and water are polar molecules. Ethanol is less polar than water. The addition of ethanol reduces DNA solubility in water and leads to its precipitation. Centrifugation then allows precipitated DNA to form a pellet at the bottom of a well. Ensuing removal of ethanol and resolving in HPLC water increases DNA purity.

25 µl of 100% ethanol were added to each well of a 96-well plate. Plates were put in a place remote of light at room temperature for 60 minutes. After one hour of incubation, plates were centrifuged at 3000 rpm for 30 minutes at 22 °C. Plates were put overhead on tissues and centrifuged at 100 rpm for about 7 seconds in order to remove the ethanol. 125 µl of 70% ethanol were added to each well and plates were centrifuged at 2000 rpm for 15 minutes at 22 °C. Plates were again put overhead on tissues and centrifuged at 600 rpm for 1 minute at 22 °C.

3.2.8 Transfer into barcode plates and sequence analysis

To perform the sequence analysis, it was necessary to dissolve precipitated DNA in water again. 50 µl HPLC water were added to each well. 25 µl of each well were transferred into a 96-well barcode plate. Prepared barcode plates were loaded into the sequencer machine which was ABI 3730 DNA Analyzer. The DNA analyzer electrophoretically separates dye-labeled termination strands in a capillary. Each of the four ddNTPs has a specific dye label which the DNA analyzer is able to recognize with a UV laser. Sequence data is created and transferred to personal computers of appliers.

3.2.9 Evaluation of created sequence data

Sequence data were evaluated with the GeneStudio Contig Editor software. This software aligns sequence data to a given reference sequence. The reference sequences for the different exons of SLC39A14 were obtained from the genome browser (https://www.genome.ucsc.edu) (University of California Santa Cruz 2012). For WDR45, reference sequences were obtained from the genome browser as well (University of California Santa Cruz 2012). With the help of the Contig Editor software, deviations from the reference sequence were identified. In addition to all coding exons, the directly adjacent 10 bp of each intron were examined. Variants were checked with dbSNP (www.ncbi.nlm.nih.gov/SNP) (National Center for Biotechnology Information 2015) and dbIHG (an in-house exome database, Institute of Human Genetics, Helmholtz Zentrum München in Neuherberg, Germany) to determine frequency. Non-synonymous variants were checked with MutationTaster (www.mutationtaster.org) (Schuelke et al. 2015) to predict possible pathogenicity. NM_01128431.2 is the reference sequence accession number that was used for the SLC39A14 gene and NM_007075.3 is the reference sequence accession number used for WDR45 (http://www.ncbi.nlm.nih.gov/refseq) (National Center for Biotechnology Information 2014).

3.2.10 X-inactivation experiments

Males with a normal karyotype have one X chromosome and one Y chromosome in every somatic cell. Females with a normal karyotype have two X chromosomes in every somatic cell. The Y chromosome only contains very few genes. In 1962, Lyon argued that for reasons of dosage compensation between male and female genes, it is necessary that one X chromosome is inactivated in each female cell. She suggested that the X-inactivation occurs randomly and early in development (Lyon 1962). If X-inactivation does not occur randomly but preferably either the paternal or the maternal X chromosome is inactivated, it is called nonrandom or skewed X-inactivation.

X-inactivation experiments were done with DNA samples from four female individuals (63700, 63701, 63702 and 63712) to look for skewed X-inactivation. The four subjects were among the 13 individuals that were identified to have mutations in WDR45 by whole exome sequencing (Haack et al. 2012).

In order to assess X-inactivation, established protocols from the laboratory (see Tables 10 to 12) were used. The experiments for X-inactivation were repeat experiments to confirm data that were obtained by technicians within the research project for WDR45. Allen et al. found out that methylation of the androgen receptor site correlates well with X-inactivation (Allen et al. 1992). The X-inactivation protocols make use of the androgen receptor site on the X chromosome and a methylation-sensitive restriction enzyme HpaII. Allen et al. reported that the first exon of the androgen receptor gene contains a highly polymorphic CAG (cytosine, adenine and guanine) short tandem repeat. There are 20 known alleles with about 90% heterozygosity in this repeat. These alleles differ in their number of CAG repeat units. Consequently, PCR products containing a different number of CAG repeat units differ in size. The size difference can be used in gel electrophoresis as a criterion to distinguish between different alleles (Allen et al. 1992). Two HpaII restriction enzyme sites are within 100 bp distance 5' to the CAG repeat (Allen et al. 1992).

Dilutions with 50 ng/µl of DNA from DNA stocks were prepared. 20 µl mixtures were prepared for each DNA sample according to the protocol shown in Table 10. One mixture was prepared with restriction enzyme HpaII (digestion mixture) and one without (control mixture). Each mixture was incubated at 37 °C for four hours on a thermo shaker, gently shaking on a low level. The enzyme HpaII digests unmethylated DNA, leaving only DNA that is

methylated. Mixtures were incubated at 65 °C for 20 minutes without shaking to inactivate HpaII.

Table 10 – Restriction enzyme protocol

Component	Digestion mixture (volume in µl)	Control mixture (volume in µl)
HPLC H2O	7.5	8
NEBuffer1 (1x)	2	2
DNA (50 ng/µl)	10	10
HpaII (10 Units/µl)	0.5	---

Table 11 – X-inactivation PCR protocol for androgen receptor DNA

PCR component	Concentration	Protocol (volume in µl)
HPLC water	-	8.32
Q-Solution (5x)	-	4
PCR buffer (10x)	-	2
dNTP mixture[3]	each dNTP 2 pmol/µl	2
Forward primer (6-carboxyfluorescein-labeled)	10 pmol/µl	0.8
Reverse primer (non-labeled)	10 pmol/µl	0.8
Taq polymerase	5 U/µl, from Qiagen	0.08
+/- digested DNA	50 ng/µl	2

Table 12 – PCR cycler conditions for androgen receptor DNA

Step	Process	Temperature	Time
1	Denaturation	95 °C	5 min
2	Denaturation	95 °C	30 sec
3	Annealing	58 °C	30 sec
4	Extension	72 °C	1 min
5	Go to Step 2: 35 times		
6	Extension	72 °C	10 min
7	Cooling Down	20 °C	1 min

[3] dNTPs: equal concentrations of dATP, dCTP, dGTP and dTTP.

Agarose gel electrophoresis was applied to clarify, if PCR was successful. Agarose gel electrophoresis was performed in the same way as described in chapter 3.2.4 using 3 µl Loading Dye (2x) and 3 µl PCR product for each well. PCR products were diluted 1: 100 mixing 1 µl PCR product and 99 µl HPLC H2O. 13.5 µl Formamide, 1.5 µl of diluted PCR product and 0.15 µl Liz500 Standard were mixed. Ten µl H2O was added to gain an end volume of 25.15 µl. 25 µl volume of this mixture were required for the DNA analyzer. Mixtures were transferred into a 96-well barcode plate and denatured at 95 °C for three minutes. After denaturation they were put on ice immediately. Rapid cooling down was done to prevent the reannealing of single strands. PCR products were then analyzed with ABI 3730 DNA analyzer. The received data then were evaluated with the GeneMapper software and with Microsoft Excel.

4 Results

4.1 Mutation screening of SLC39A14

Altogether, 251 DNA samples were completely screened and provided sufficient data for each exon. At the beginning of the study, 285 DNA samples were arranged in three plates with 95 DNA samples for each plate. Of these 285 DNA samples 34 dropped out during the study for several reasons. Some did not provide sufficient sequence data for each exon despite repeated tests and some turned out to be mutation-positive for another NBIA subtype while tests were done for SLC39A14.

In the 251 DNA samples several homozygous and heterozygous variants were found in the gene SLC39A14. Most variants were found in exon 2. A part of these variants was synonymous and a part of these was non-synonymous. All variants that were identified are listed in Table 13.

4.1.1 Synonymous variants

Four synonymous variants were identified in the present investigation. The variants {c.[156C>T], p.[Gly52Gly]} and {c.[195A>G], p.[Leu65Leu]} were found both in a heterozygous and homozygous state. The variants {c.[321G>A], p.[Ser107Ser]} and {c.[1041T>C], [p.His347His]} were identified only in a heterozygous state. ‘Synonymous’ means that there is a change in the DNA but no change in the amino acid chain. The minor allele frequency of these synonymous variants was above 1% in this study except for the variant {c.[321G>A hetero], p.[Ser107Ser hetero]}. The latter variant was found only once in the present investigation. The variant {c.[156C>T], p.[Gly52Gly]} was identified to be heterozygous in 22 individuals and homozygous in 11 individuals. The variant {c.[195A>G], p.[Leu65Leu]} was found to be heterozygous in two individuals and homozygous in 52 individuals.

4.1.2 Intronic variants

In addition to all coding exons, 10 bp of each directly adjacent intron were examined. The variants c.[751-4C>A hetero], c.[939+8G>A hetero] and c.[939+8G>C hetero] were detected in introns and were all heterozygous. The variant c.[939+8G>C hetero] was found five times in this study which corresponds to a minor allele frequency of 1%. The variant c.[751-4C>A hetero] was detected two times (frequency of 0.4%) and c.[939+8G>A hetero] was found once in this study.

4.1.3 Non-synonymous variants

Five non-synonymous variants were detected in the gene SLC39A14, two of them were very frequent and three of them were detected only once each. The variants {c.[6_11del6], p.[Lys2_Leu4delinsLys]} and {c.[98T>C], p.[Leu33Pro]} in exon 2 were found frequently in the cohort of this study. The variant {c.[6_11del6], p.[Lys2_Leu4delinsLys]} is an in-frame deletion. This variant results in the deletion of two leucine amino acids in the ZIP14 protein. This variant was found in a homozygous state in 11 individuals and in a heterozygous state in 22 individuals. The minor allele frequency was 8.8% in the present study. The variant {c.[98T>C], p.[Leu33Pro]} was identified to be homozygous in 54 subjects and heterozygous in one subject. The minor allele frequency was 21.7% in the present investigation. The remaining three non-synonymous variants {c.[607C>T hetero], p.[Leu203Phe hetero]}, {c.[838G>A hetero], p.[Gly280Arg hetero]} and {c.[1415G>A hetero], p.[Arg472Gln hetero]} were identified each only once in the present study. These three variants are located in exons 4, 6 and 9b, respectively.

Table 13 – Heterozygous and homozygous variants in SLC39A14

Exon	Variant (RefSeq NM_01128431.2)	Frequency	Total allele frequency	Relative allele frequency
Exon 2	{c.[6_11del6 hetero], p.[Lys2_Leu4delinsLys hetero]} {c.[6_11del6 homo], p.[Lys2_Leu4delinsLys homo]}	22 11	44	8,8%
	{c.[98T>C hetero], p.[Leu33Pro hetero]} {c.[98T>C homo], p.[Leu33Pro homo]}	1 54	109	21,7%
	{c.[156C>T hetero], p.[Gly52Gly hetero]} {c.[156C>T homo], p.[Gly52Gly homo]}	22 11	44	8,8%
	{c.[195A>G hetero], p.[Leu65Leu hetero]} {c.[195A>G homo], p.[Leu65Leu homo]}	2 52	106	21,1%
Exon 3	{c.[321G>A hetero], p.[Ser107Ser hetero]}	1	1	0,2%
Exon 4	{c.[607C>T hetero], p.[Leu203Phe hetero]}	1	1	0,2%
Intron between exon 5 and 6	c.[751-4C>A hetero]	2	2	0,4%
Exon 6	{c.[838G>A hetero], p.[Gly280Arg hetero]}	1	1	0,2%
Intron between exon 6 and 7	c.[939+8G>A hetero]	1	1	0,2%
	c.[939+8G>C hetero]	5	5	1,0%
Exon 7	{c.[1041T>C hetero], [p.His347His hetero]}	31	31	6,2%
Exon 9b	{c.[1415G>A hetero], p.[Arg472Gln hetero]}	1	1	0,2%

Synonymous

non-synonymous

Intron

4.2 Mutation screening of WDR45

In six selected DNA samples, one individual (DNA sample number 49841) was found with an X-linked dominant WDR45 mutation (Haack et al. 2012). The remaining five DNA samples showed no clinically relevant mutations in WDR45.

4.2.1 Description of the identified mutation

The identified mutation in exon 3 of WDR45 was found in one male individual investigated. The mutation is {c.[19dupC, hemizygous], p.[Arg7Profs*64, hemizygous]} (Haack et al. 2012). The cytosine at position c.19 is duplicated. This is near the start triplet ATG in exon 3, which is the first coding exon in WDR45. The duplication can formally also be described as an insertion of a single nucleotide c.[19insC, hemizygous]. The duplication of cytosine 19 leads to a frameshift. This changes the amino acids from the seventh amino acid on. The first six amino acids are unaffected. The seventh amino acid is arginine and is changed to proline. The frameshift moreover leads to a premature stop codon which results in a reduced amino acid length of the transcribed protein. The following figures (Figures 9 to 11) illustrate the change in the DNA and the amino acid sequence.

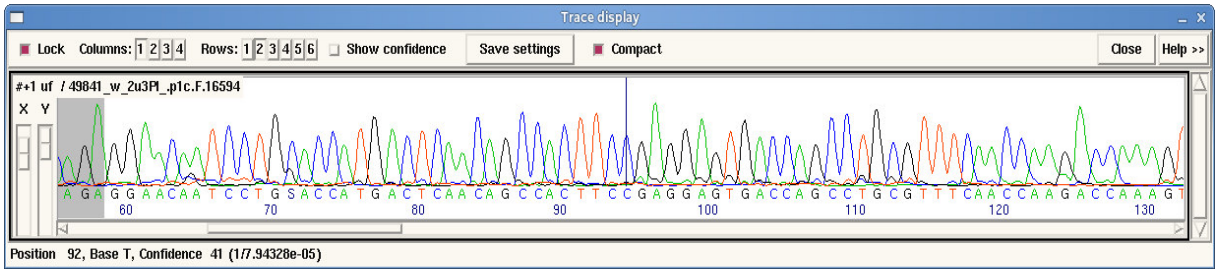

Figure 9 – Sequencing electropherogram demonstrating the WDR45 mutation

The sequencing electropherogram which was generated with Contig editor software shows the hemizygous WDR45 mutation {c.[19dupC], p.[Arg7Profs*64]}. There is a duplication of a cytosine 19 in exon 3.

WT:	Met	Thr	Gln	Gln	Pro	Leu	Arg	Gly	Val	Thr	Ser	Leu	Arg	Phe
WT:	ATG	ACT	CAA	CAG	CCA	CTT	CGA	GGA	GTG	ACC	AGC	CTG	CGT	TTC
mut:	ATG	ACT	CAA	CAG	CCA	CTT	CCG	AGG	AGT	GAC	CAG	CCT	GCG	TTT
mut:	Met	Thr	Gln	Gln	Pro	Leu	***Pro***	***Arg***	***Ser***	***Asp***	***Gln***	***Pro***	***Ala***	Phe
WT:	Asn	Gln	Asp	Gln	Ser	Cys	Phe	Cys	Cys	Ala	Met	Glu	Thr	Gly
WT:	AAC	CAA	GAC	CAA	AGC	TGC	TTT	TGC	TGC	GCC	ATG	GAG	ACA	GGT
mut:	CAA	CCA	AGA	CCA	AAG	CTG	CTT	TTG	CTG	CGC	CAT	GGA	GAC	AGG
mut:	***Gln***	***Pro***	***Arg***	***Pro***	***Lys***	***Leu***	***Leu***	***Leu***	***Leu***	***Arg***	***His***	***Gly***	***Asp***	***Arg***
WT:	Val	Arg	Ile	Tyr	Asn	Val	Glu	Pro	Leu	Met	Glu	Lys	Gly	His
WT:	GTG	CGC	ATC	TAC	AAC	GTG	GAG	CCC	TTG	ATG	GAG	AAG	GGG	CAT
mut:	TGT	GCG	CAT	CTA	CAA	CGT	GGA	GCC	CTT	GAT	GGA	GAA	GGG	GCA
mut:	***Cys***	***Ala***	***His***	***Leu***	***Gln***	***Arg***	***Gly***	***Ala***	Leu	***Asp***	***Gly***	***Glu***	Gly	***Ala***
WT:	Leu	Asp	His	Glu	Gln	Val	Gly	Ser	Met	Gly	Leu	Val	Glu	Met
WT:	CTG	GAC	CAC	GAG	CAG	GTG	GGC	AGC	ATG	GGC	TTG	GTG	GAG	ATG
mut:	TCT	GGA	CCA	CGA	GCA	GGT	GGG	CAG	CAT	GGG	CTT	GGT	GGA	GAT
mut:	***Ser***	***Gly***	***Pro***	***Arg***	***Ala***	***Gly***	Gly	***Gln***	***His***	Gly	Leu	***Gly***	***Gly***	***Asp***
WT:	Leu	His	Arg	Ser	Asn	Leu	Leu	Ala	Leu	Val	Gly	Gly	Gly	Ser
WT:	CTG	CAC	CGC	TCC	AAC	CTT	CTG	GCC	TTG	GTG	GGC	GGT	GGT	AGT
mut:	GCT	GCA	CCG	CTC	CAA	CCT	TCT	GGC	CTT	GGT	GGG	CGG	TGG	TAG
mut:	***Ala***	***Ala***	***Pro***	***Leu***	***Gln***	***Pro***	***Ser***	***Gly***	Leu	***Gly***	Gly	Arg	Trp	*

Figure 10 – Comparison of DNA and amino acids between wild type and mutation

DNA and amino acids of wild type (WT) and mutation (mut) are demonstrated for the hemizygous WDR45 mutation {c.[19dupC], p.[Arg7Profs*64]}. DNA and amino acids are shown until the premature stop codon (indicated by '*') of the WDR45 mutation. Amino acids that changed because of the mutation are marked bold and italic. The mutation site is marked red.

WT: MTQQPLRGVTSLRFNQDQSCFCCAMETGVRIYNVEPLMEKGHLDHEQVGS
mut: MTQQPL***PRSDQPAFQPRPKLLLLRHGDRCAHLQRGALDGEGASGPRAGGQ***

WT: MGLVEMLHRSNLLALVGGGSSPKFSEISAVLIWDDAREGKDSKEKLVLEF
mut: ***HGLGGDAAPLQPSGLGGRW**

WT: TFTKPVLSVRMRHDKIVIVLKNRIYVYSFPDNPRKLFEFDTRDNPKGLCD
mut:

WT: LCPSLEKQLLVFPGHKCGSLQLVDLASTKPGTSSAPFTINAHQSDIACVS
mut:

WT: LNQPGTVVASASQKGTLIRLFDTQSKEKLVELRRGTDPATLYCINFSHDS
mut:

WT: SFLCASSDKGTVHIFALKDTRLNRRSALARVGKVGPMIGQYVDSQWSLAS
mut:

WT: FTVPAESACICAFGRNTSKNVNSVIAICVDGTFHKYVFTPDGNCNREAFD
mut:

WT: VYLDICDDDDF*
mut:

Figure 11 – Comparison of wild type and mutation of the whole protein WDR45
Amino acids of wild type (WT) and mutation (mut) are demonstrated for the hemizygous WDR45 mutation {c.[19dupC], p.[Arg7Profs*64]}. Due to the frameshift the protein resulting from the mutation is truncated. The stop codon is indicated by '*'. Amino acids that changed because of the mutation are marked bold and italic.

4.2.2 Confirmation of mutation

After the detection of the mutation, another DNA sample was obtained from the affected individual to confirm the mutation. DNA was available from the individual's mother and was also investigated. Exon 3 of the mother's DNA did not show the mutation, but was homozygous for the wild type.

4.2.3 Case report of the male individual with the mutation in WDR45

The major facts of the following case report have already been published (Haack et al. 2012; Hayflick et al. 2013). The affected male individual (DNA sample number 49841) was born in 1981. The pregnancy and the delivery were normal. There were no perinatal complications. He was born to nonconsanguineous parents. The individual has one sister. Both the sister and the parents are clinically unaffected. No one of his relatives is reported to be affected. The male individual has shown delayed and impaired psychomotor development from infancy on. He had epileptic seizures until adolescence. He had one grand mal seizure in infancy that led to cardiac arrest with the need of cardiopulmonary resuscitation. He had febrile seizures in childhood as well. The individual never learned to speak. He had severe cognitive deficits already as a child. He had used to eat on his own and to walk alone before deterioration started. Clinical deterioration started relatively suddenly at the age of 28 years. At the beginning of the deterioration he had marked gait abnormalities with small steps and a broad based bent-forward gait. Within 6 months he became wheelchair-bound. In 2012, the individual had prominent generalized dystonia and spastic tetraparesis. Spastic tetraparesis was greater in lower than in upper limbs. He had flexion contractures in both upper and lower limbs. Since clinical deterioration, his scoliosis has worsened as well. Further, he had sleeping difficulties. He had problems to fall asleep and sometimes he made choreiform movements especially at night. The individual did not show Rett-like features. He never received levodopa medication.

An MRI done at the time of deterioration showed hypointensities in T2 in globus pallidus, striatum and substantia nigra. A T1 hyperintense halo could not be identified. The MR images further showed global cerebral atrophy with dilated ventricles. The routine laboratory parameters were normal except for a light elevation of creatine kinase.

4.3 X-inactivation studies in four individuals with WDR45

X-inactivation studies were done with DNA from four female individuals (63700, 63701, 63702 and 63712) with WDR45 mutations as described in chapter 3.2.10 of this thesis. The X chromosome allele specific methylation pattern was rated as random (50:50 to 75:25), skewed (75:25 to 90:10), and extremely skewed (> 90:10) (Haack et al. 2012). Individual 63700 showed a methylation ratio of 67:33 and 63701 had a methylation ratio of 68:32. Thus, both subjects 63700 and 63701 showed a methylation ratio that belongs to the category of random X-inactivation (ratio of 50:50 to 75:25). Individuals 63702 and 63702 both displayed extremely skewed X-inactivation patterns (ratio of > 90:10). Subject 63702 had a methylation ratio of 91:9 and subject 63712 had a methylation ratio of 96:4 (Haack et al. 2012). In Figure 12, the allele specific methylation ratios are illustrated for all four investigated subjects.

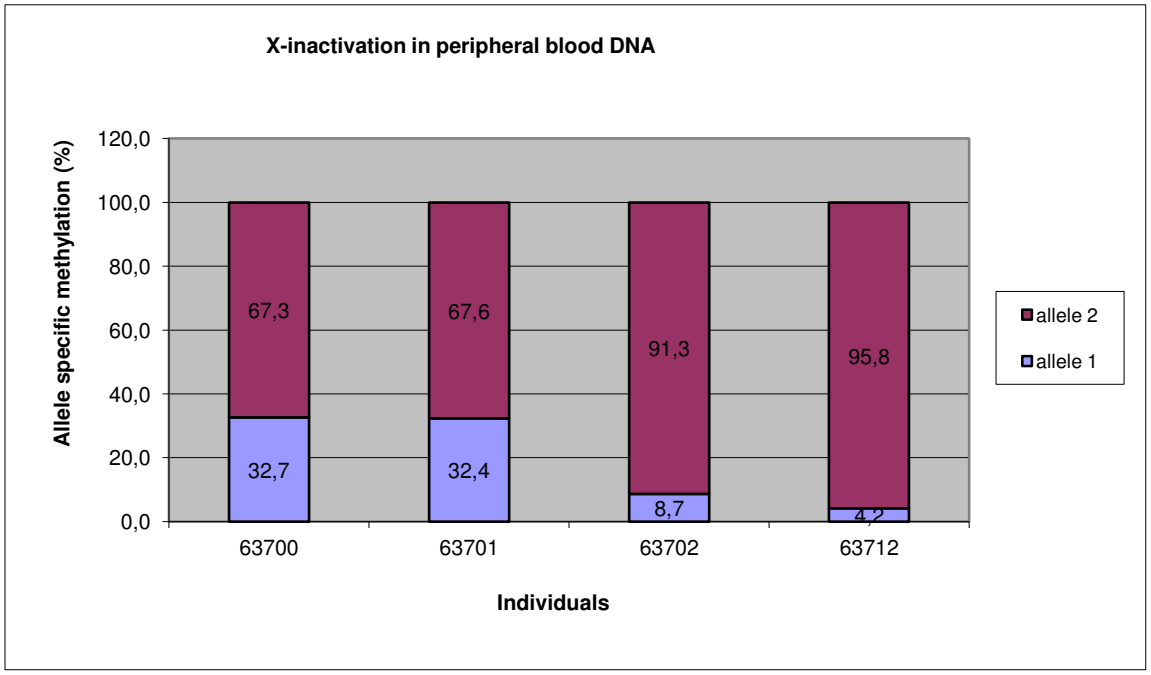

Figure 12 – X-inactivation in peripheral blood DNA

The X axis shows the DNA sample numbers of the four investigated individuals. The Y axis displays the allele specific methylation ratios in percent (%).

5 Discussion

5.1 General aspects of SLC39A14 and WDR45 mutation screening

For the patient group to be screened for SLC39A14 mutations, no detailed clinical dataset was available. Hence, all DNA samples within the large cohort of idiopathic NBIA cases were examined. This approach had the theoretical advantage of being able to measure the frequency of SLC39A14 mutations and of identifying atypical cases with mutations in this gene. In contrast to SLC39A14, detailed clinical data were available for WDR45 prior to this study. Thirteen sporadic index patients formed a distinct clinical subgroup suspected to have SENDA (static encephalopathy of childhood with neurodegeneration in adulthood) (Haack et al. 2012). These thirteen individuals were identified to have WDR45 mutations prior to this study (Haack et al. 2012). Based on clinical information, a screening for WDR45 mutations was done in preselected individuals with idiopathic NBIA. The advantage of this approach was to save time, materials including DNA and costs. However, there are two disadvantages of this approach, which have to be noticed. Firstly, frequency data could not be obtained for WDR45. Secondly, individuals with an atypical phenotype might have been missed.

For both SLC39A14 and WDR45, Sanger sequencing was applied to obtain sequence data. Sanger sequencing has the advantage to be easily available, relatively inexpensive and to provide accurate results with only few sequence errors. However, Sanger sequencing is both time-consuming and material-consuming.

From the view of NBIA research, it would be useful in future to do whole exome sequencing with much more idiopathic NBIA DNA samples. Currently, costs for whole exome sequencing are a limiting factor. When new generation sequencing will become cheaper, it is to be expected that more individuals with idiopathic NBIA will profit from whole exome sequencing.

5.2 SLC39A14

5.2.1 Mutation screening of SLC39A14

Several homozygous and heterozygous variants were found in the gene SLC39A14 in 251 individuals with idiopathic NBIA. The variants in SLC39A14 that were described and explained in chapter 4.1 (results) shall be discussed in the following. Three databases were used to compare the frequency data obtained in this study. The three databases are the Exome Aggregation Consortium (ExAC) database with 60,706 exomes (http://exac.broadinstitute.org) (Exome Aggregation Consortium 2015), dbIHG (an in-house exome database, Institute of Human Genetics, Helmholtz Zentrum München in Neuherberg, Germany) with 5,549 exomes and the SNP database (dbSNP) (http://www.ncbi.nlm.nih.gov/SNP) (National Center for Biotechnology Information 2015). Frequency data of all three databases were obtained on February 23, 2015.

5.2.1.1 Recessive model for SLC39A14

Recessive inheritance would seem to be the most appropriate model for a rare monogenic neurodegenerative disease associated with SLC39A14 mutations for the following reasons. Firstly, the five affected family members of the two index families mentioned in chapter 2 that were identified by collaborating foreign research groups (personal communication[4]) all had homozygous SLC39A14 mutations. Secondly, as will be explained in more detail in chapter 5.2.2, other human diseases associated with SLC39 gene mutations such as SCL39A4 and SLC39A13 demonstrate an autosomal recessive inheritance pattern. Thirdly, the results obtained from the databases dbIHG and ExAC argue for a recessive model for SLC39A14 variants, as well. The in-house exome database dbIHG was searched for both homozygous and heterozygous variants. Except for four very frequent variants in exon 2, which were identified in this study as well (see Table 14), no other homozygous variants were found. In 4762 in-house exomes, 16 heterozygous non-synonymous variants were provided from the database (11 times ‘missense’, three times ‘missense in introns’, one ‘frameshift’ and one ‘splice defect’). That is about one heterozygous variant in 300 exomes. Furthermore, the

[4] Kurian, M.A., Neurosciences Unit, Institute of Child Health, University College London, London, UK, 03/2012.

ExAC database provides data for the amount of loss-of-function variants in SLC39A14 alleles. In about 120,000 alleles, eight heterozygous loss-of-function variants were found (http://exac.broadinstitute.org) (Exome Aggregation Consortium 2015). This is about one loss-of function variant in 15,000 alleles. All this argues for an autosomal recessive model.

Table 14 – Variants in SLC39A14 with allele frequencies in this study and in reference databases

Exon	Variant (RefSeq NM_01128431.2)	Reference number (dbSNP)	Frequency (this study)	Relative allele frequency (this study)	MAF (dbSNP)	MAF (dbIHG)	MAF (ExAC)
Exon 2	c.[6_11del6 hetero]	rs111662782	22	8,8%	31,8%	18,7%	22,1%
	c.[6_11del6 homo]	rs111662782	11				
	c.[98T>C hetero]	rs896378	1	21,7%	37,1%	47,7%	53,1%
	c.[98T>C homo]	rs896378	54				
	c.[156C>T hetero]	rs33999442	22	8,8%	16,5%	18,3%	17,7%
	c.[156C>T homo]	rs33999442	11				
	c.[195A>G hetero]	rs2293144	2	21,1%	32,5%	48,0%	55,3%
	c.[195A>G homo]	rs2293144	52				
Exon 3	c.[321G>A hetero]	rs138114438	1	0,2%	n.a.	0,05%	0,01%
Exon 4	c.[607C>T hetero]	n.a.	1	0,2%	n.a.	n.a.	n.a.
Intron	c.[751-4C>A hetero]	rs140164699	2	0,4%	0,3%	n.a.	0,4%
Exon 6	c.[838G>A hetero]	rs111637707	1	0,2%	0,02%	0,05%	0,02%
	c.[939+8G>A hetero]	n.a.	1	0,2%	n.a.	n.a.	n.a.
Intron	c.[939+8G>C hetero]	rs137890800	5	1,0%	0,7%	1,8%	1,7%
Exon 7	c.[1041T>C hetero]	rs6558052	31	6,2%	28,6%	6,5%	12,9%
Exon 9b	c.[1415G>A hetero]	n.a.	1	0,2%	n.a.	0,02%	n.a.

Synonymous

non-synonymous

Intron

n.a.: not available

5.2.1.2 Synonymous variants

The variants {c.[156C>T hetero], p.[Gly52Gly hetero]}, {c.[156C>T homo], p.[Gly52Gly homo]}, {c.[195A>G hetero], p.[Leu65Leu hetero]}, {c.[195A>G homo], p.[Leu65Leu homo]}, {c.[321G>A hetero], p.[Ser107Ser hetero]} and {c.[1041T>C hetero], [p.His347His hetero]} are synonymous variants in a sense that the DNA is changed compared to the wildtype, although there is no change in the amino acid chain. Synonymous variants, however, have the potential to alter splicing of the transcript or to interfere with regulatory mechanisms which depend on the primary DNA sequence. Such mechanisms have not been investigated in this study.

5.2.1.3 Intronic variants

In the following, intronic and non-synonymous variants in SLC39A14 will be examined with regard to their potential to cause NBIA. This will be done if applicable by referring to their frequency, their hetero- or homozygosity and their potential pathogenicity. Because NBIA is a very rare disease, relatively high frequencies of variants argue against a role in NBIA. A recessive inheritance model as explained in detail in chapter 5.2.1.1 argues against heterozygous SLC39A14 variants to be causing NBIA. In order to assess the potential pathogenicity, the program MutationTaster was used. This is an online software-tool with the aim to predict the pathogenicity of variants (www.mutationtaster.org) (Schuelke et al. 2015; Schwarz et al. 2014).

The variants c.[751-4C>A hetero], c.[939+8G>A hetero] and c.[939+8G>C hetero] were found in intronic regions within 10 bp distance to adjacent coding exons. Intronic variants can potentially lead to an alteration of the amino acid sequence by interfering with splice sites. The three intronic variants have a minor allele frequency of 0.2 to 1% (see Table 14) in this study. In the three abovementioned databases (ExAC, dbSNP and dbIHG), frequency data was not available for c.[939+8G>A hetero] and was between 0.3 and 1.8% for the two other variants.

The three variants were tested with MutationTaster. For c.[939+8G>A hetero] and c.[939+8G>C hetero], the prediction from MutationTaster was ‘polymorphism’. According to MutationTaster, the distance to the next splice site is eight base pairs. This makes an interruption of the splicing process unlikely. For c.[751-4C>A hetero], the prediction was

‘disease causing’. According to MutationTaster, the distance to the next splice site is only four base pairs which is more likely to interfere with the splicing process. However, like the two other intronic variants, the variant c.[751-4C>A hetero] is heterozygous. Neither homozygous nor compound heterozygous intronic variants were identified in the present study. Because of the recessive model of inheritance for SLC39A14 associated with NBIA, none of the three intronic variants qualifies to be disease causing for NBIA.

5.2.1.4 Non-synonymous variants

Five non-synonymous variants were detected in the gene SLC39A14. The two variants {c.[6_11del6], p.[Lys2_Leu4delinsLys]} and {c.[98T>C], p.[Leu33Pro]} were found both in a heterozygous and a homozygous state. Both variants were very frequent in the present study. In c.[6_11del6], there is a deletion of two leucines and in c.[98T>C], a leucine is replaced by proline. In general, a homozygous deletion of two amino acids or a homozygous change in one amino acid can possibly be the cause for a genetic disease. However, in these two cases, both variants have very high allele frequencies in the general population which makes a causative association with NBIA highly unlikely. In dbSNP, the variants c.[6_11del6] and c.[98T>C] have a minor allele frequency of 31.8% and 37.1%, respectively.

The three variants {c.[607C>T hetero], p.[Leu203Phe hetero]}, {c.[838G>A hetero], p.[Gly280Arg hetero]} and {c.[1415G>A hetero], p.[Arg472Gln hetero]} were also non-synonymous. All three variants were found only once in the present investigation and were identified in three different individuals. Both c.[838G>A hetero] and c.[1415G>A hetero] had a minor allele frequency below 0.1% in dbIHG. The variant c.[607C>T hetero] was neither present in dbSNP (www.ncbi.nlm.nih.gov/SNP) (National Center for Biotechnology Information 2015) nor dbIHG nor ExAC. That means, all three variants are quite rare, which is a prerequisite for NBIA. In MutationTaster all three variants were predicted to be “disease causing”. All three variants alter one amino acid. They do not result in a frame shift. MutationTaster allows the comparison of alignments of the DNA and amino acids to other species. There, all three variants demonstrate a high degree of conservation. That means if any of these three variants were homozygous, the suspicion for a causal role in NBIA would be high. However, all three variants were found in a heterozygous state only. As was outlined in chapter 5.2.1.1, important facts argue for a recessive model of SLC39A14 associated with

NBIA. In the present study, all three variants were neither homozygous nor compound heterozygous. In conclusion, all three variants are unlikely to have a pathogenetic role.

5.2.1.5 Allele frequency data in exon 2

The allele frequency data obtained for the four variants in exon 2 differ from frequency data provided in dbSNP (www.ncbi.nlm.nih.gov/SNP) (National Center for Biotechnology Information 2015), ExAC (http://exac.broadinstitute.org) (Exome Aggregation Consortium 2015) and dbIHG. All four variants are less frequent in the present study then in the reference databases. Homozygosity rates and heterozygosity rates do not fit to each other. As presented in Table 14, the variant {c.[98T>C], p.[Leu33Pro]} was found 'heterozygous' only once and 'homozygous' 54 times and {c.[195A>G], p.[Leu65Leu]} was found 'heterozygous' twice and 'homozygous' 52 times. These rates are statistically not reasonable. Exon 2 was the exon where most experimental repeats were necessary to achieve sufficient sequencing data during the practical work of this study. The most likely explanation for the deviations is that one of the two primers for exon 2 did not work sufficiently. Most probably, this resulted in some DNA samples where only one allele was amplified. If in a DNA sample heterozygous for {c.[98T>C], p.[Leu33Pro]} only the allele containing the variant was amplified, then this would falsely result in a 'homozygous' designation of the variant. If, in contrast, in DNA sample heterozygous for {c.[98T>C], p.[Leu33Pro]} only the WT variant was amplified, then the heterozygous state of the gene would be missed. This would explain both the lower frequency rates of variants in exon 2 compared to frequency rates in dbSNP, ExAC and dbIHG and the relatively higher homozygosity rates in exon 2 mentioned above.

Nevertheless, this obvious deviation has no major impact for the purpose of this study. As mentioned above, heterozygous missense variants are quite frequent in the general population. Hence, only homozygous, non-synonymous variants would be candidates to be of clinical relevance for NBIA. But only heterozygous variants could have been missed by the problem described above.

5.2.1.6 Conclusions for variants in SLC39A14

In conclusion, clinically relevant SLC39A14 variants were not found in the investigated cohort. This argues against SLC39A14 as an NBIA candidate gene. Nevertheless, the absence

of pathogenic mutations cannot finally answer the question whether SLC39A14 is a gene associated with NBIA. Mutations in SLC39A14 could still – based on this information – be associated with NBIA. Moreover, the cohort of individuals with idiopathic NBIA might have been too narrow to find individuals with SLC39A14 mutations. Perhaps, SLC39A14 mutations will be found in other neurodegenerative genetic diseases. More research is needed to elucidate this issue.

In fact, after these investigations had been done, collaborating researchers within the joint gene identification project but outside this work discovered that SLC39A14 mutations cause a neurodegenerative disease by the accumulation of manganese in the brain. In addition to the two families with homozygous SLC39A14 mutations mentioned above, they identified three further families with homozygous SLC39A14 mutations. The still unpublished data show clear evidence for the causal association of SLC39A14 mutations and manganese accumulation in the brain (personal communication[5]).

5.2.2 ZIP transporters and human diseases

Until today, mutations in SLC39 genes are known to be associated with two genetic disorders in humans (Jeong and Eide 2013). Loss of function mutations in SLC39A4 were identified in patients affected with acrodermatitis enteropathica (AE) (Wang et al. 2002; Küry et al. 2002). Furthermore, mutations in SLC39A13 were found in individuals suffering from a subtype of Ehlers-Danlos syndrome (Giunta et al. 2008; Fukada et al. 2008).

5.2.2.1 SLC39A4 and acrodermatitis enteropathica

In 2002, Wang et al. discovered mutations in the gene SLC39A4 in acrodermatitis enteropathica (AE) patients (Wang et al. 2002). Acrodermatitis enteropathica is an inherited disease associated with mutations in the gene SLC39A4. SLC39A4 is located on chromosome 8q24.3. SLC39A4 encodes the protein ZIP4 and belongs to the family of ZIP transporters. It belongs to the LIV-1 subfamily of ZIP transporters, the same subfamily that ZIP14 belongs to as well. Acrodermatitis enteropathica is inherited in an autosomal recessive fashion (Wang et

[5] Tuschl, K., Genetics and Genomic Medicine, Institute of Child Health, University College London, London, UK, 07/2015.

al. 2002). Küry et al. also discovered mutations in SLC39A4 in individuals with AE in 2002 (Küry et al. 2002). Acrodermatitis enteropathica has a prevalence of about 1:500,000 (Jung et al. 2011).

Danbolt and Closs first systematically described signs and symptoms of acrodermatitis enteropathica. Patients with AE usually present in infancy. Individuals that were breast-fed typically develop symptoms shortly after weaning. Frequent symptoms are periacral dermatitis, nail dystrophy, alopecia and diarrhea. Without appropriate treatment, AE manifests as a chronic disease with frequent exacerbations (Danbolt and Closs 1942). Moynahan and Barnes noticed that the symptoms of acrodermatitis enteropathica are due to a zinc deficiency. They demonstrated that the restoration of systemic zinc levels correlated with a rapid and complete relief of the symptoms of the disease (Moynahan and Barnes 1973; Moynahan 1974).

The example of acrodermatitis enteropathica demonstrates the clinical impact that pathogenic mutations of metal transporters such as SLC39A4 can have.

5.2.2.2 SLC39A13 and the spondylocheiro dysplastic form of the Ehlers-Danlos syndrome (SCD-EDS)

In 2008, Giunta et al. identified homozygous 9 base pair in-frame deletions in the gene SLC39A13 in six affected individuals of two consanguineous families. The gene SCL39A13 encodes for ZIP13 and is located on chromosome 11p (Giunta et al. 2008). According to Giunta et al., individuals with the abovementioned pathogenic mutations in SLC39A13 show Ehlers-Danlos syndrome-like features like thin, hyperelastic and bruisable skin, hypermobile small joints, contractures, atrophy of hand muscles, hands with finely wrinkled palms and protruding eyes with bluish sclerae. Affected individuals further show a skeletal dysplasia that includes platyspondyly (flattened vertebral bodies) with moderate short stature, osteopenic bones and widened metaphyses. The generalized skeletal dysplasia that involves mainly the spine (spondylo) and the hands (cheiro) in addition to the EDS-like features, gave rise to the subtype name ‘spondylocheiro dysplastic form of the Ehlers-Danlos syndrome’ (SCD-EDS) (Giunta et al. 2008).

It is worthwhile to have a closer look at a possible pathomechanism of the ZIP13 defect in SCD-EDS. As Giunta et al. pointed out, it is not a generalized zinc deficiency that causes the

signs and symptoms of SCD-EDS but most likely a local subcellular disturbance in proper zinc concentration (Giunta et al. 2008). Giunta et al. provided some evidence why ZIP13 may be located at the endoplasmic reticulum (ER) membrane (Giunta et al. 2008). Bin et al. also argued for an intracellular location of ZIP13 and suggested that ZIP13 is located at the Golgi apparatus (Bin et al. 2011). Giunta et al. pointed towards two studies by Puistola et al. and Tuderman et al. that investigated the effect of zinc on lysyl hydroxylase (Puistola et al. 1980) and on prolyl hydroxylase (Tuderman et al. 1977; Giunta et al. 2008). Lysyl hydroxylase and prolyl hydroxylase hydroxylate lysine residues and prolyl residues, respectively and are thus important for collagen (Turpeenniemi-Hujanen and Myllylä 1984). Puistola et al. demonstrated that zinc is a competitive inhibitor for lysyl hydroxylase with respect to ferrous iron (Fe^{2+}) (Puistola et al. 1980), whereas Tuderman et al. provided evidence that zinc is a competitive inhibitor for prolyl hydroxylase with respect to ferrous iron (Fe^{2+}) (Tuderman et al. 1977). The genetic defect in SLC39A13 is an example of how a zinc transporter can have a major systemic impact on certain tissues by disturbing subcellular metal ion concentrations.

5.2.3 ZIP transporters and knockout mice

In the group of SLC39 transporters, various knockout animals (KO) were generated in the past years (Fukada et al. 2008; Hojyo et al. 2011; Gálvez-Peralta et al. 2012). Because all 14 SLC39 genes in mouse and human are highly conserved (Girijashanker et al. 2008), it is likely, that the knockout of such genes has a major impact on mammals. It is worthwhile to have a closer look at the knockout of SLC39A13, SLC39A8 and in particular of SLC39A14 in the mouse.

5.2.3.1 SLC39A13 knockout mouse

Mutations in human SLC39A13 are associated with the spondylocheiro dysplastic form of Ehlers-Danlos syndrome (SCD-EDS) as described above (Giunta et al. 2008). Fukada et al. developed a mouse model with a homozygous knockout of SLC39A13. Signs and symptoms of SLC39A13-KO mice include growth retardation, kyphosis, osteopenia, generalized skeletal dysplasia and reduced skin tension. The histopathology of skin and cornea showed reduced dermal and corneal collagen. The KO mice display a syndrome that resembles SCD-EDS (Fukada et al. 2008). Hence, SLC39A13-KO mice are an excellent animal model to study the

pathomechanism of SCD-EDS. Moreover, it illustrates the high degree of conservation of protein function at the phenotype level.

5.2.3.2 SLC39A8 knockout mouse

Gálvez-Peralta et al. generated a SLC39A8 knockout mouse model by inserting a neomycin-coding sequence. The so-developed SLC39A8 (neo/neo) mice showed significantly decreased ZIP8 mRNA levels and marked phenotypic consequences. Homozygous SLC39A8-KO mice displayed marked neonatal lethality and died between gestational day 18.5 and 48 h postpartum. Growth and normal organ development were hampered. The mice showed malformed craniums, underdeveloped eyes and hypoplastic limbs. Internal organs were smaller than controls with a nearly absent spleen and hypoplasia of kidneys, liver and lungs. The KO mice showed severe anemia with low hemoglobin, low hematocrit and low serum iron (Gálvez-Peralta et al. 2012). According to Gálvez-Peralta et al., ZIP8 appears to be an essential protein for embryo development of mice. Homozygous SLC39A8-KO mice are grossly malformed and are not viable postpartum (Gálvez-Peralta et al. 2012).

In the SLC39 gene family, SLC39A8 and SLC39A14 are most closely related (Girijashanker et al. 2008). The corresponding proteins, ZIP8 and ZIP14, share identical amino acids in about 50% of positions (Jenkitkasemwong et al. 2012). Within the LIV-1 subfamily of ZIP proteins, that is marked by a unique amino acid motive HEXPHEXGD, ZIP8 and ZIP14 set themselves apart by a unique EEXPHEXGD sequence (Begum et al. 2002; Taylor et al. 2005).

5.2.3.3 SLC39A14 knockout mouse

Among the various animal knockout models within the SLC39 gene group, the knockout of SLC39A14 in mice is the most interesting one for the present investigation. Hojyo et al. generated knock out mice that lack the SLC39A14 gene. They constructed a vector that eliminated exons 5 to 8 in the SLC39A14 gene. Homozygous knock out mice were then studied for morphological and biochemical abnormalities. They observed several features that indicate that SLC39A14 participates in the regulation of systemic growth in mice. Knock out mice displayed growth retardation, dwarfism, scoliosis, torticollis and osteopenia. They noticed that pituitary zinc and pituitary cAMP were lower than in control mice. Furthermore,

lower serum IGF-1 levels than in controls and impaired growth hormone (GH) production were identified (Hojyo et al. 2011). Hojyo et al. suggested that SLC39A14 influences the signaling mediated by pituitary growth hormone releasing hormone receptor (GHRHR) by maintaining cAMP levels (Hojyo et al. 2011). GHRHR belongs to the group of G-protein coupled receptors (GPCR) (Mayo 1992).

Hojyo et al. further studied zinc and iron levels in the liver of knock out mice. They noticed lower zinc levels than in controls but normal iron levels in the liver. SLC39A14 knock out mice also showed reduced ability to maintain plasma glucose level during fasting which might be explained by impaired gluconeogenesis in the liver (Hojyo et al. 2011). Hojyo et al. did not describe neurological symptoms in the knock out mice (Hojyo et al. 2011). The absence of neurologic symptoms makes the association of NBIA and SLC39A14 gene mutations in the human less likely.

Interestingly, the SLC39A13 knock out mouse, discussed in chapter 5.2.3.1, and the corresponding mutations in SLC39A13 in humans, discussed in chapter 5.2.2.2 correlate very well with each other (Fukada et al. 2008). Although the SLC39A14 knock out mouse model does not support the idea of an association of NBIA and SLC3914, it does not exclude the possibility of such an association, as results in animals cannot always be transferred to humans.

One example in NBIA research, where mouse models cannot be easily transferred to humans, is PKAN. In order to understand PKAN better, Kuo et al. developed a pantothenate kinase 2 knock out mouse model. This animal model did not represent the disease in humans. Except for retinal degeneration, PANK2 knock out mice were neurologically asymptomatic and showed no brain iron accumulation. PANK2 knock out mice showed growth retardation, although they had no difficulties with food access or eating behavior (Kuo et al. 2005). Later, Garcia et al. developed double knock out mouse models where two pantothenate kinase isoforms were removed simultaneously. These animal models died early but did not represent PKAN of humans, either (Garcia et al. 2012).

In conclusion, the knock out mouse model for SLC39A14 does not support an association of SLC39A14 mutations and a neurodegenerative human disease. SLC39A14 mutations were not identified in individuals with idiopathic NBIA in this work. However, further investigations done by collaborating researchers within the NBIA gene identification project

revealed a causal association of a progressively neurodegenerative disease and homozygous human SLC39A14 mutations. In contrast to NBIA, not iron, but manganese was identified to be accumulated in the brain of affected individuals (personal communication[6]).

5.2.4 SLC30A10 and hypermanganesemia

Recently, Quadri et al. and Tuschl et al. simultaneously identified mutations in SLC30A10 in individuals with hypermanganesemia but without environmental manganese overexposure. They both investigated consanguineous families with homozygosity mapping. SLC30A10 is a metal ion transporter that was previously presumed to be a zinc transporter (Quadri et al. 2012; Tuschl et al. 2012). As its name indicates, SLC30A10 belongs to the superfamily of solute carriers (SLC).

Tuschl et al. used manganese-sensitive yeasts to study the effects of mutations in SLC30A10. They provided evidence that the protein encoded by SLC30A10 is a potent manganese transporter (Tuschl et al. 2012). According to Quadri et al., affected human individuals with mutations in SLC30A10 show juvenile-onset dystonia, adult-onset parkinsonism, chronic liver disease, polycythemia and laboratory evidence of hypermanganesemia. It is thus a disorder with neurologic, hepatic and hematologic disturbances (Quadri et al. 2012). However, the phenotypical spectrum of this disease is wide, particularly with regard to neurologic and liver dysfunction (Stamelou et al. 2012; Quadri et al. 2012; Tuschl et al. 2012). Manganese whole blood levels are highly elevated in patients with SLC30A10 mutations (Tuschl et al. 2012).

In NBIA, MRI changes are best seen on T2-weighted images or even T2* (gradient-echo) weighted images, as iron appears hypointense on T2 (Mutoh et al. 1988; McNeill et al. 2008a; Kruer et al. 2012). In contrast, according to Tuschl et al., in individuals with SLC30A10 mutations, manganese accumulation is best seen on T1-weighted images. T2-weigthed images may show changes, but are often reported as normal (Tuschl et al. 2012). Quadri et al. and Tuschl et al. both report about hyperintensities in the globus pallidus, putamen, caudate nucleus and various other brain areas on T1-weighted MRI (Quadri et al. 2012; Tuschl et al.

[6] Tuschl, K., Genetics and Genomic Medicine, Institute of Child Health, University College London, London, UK, 07/2015.

2012). Chelation therapy may provide marked clinical benefit (Quadri et al. 2012; Tuschl et al. 2012). Tuschl et al. reported about one individual who received chelation therapy where long-term follow-up data were available. The individual showed significant improvement of neurologic symptoms. Furthermore, polycythemia resolved and liver manganese content normalized without further progression of liver cirrhosis (Tuschl et al. 2012).

In contrast to neurodegeneration with brain iron accumulation, not iron but manganese is accumulated in the brain (Quadri et al. 2012; Tuschl et al. 2012). In both NBIA and the presented disease with hypermanganesemia, case reports are available that show some benefit from chelating therapy. However, improvements seem to be more promising in individuals with SCL30A10 mutations (Quadri et al. 2012; Tuschl et al. 2012; Kwiatkowski et al. 2012; Cossu et al. 2014). In the literature there is no common name for the new disease of manganese accumulation so far. Stamelou et al. entitle it 'dystonia with brain manganese accumulation' (Stamelou et al. 2012).

In conclusion, there are interesting parallels between NBIA and the presented disease of hypermanganesemia associated with mutations in SLC30A10. Taking into account the similarities between the described disease and NBIA, the disorder might also be named NBMA: Neurodegeneration with Brain Manganese Accumulation.

5.2.5 ZIP transporters and prion diseases

The 14 SLC39 genes code for ZIP transporters ZIP1 - ZIP14 (Grotz et al. 1998; Taylor 2000; Girijashanker et al. 2008). In the following, possible connections between ZIP transporters and prion diseases will be discussed.

5.2.5.1 Prion diseases

Prion diseases are a unique group of neurodegenerative diseases that are associated with infectious prions (Prusiner 1982). Griffith introduced the idea of self-replication of prions (Griffith 1967). Due to its unconventional characteristics, Prusiner suggested a new term for the infectious agent that was formerly called scrapie agent. He proposed the term 'prion' because of its *pro*teinaceous and *in*fectious properties (Prusiner 1982). The normal cellular prion protein (PrP^{C}) and the infective scrapie prion protein (PrP^{Sc}) are derived from the same

gene (Basler et al. 1986). The scrapie prion protein is generated post-translationally from normal cellular prion protein (Caughey and Raymond 1991; Kocisko et al. 1994). Interestingly, transgenic mice without neuronal PrP^{C} expression are resistant to prion disease infection with PrP^{Sc} (Mallucci et al. 2003).

In their review, Head and Ironside provide a list of human prion diseases. The human prion diseases comprise Creutzfeldt-Jakob disease (CJD), Gerstmann-Sträussler-Scheinker disease, Kuru, fatal familial and sporadic fatal insomnia, prion protein cerebral amyloid angiopathy and variably protease-sensitive prionopathy. The Creutzfeldt-Jakob disease can be subdivided into familial CJD, sporadic CJD, iatrogenic CJD and variant CJD (Head and Ironside 2012). After the epidemic of bovine spongiform encephalopathy (BSE) in cattle, surveillance systems were initiated in several European countries (Will et al. 1996). In 1996, Will et al. noted a sudden increase in the prevalence of Creutzfeldt-Jakob disease in the United Kingdom. Individuals affected presented in an atypical fashion. Individuals were younger than usual. This new form of CJD was called new variant CJD (Will et al. 1996).

5.2.5.2 Sequence similarities between ZIP transporters and prions

Schmitt-Ulms et al. noted similarities between the prion protein on the one hand and representatives of the ZIP family of metal ion transporters on the other hand. They first generated quantitative interactome data of the prion protein. This revealed the spatial proximity of murine prion protein to metal ion transporters of the ZIP family. Subsequent analysis demonstrated the presence of a prion protein-like amino acid sequence within the extracellular, N-terminal domain of specific ZIP transporters. In particular, ZIP5, ZIP6 and ZIP10 showed partial amino acid sequence homology with the prion protein (see Figure 13). This may suggest a common evolutionary descent of the ZIP genes and the prion genes (Schmitt-Ulms et al. 2009).

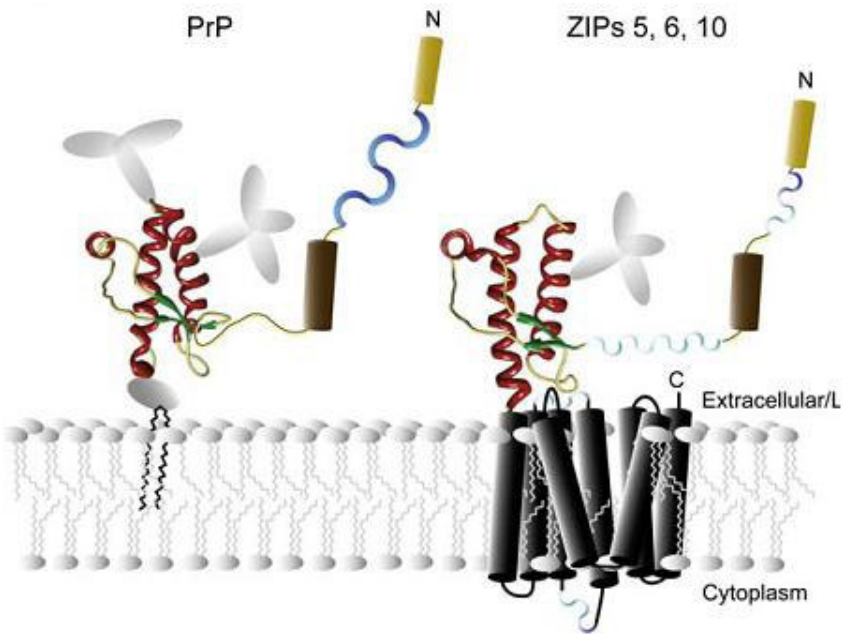

Figure 13 – Comparison of the prion protein and the ZIP transporters 5, 6 and 10

Similarities of the prion protein and the ZIP transporters 5, 6 and 10 are graphically demonstrated. Similar domains are displayed with the same color. The amino terminus is marked with N. The carboxy terminus is marked with C (Ehsani et al. 2011, p. 407). With kind permission from Progress in Neurobiology, Elsevier.

Interestingly, the ZIP gene family is widely distributed among diverse kingdoms of life including plants, animals and prokaryotes whereas sequences related to the prion protein can be found only in the chordate lineage (Schmitt-Ulms et al. 2009). Schmitt-Ulms et al. proposed a common ancestor for today's ZIP and prion genes. More precisely, they suggested that prion genes are a divergent branch from ancient ZIP genes. They compared orthologous sequences of the prion protein and ZIP10 across various species of the chordate lineage. They investigated sequence identities with regard to the prion protein and ZIP10 in close and distant members of the chordate lineage. They demonstrated relatively high sequence identity percentages between prion protein and ZIP10 in fish and relatively low sequence identity percentages in mammals. They displayed intermediate sequence identity percentages in turtle, frog and chicken, organisms which lie evolutionary between fish and mammals. They thus argued for a common evolutionary origin of the prion protein and ZIP10 (Schmitt-Ulms et al. 2009). More precisely, Ehsani et al. suggested, that 500 million years ago, a spliced transcript encoding for a prion protein-like ZIP ectodomain may have been inserted back into the genome of a vertebrate ancestor. Thus, a prion founder gene could have been created (Ehsani et al. 2012b).

Interestingly, ZIP5, ZIP6 and ZIP10 are members of the same ZIP family subgroup like ZIP14 which is the LIV-1 subfamily (Taylor 2000; Jenkitkasemwong et al. 2012). This subfamily has the sequence motive ((H/E)EXPHEXGD) in common (Taylor 2000; Taylor et al. 2005). This motif is similar to a zinc-binding motif known from zinc metalloproteases (HEXXH) (Jongeneel et al. 1989; Taylor 2000).

5.2.5.3 Prions and metals

In the last decades a lot of research has been done on the prion protein. In the light of the likely common evolutionary origin of prion protein and ZIP transporters mentioned above, it is worthwhile to note a growing literature linking the prion protein to various trace metals. In 1997, Brown et al. demonstrated that cellular prion protein (PrP^C) binds copper *in vivo* (Brown et al. 1997). It has been established, that not only copper, but also zinc may interact with the prion protein (Perera and Hooper 2001). Both copper (Pauly and Harris 1998; Perera and Hooper 2001) and zinc (Perera and Hooper 2001) were shown to induce prion protein endocytosis *in vitro*.

Watt et al. suggest in their review, that prion protein is as a zinc sensor that does not transport zinc itself, but may induce the transportation of zinc by other proteins. They suggest that the octarepeat region of the prion protein acts as zinc sensing element. They propose that the prion protein interacts with glutamatergic AMPA receptors and promotes for zinc influx by that receptor (Watt et al. 2013).

Iron plays an important role with the prion protein as well. Singh et al. provide evidence that the prion protein functions as ferrireductase and is important for maintaining systemic iron levels in mice (Singh et al. 2013). Prion protein knockout mice (PrP-/-) develop systemic iron deficiency. This is demonstrated by relatively poor iron staining on bone marrow preparations. The iron deficiency can be overcome by chronic feeding with excess dietary iron. However, if PrP-/- mice are fed on normal diet again, they redevelop systemic iron deficiency (Singh et al. 2013).

The presumed evolutionary proximity of prion protein and the LIV-1 subfamily of ZIP transporters which includes ZIP14 may provide new insights into ZIP14. It may well be possible to adapt concepts and mechanisms observed in the context of prion protein to ZIP14 or other ZIP transporters.

There is much more research literature about the prion protein than about ZIP14 today. According to Ehsani et al. it is one of the most intensively studied proteins in biology (Ehsani et al. 2012a). However, the physiologic function of the prion protein is also still ambiguous (Singh et al. 2009) and information about ZIP14 and other LIV-1 ZIP transporters may possibly provide a better understanding of the prion protein and prion diseases. Ehsani et al. further provided evidence, that there is not only a common evolutionary origin from prion protein and ZIP transporters but also some functional similarities between both. They described, how the starvation of cells of manganese or zinc, but not copper, is followed by protein shedding of fragments of the cellular prion protein and of the ectodomain of ZIP10 (Ehsani et al. 2012b).

5.3 WDR45

5.3.1 Mutation screening of WDR45

In the following, the mutation {c.[19dupC, hemizygous], p.[Arg7Profs*64, hemizygous]}, that was detected in the DNA of a male individual (see chapter 4.2) (Haack et al. 2012), will be discussed. The gene WDR45 (WIPI-4), in which the mutation was found, is located on the X chromosome. A karyotype was obtained from blood of the affected individual to look for possible aneuploidy or X chromosome abnormalities. The karyotype analysis was done by staff in the Institute of Human Genetics in Munich[7]. The karyotype turned out to be normal (46, XY). The male individual is thus hemizygous for the mutation.

The mentioned WDR45 mutation leads to a frameshift with a premature stop codon. The seventh amino acid which is arginine in wild type is exchanged for proline which results in a subsequent frameshift. The premature stop codon leads to a markedly reduced amino acid length of the protein. The resulting protein has 69 amino acids compared to 361 amino acids in the wild type protein. This is only about 19% of the wild type amino acid length. Consequently, the mutation renders a complete loss of function. The transcribed protein is truncated. It most likely will be either degraded by intracellular clearance systems or accumulate within the cell.

In six selected DNA samples, the abovementioned male individual was found with an X-linked dominant WDR45 mutation. His asymptomatic mother had wild type alleles in both her X chromosomes. Hence, the male affected subject has a de novo mutation. The genetic and clinical information which was gained by the identified mutation contributed to define the disease characteristics of BPAN. A case report of the clinical information is provided in chapter 4.2.3. The remaining five DNA samples did not show WDR45 mutations. Conclusions about frequency data on WDR45 cannot be drawn from the present study.

[7] Institute of Human Genetics, Technische Universität München, Trogerstraße, Munich, Germany.

5.3.2 Beta-propeller protein-associated neurodegeneration (BPAN)

In 2012, Haack et al. reported about beta-propeller protein-associated neurodegeneration as a new type of NBIA. It is an X-linked dominant neurodegenerative disease associated with mutations in the gene WDR45. The gene is located at Xp11.23 (Haack et al. 2012). Individuals with BPAN show markedly uniform disease characteristics (Haack et al. 2012; Hayflick et al. 2013).

Hayflick et al. analyzed and compared phenotype data of 23 individuals with BPAN (Hayflick et al. 2013). The male individual 49841, who was identified to have a deleterious mutation in WDR45 in the present study (see case report in chapter 4.2.3) was part of the cohort of 23 subjects with BPAN. There are much more female individuals than male individuals affected with BPAN. Out of the cohort of 23 individuals, there were 20 women and three men. The mean age at time of deterioration was 25.3 years and ranged from 15 to 37 years (Hayflick et al. 2013). The male subject 49841 displayed deterioration at 28 years of age. All 23 individuals with BPAN showed developmental delay and cognitive deficits in childhood. Most children were reported to have severe speech deficits and displayed gait abnormalities. Six children had spasticity in childhood. Particular characteristic of the disease is a major worsening of neurologic symptoms in the adolescence or early adulthood. With deterioration of the disease, dystonia and parkinsonian symptoms manifest or become more prominent (Hayflick et al. 2013). Out of the abovementioned cohort, 23/23 developed dystonia and 21/23 developed parkinsonism in the course of the disease, including the subject 49841. Bradykinesia and rigidity were the predominant clinical features, whereas tremor was only seen in 2/23 subjects. With 11/11 individuals who received levodopa, marked clinical improvement was noted. However, the beneficial effects of levodopa were only of short duration. About half of all individuals had seizures in childhood, including the individual 49841 (Hayflick et al. 2013). Multiple seizure types were reported, sometimes also different seizure types in one affected subject. Rett-like features were seen in 7/23 persons. Diverse eye abnormalities such as myopia, pupillary defects and retinal abnormalities were reported. Visually evoked potentials showed increased latency in the individual 49841. A minority of 6/23 individuals, including the subject 49841, had sleeping abnormalities (Hayflick et al. 2013).

In 22/23 individuals, MR images were available. T2-weighted MR images showed hypointensities of the substantia nigra and the globus pallidus. The hypointensities were more

prominent in the substantia nigra than in the globus pallidus. In 20/22 subjects, brain MR images displayed a distinctive halo of hyperintensity surrounding hypointense substantia nigra. This radiologic particularity was not seen in the MR images of the male individual 49841. The two other men of the cohort demonstrated this feature, though (Hayflick et al. 2013). Figure 14 demonstrates typical MR imaging features in BPAN.

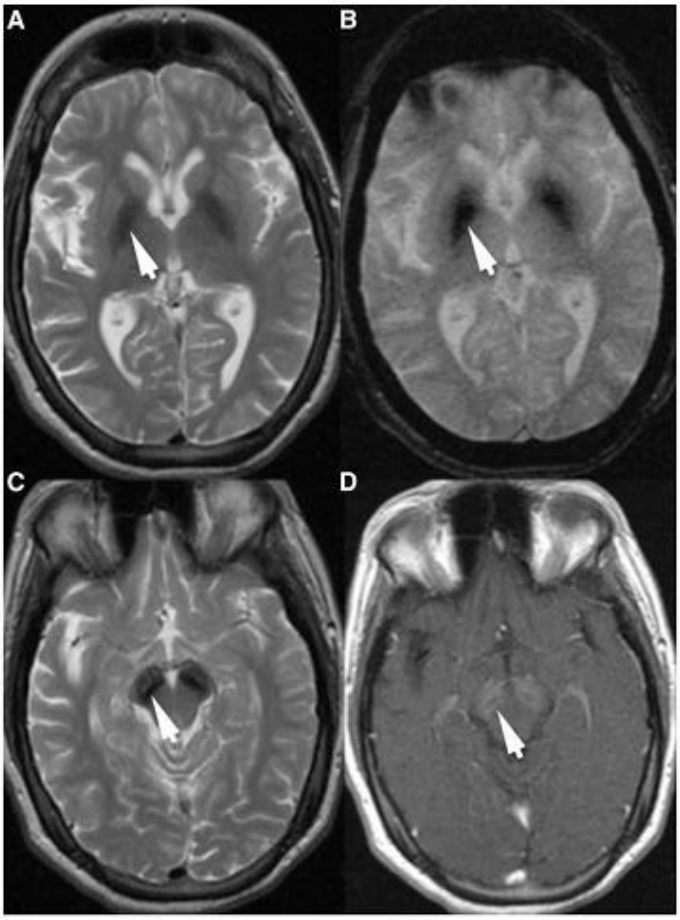

Figure 14 – Axial MR imaging of an individual with BPAN

Different MRI sequences are shown which demonstrate typical MRI characteristics in BPAN. (A, arrow) indicates a hypointensity in the globus pallidus on T2-weighted TSE (turbo-spin-echo) sequence which is seen more clearly on FLAIR (fluid-attenuated inversion-recovery) sequence (B, arrow). (C, arrow) indicates a hypointensity in the substantia nigra on T2-weighted TSE. (D, arrow) shows a hyperintense halo in the substantia nigra on T1-weighted imaging (Haack et al. 2012, p. 1145). With kind permission from American Journal of Human Genetics, Elsevier.

MPAN and PLAN, which are among the three most common subtypes of NBIA, have been reported to develop Lewy bodies and Tau accumulations in the brain (Hartig et al. 2011; Paisán-Ruiz et al. 2012). In BPAN, neuropathological investigations performed by Hayflick et

al., did not elucidate Lewy bodies. However, tau-positive neurofibrillary tangles in the hypothalamus and the hippocampus were identified (Hayflick et al. 2013).

5.3.3 WDR45 and autophagy

In her review, Tanida differentiates between macroautophagy, microautophagy and chaperone-mediated autophagy. Macroautophagy is a process of intracellular sequestration of proteins, lipids and organelles. The sequestration involves the formation of autophagosomes, the intake of intracellular content into the autophagosome and thereafter the fusion with lysosomes by which autolysosomes are formed. Macroautophagy is unique in that vesicles with double-layer lipid membranes, so-called autophagosomes, are formed. Microautophagy is the sequestering of proteins, lipids and organelles by lysosomes themselves without autophagosome formation. In contrast to both macroautophagy and microautophagy, chaperone-mediated autophagy comprises the degradation of proteins only (Tanida 2011). In her review, Tanida summarizes that autophagy has been associated with various pathologies, among them tumor development, diabetes mellitus, infectious diseases and neurodegenerative diseases such as Parkinson's disease, Alzheimer's disease and Creutzfeldt-Jakob disease (Tanida 2011).

The human WIPI WD40 repeat family has been shown to be involved in autophagy processes (Proikas-Cezanne et al. 2004). Autophagy regulation has been intensely investigated in the yeast Saccharomyces cerevisiae (Barth et al. 2001; Guan et al. 2001) ATG18 is the WIPI-1 homologue in S. cerevisiae and has been shown to be an important protein in autophagy (Barth et al. 2001; Guan et al. 2001; Proikas-Cezanne et al. 2004). There is growing evidence for the involvement of WDR45 (WIPI-4) in autophagy regulation as well since WDR45 interacts with ATG2A and ATG2B which are two other important autophagy proteins (Behrends et al. 2010). WIPI-1 binds phosphatidylinositol-3-phosphat, a phospholipid which belongs to the phosphoinositides (Behrends et al. 2010). Whether WDR45 (WIPI-4) binds to phosphatidylinositol-3-phosphat as well remains unclear so far (Behrends et al. 2010). More research is needed to elucidate the association of WDR45 and autophagy more clearly. It is to hope that a better understanding of autophagy and its role in the pathophysiology of neurodegenerative diseases will help to identify treatment opportunities in neurodegenerative diseases.

5.3.4 LRRK2 and its WD40 repeat domain

According to Paisan-Ruiz et al., LRRK2 is the most important gene in Parkinson's disease (Paisán-Ruíz et al. 2008). The most common genetic form of Parkinson's disease is associated with mutations in the gene LRRK2 (leucine-rich repeat kinase 2) which is PAKR8 (Funayama et al. 2002; Zimprich et al. 2004; Paisán-Ruíz et al. 2008). As BPAN associated with mutations in WDR45 shows features of parkinsonism (Haack et al. 2012) and LRRK2 contains a WD40 repeat domain (Paisán-Ruíz et al. 2004), it is worthwhile to have a closer look at LRRK2. In addition to that, WDR45 was proposed as a new PARK gene (Haack et al. 2012).

5.3.4.1 Gene structure of LRRK2 and mutations in LRRK2

The LRRK2 gene comprises 51 exons and encodes for a very large protein with 2527 amino acids (Zimprich et al. 2004). Interestingly, the protein LRRK2 not only contains a leucine-rich repeat and a kinase, after which it was named, but also a WD40 repeat domain (Paisán-Ruíz et al. 2004). According to Zimprich et al. as well as Bosgraaf and van Haastert, other domains are Roc (Ras of complex (GTPase)), COR (C-terminal of Ras) and MAPKKK (mitogen-activated protein kinase kinase kinase). The Roc domain of LRRK2 together with the COR domain which is located directly C-terminal to the Roc domain belong to the Ras-related superfamily of small GTPases (Zimprich et al. 2004; Bosgraaf and van Haastert 2003). The WD40 repeat domain is located at the C-terminus of the protein (Bosgraaf and van Haastert 2003; Mata et al. 2006). The estimated domain boundaries are the amino acids at the positions 2142 and 2498. This means the domain consists of about 357 amino acids (Mata et al. 2006). Thus, the WD40 repeat domain of LRRK2 has about the same length as WDR45, which consists of 361 amino acids (Saitsu et al. 2013).

Most reported pathogenic LRRK2 mutations that segregate with PD are in the Ras and the kinase domain of the protein (Paisán-Ruíz et al. 2008). However, there is growing evidence for the importance of the WD40 repeat domain in the development of LRRK2-associated Parkinson's disease (Mata et al. 2005; Jorgensen et al. 2009; Sheng et al. 2010). In 2005, Mata et al. identified several new mutations in the LRRK2 gene, among them the mutation Gly2385Arg which is located in the WD40 repeat domain of the LRRK2 gene (Mata et al. 2005). This mutation is of particular interest. According to Di Fonzo et al. and Farrer et al.,

the mutation Gly2385Arg is especially prevalent in the Asian population. They demonstrated that Gly2385Arg is a risk factor for the development of Parkinson's disease (Di Fonzo et al. 2006; Farrer et al. 2007). Both Di Fonzo et al. and Farrer et al. calculated an odds ratio of 2.2 for Parkinson's disease for heterozygous Gly2385Arg mutation carriers (Di Fonzo et al. 2006; Farrer et al. 2007).

5.3.4.2 Lack of the WD40 repeat domain of LRRK2 in neuron cell culture

Jorgensen et al. investigated the effect of abolishing the WD40 repeat domain in LRRK2 in a mouse neuron cell culture (Jorgensen et al. 2009). They developed LRKK2 constructs that lack the WD40 repeat domain. They noticed that two common mutations in LRRK2 in the GTPase and MAPKKK domain, Arg1441Cys and Gly2019Ser, respectively lacked neurotoxicity if the WD40 repeat domain was deleted. Whereas usually the two mutations lead to an increased rate of apoptosis in cell culture, the apoptosis rate was normal, if the WD40 repeat domain was missing (Jorgensen et al. 2009). Jorgensen et al. concluded that the WD40 repeat domain in LRRK2 may be necessary to convey deleterious effects of mutations in LRRK2. They further noticed that LRRK2 autophosphorylation activity *in vitro* and dimerization of LRRK2 *in vitro* is lost when the WD40 repeat domain is deleted (Jorgensen et al. 2009). The *in vitro* findings of Jorgensen et al. may suggest that the lack of the WD40 repeat domain may be protective. However, the following animal model by Sheng et al. implies that the deletion of the WD40 repeat domain is not protective but leads to a Parkinson's disease-like phenotype (Sheng et al. 2010). This is in accordance with the abovementioned Gly2385Arg mutation that conveys an increased risk in developing Parkinson's disease (PD) in humans (Di Fonzo et al. 2006; Farrer et al. 2007).

5.3.4.3 Lack of the WD40 repeat domain of LRRK2 in the zebrafish

The first study about the function of the WD40 repeat domain in LRRK2 in a vertebrate model was done by Sheng et al. (Sheng et al. 2010). They investigated the deletion of the WD40 repeat motif in LRRK2 in zebrafish. In the following, this will be discussed here in more detail because of its possible value in the context of WDR45 mutations. They identified the zebrafish homologue of human LRRK2. Zebrafish LRRK2 contains the same abovementioned motifs as the human LRRK2, including the WD40 repeat motif. 47% of the amino acids of human and zebrafish LRRK2 are conserved. Within the WD40 repeat domain

38% of the amino acids are conserved (Sheng et al. 2010). Sheng et al. used morpholinos to interrupt splicing of exon 45 in zebrafish LRRK2. They so generated a truncated zebrafish LRRK2 protein lacking the C-terminal WD40 repeat domain. Introduced into zebrafish embryos, the zebrafish subsequently developed Parkinsonism-like phenotypes. Both locomotion defect (reduced swimming activity) and loss of diencephalic dopaminergic neurons were observed. Overexpression of human LRRK2 or zebrafish LRRK2 mRNA allowed to overcome both the morphological and functional abnormalities. Moreover, locomotion effects, but not the pathological changes in the diencephalon were shown to be rescued with levodopa administration (Sheng et al. 2010). This is interesting because levodopa is well-known to be an effective symptom-reducing treatment in humans with Parkinson's disease.

5.3.4.4 Parkinson's disease associated with LRRK2 and BPAN

In the following, it shall be emphasized what Parkinson's disease associated with mutations in LRRK2 and beta-propeller protein-associated neurodegeneration (BPAN) share in common and what distinguishes one from another. Both LRKK2 and WDR45 are genes associated with neurodegeneration and parkinsonism (Zimprich et al. 2004; Haack et al. 2012). LRRK2 is a PARK gene (Funayama et al. 2002; Paisán-Ruíz et al. 2004) and WDR45 has been proposed as such (Haack et al. 2012). Mutations in both genes exhibit dominant effect, LRRK2, located on chromosome 12, autosomal dominant (Zimprich et al. 2004) and WDR45 X-linked dominant (Haack et al. 2012). Both genes seem to be involved in autophagy processes (Gómez-Suaga et al. 2012; Behrends et al. 2010). Both diseases respond well to levodopa, although the effect seems to be very short in BPAN (Paisán-Ruíz et al. 2004; Hayflick et al. 2013).

In future research, it is worthwhile to be aware of the similarities between LRRK2 and WDR45. These similarities might reflect underlying important disease mechanisms. It is only little known about WDR45 so far. A better knowledge of the functional role of WDR45 would be promising to enhance understanding of LRRK2-related PD and thus understanding of Parkinson's disease in general. A functional analysis about possible protein-protein interactions with respect to LRRK2 and WDR45 would be interesting.

5.3.5 Rett syndrome – a disease with similarities to BPAN

Rett syndrome is an X-linked dominant disease with an estimated prevalence of about 1 in 10,000 girls (Hagberg 1985). In 1999, Amir et al. identified the main gene associated with Rett syndrome which is MECP2. The MECP2 gene is encoding for Methyl-CpG-binding protein 2. This protein is involved in transcriptional inhibition by the selective binding of CpG dinucleotides and the interaction with histone proteins (Amir et al. 1999). More recent investigations suggest that the lack of transcriptional repression due to MECP2 mutations changes synaptic neurotransmission (Nelson et al. 2011). There are at least two other genes that are known to be associated with Rett syndrome. One gene is CDKL5, also called STK9, which is located on the X chromosome as well (Kalscheuer et al. 2003; Tao et al. 2004). The other gene is FOXG1, which is located on chromosome 14 (Ariani et al. 2008).

Rett syndrome is similar to BPAN in several aspects (Hayflick et al. 2013) which shall be emphasized in the following. All individuals with BPAN reported by Haack et al., Hayflick et al. and Saitsu et al., where sufficient information was available, had de novo mutations (Haack et al. 2012; Hayflick et al. 2013; Saitsu et al. 2013). Rett syndrome is sporadic in the vast majority of cases as well and familial Rett syndrome is very rare (Schanen et al. 1997). In both diseases, females are the predominantly affected sex (Rett 1966; Haack et al. 2012). Individuals with Rett syndrome show delayed development and regression of motor, cognitive and communication skills (Rett 1966; Hagberg et al. 1983) as do individuals with BPAN (Hayflick et al. 2013). Both show gait abnormalities, severe motor deficits and severe cognitive decline (Rett 1966; Hayflick et al. 2013). Seizures are frequently encountered in both entities (Rett 1966; Hayflick et al. 2013). Rett-like features such as stereotypic hand movements which Rett syndrome is most typical for (Rett 1966; Hagberg et al. 1983), were found in 7/23 individuals with BPAN (Hayflick et al. 2013).

Although reduced cerebral volume is very common in both diseases, microcephaly seems to be a feature occurring only in Rett syndrome (Murakami et al. 1992; Hayflick et al. 2013). In contrast, the male individual with BPAN and reduced cerebral volume investigated in the present study showed relative macrocephaly. Furthermore, autonomic dysfunctions such as vasomotor disturbances of the lower limbs are only known for Rett syndrome so far (Rett 1966; Hagberg et al. 1983). MR imaging shows hypointensities in globus pallidus and striatum in individuals with BPAN (Haack et al. 2012; Hayflick et al. 2013). In Rett syndrome, similar MRI changes are not reported (Murakami et al. 1992).

As shown above, there is considerable overlap between BPAN and Rett syndrome. Individuals with symptoms of Rett syndrome without a molecular diagnosis should therefore be tested for WDR45 (Hayflick et al. 2013). It is to be expected, that this will broaden the understanding of genotype-phenotype correlations in BPAN in particular and in Rett syndrome as well.

5.3.6 Males with BPAN and the X chromosomal location of WDR45

The WDR45 gene is located on the X chromosome. However, BPAN does not show the typical constellation expected for an X-linked disease (Haack et al. 2012). Until now, much more females than males affected with BPAN have been identified, although the phenotype in males and females is indistinguishable (Haack et al. 2012; Hayflick et al. 2013).

In Rett syndrome, males with somatic mosaicism as well as X chromosomal aneuploidy have been described. Schwartzman et al. reported a male with Klinefelter syndrome (47, XXY) who developed Rett syndrome (Schwartzman et al. 1999). Clayton-Smith et al. described another male individual with Rett syndrome where somatic mosaicism was demonstrated (Clayton-Smith et al. 2000).

Extra X chromosomes in males such as in Klinefelter syndrome (47, XXY) could explain the phenomenon in BPAN as well. However, the karyotypes obtained in all three individuals investigated by Haack et al. (Haack et al. 2012) including the male identified in this study were normal. To analyze karyotypes, peripheral blood cells are used and not neurons. Thus, chromosomal mosaicism in cells other than peripheral blood cells would still be a possible explanation. However, two different events, both a chromosomal mosaicism and a de novo mutation in the WDR45 gene would have to occur in the same individual which is highly unlikely. Another, but also rather unlikely explanation would be the coincidence of a WDR45 gene duplication and a de novo mutation in one of the two genes.

One male investigated by Haack et al. showed two different WDR45 DNA populations, one wild type and one mutated in peripheral blood cells. Thus the most likely explanation is somatic mosaicism resulting from a postzygotic WDR45 de novo mutation in males (Haack et al. 2012).

5.3.7 X-inactivation studies and skewing in WDR45

The methods that were used for the X-inactivation studies are described in chapter 3.2.10. Control experiments had previously been done prior to this study, when the X-inactivation protocols had been established in the laboratory. The results for the X-inactivation studies done in this investigation are described in chapter 4.3 and have been incorporated in the publication of Haack et al. (Haack et al. 2012).

Extremely skewed X-inactivation patterns were identified in two of four subjects that were investigated. This proportion suggests that X-inactivation skewing is of importance for disease characteristics in females with BPAN. However, these data alone are not sufficient to prove that skewed X-inactivation is a relevant pathomechanism for BPAN. The ratios in the two extremely skewed subjects do not indicate whether the paternal or maternal X chromosome was preferentially inactivated. They do not allow determining whether the mutated or the non-mutated chromosome is preferentially inactivated, either. More research in the future is needed to answer these questions.

In his review, Dobyns et al. differentiates between favorable skewing and unfavorable skewing. Favorable skewing is seen when the wild type allele is preferably active. In contrast, unfavorable skewing is seen when the mutant allele is primarily active (Dobyns et al. 2004). Unfavorable skewing is rare (van den Veyver 2001). One presumed example may be X-linked adrenoleukodystrophy (Migeon et al. 1981; van den Veyver 2001). Migeon et al. investigated clonal fibroblast cells with an X-linked adrenoleukodystrophy defect. They provided evidence for *in vitro* selection of the mutant allele in fibroblasts. However, they were not able to provide evidence for *in vivo* selection of the mutant allele in erythrocytes and leukocytes (Migeon et al. 1981). In contrast, favorable skewing of X-inactivation has been shown in a variety of X-linked disorders (Conley et al. 1986; Fearon et al. 1988; Puck et al. 1992). A mutation in a gene may well be a reason for suboptimal cell growth, thus favoring those cells that harbor no mutation (van den Veyver 2001). Conley et al. investigated X-linked agammaglobulinemia and demonstrated extremely skewed X-inactivation patterns in B cells of affected individuals. Only B cells with active wild type X chromosome are present. This is probably because B cell precursors that harbor the X-linked genetic defect fail to differentiate (Conley et al. 1986). Conley et al. further showed normal X-inactivation patterns for other immune cells such as T lymphocytes or neutrophils in X-linked agammaglobulinemia (Conley

et al. 1986). This example demonstrates that skewed X-inactivation patterns can be very cell-specific.

Sharp et al. investigated skewing of X chromosomes in randomly selected women. They found out that the prevalence of severely skewed X-inactivation (ratio of 90:10 or more) is higher in older women. The portion of severely skewed X-inactivation increased from 7% in women being 25 years of age or younger to 16% in women being 60 years of age or older. These data were obtained with blood cells (Sharp et al. 2000).

The four subjects investigated in the present study (63700, 63701, 63702 and 63712) fell into 50% (2/4) of random X-inactivation and 50% (2/4) of extremely or severely skewed X-inactivation. The two individuals in the present investigation who had extremely skewed X-inactivation patterns were only 29 and 37 years old when investigations were performed. This means that X-inactivation patterns could possibly be important for BPAN. One needs to consider, however, that the DNA was obtained from peripheral blood cells. X-inactivation data from peripheral blood cells may possibly not adequately reflect X-inactivation patterns of cells in the brain. Post mortem X-inactivation studies in neurons and maybe also glia cells would be needed to answer that question in the future.

The abovementioned four females (63700, 63701, 63702 and 63712) were part of the 13 index patients with WDR45 mutations identified by Haack et al. (Haack et al. 2012). Twelve of these 13 index patients were females. Collaborating researchers that co-authored the paper from Haack et al. investigated X-inactivation patterns in the remaining eight female individuals (Haack et al. 2012).

In 2013, Saitsu et al. published data on five subjects with WDR45 mutations. They also did X-inactivation studies and identified extremely skewed X-inactivation patterns (ratio > 90:10) in two individuals, skewed X-inactivation patterns in one individual and random X-inactivation in one individual. The fifth subject was non-informative as the alleles used for X-inactivation studies were homozygous (Saitsu et al. 2013). In the supplemental materials from Saitsu et al. it is explained that the individual with random X-inactivation had a methylation ratio of 78:22 at the androgen receptor site (Saitsu et al. 2013). According to the rating used by Haack et al. (Haack et al. 2012) and also used in this thesis, the subject with a ratio of 78:22 belongs to the category of skewed X-inactivation (ratio 75:25 to 90:10).

Taking together the data of the 12 female individuals published by Haack et al. including the four females investigated in this study (Haack et al. 2012) and the four informative individuals investigated by Saitsu et al. (Saitsu et al. 2013), there are 16 individuals with informative X-inactivation studies. Of these, two are to be rated as random (12.5%), eight are to be rated as skewed (50%) and six are to be rated as extremely skewed (37.5%). Nevertheless, with all 16 individuals, the information about X-inactivation patterns was obtained from peripheral blood cells. Hence, as already mentioned above, the results may not necessarily correctly represent X-inactivation patterns of affected cells in the brain (Haack et al. 2012; Saitsu et al. 2013).

Sharp et al. investigated blood cells and two other tissues in their general studies on X-inactivation. They studied X-inactivation in buccal and urinary epithelia, but not neuronal tissue. They noticed similar skewing patterns with buccal epithelia, urinary epithelia and blood cells in young women. However, in the older women, skewed X-inactivation was more prominent in the blood cells than in buccal or urinary epithelia. This might be explained by a higher turnover of blood cells (Sharp et al. 2000).

The data obtained by Sharp et al. indicate, that firstly, skewed X-inactivation is relatively common in the general population and secondly skewed X-inactivation may be acquired with age. Sharp et al. point out that blood cells have a high turnover. Polymorphisms in X-linked genes would need to have only minimal selective pressures to exert an effect over several decades (Sharp et al. 2000). In his review, van den Veyver refers to the data obtained by Sharp et al. He points out that age-matched controls should be used in X-inactivation experiments wherever possible to avoid an age-related bias. This is particularly true for skewed X-inactivation results that are borderline and not extreme (van den Veyver 2001).

However, the abovementioned X-inactivation results with WDR45 are not borderline. In conclusion, there are similar results with the abovementioned 16 female individuals that have been investigated by different researchers. The results are consistent with each other. It is thus very likely, that X-inactivation is a relevant feature of female subjects with BPAN. Future research is needed to further clarify X-inactivation patterns in BPAN.

6 Summary

Neurodegeneration with brain iron accumulation or NBIA is a group of rare monogenic diseases which are characterized by a progressive neurodegenerative disease process and an accumulation of iron in the brain. Most characteristic is the accumulation of iron in the basal ganglia of the brain. Currently, there are ten recognized NBIA subtypes. Despite significant advances in the identification of genes associated with NBIA, still about 30% of individuals with NBIA remain without a genetic diagnosis.

The present study was part of a gene identification project. The aim of this study was to search for mutations in two predefined NBIA candidate genes, namely SLC39A14 and WDR45. Both genes had been identified as candidate genes prior to the start of this study. In SLC39A14, two index patients with homozygous mutations had been identified by collaborating researchers. In WDR45, 13 index patients had been found to have WDR45 mutations in the local research group in collaboration with a US research group prior to this study.

Overall, 251 DNA samples with idiopathic NBIA were tested for mutations in SLC39A14. Six selected DNA samples belonging to a clinically defined subgroup of NBIA were tested for WDR45 mutations. Mutation screening was done by Sanger sequencing. Furthermore, X-inactivation studies were done in four individuals with molecularly confirmed WDR45 mutations to look for skewed X-inactivation patterns.

In the 251 DNA samples that were investigated, several homozygous and heterozygous variants were found in SLC39A14. However, all these variants were interpreted as non-pathogenic. The absence of pathogenic SLC39A14 mutations in the cohort means that SLC39A14 could not be confirmed as NBIA candidate gene. During further investigations within the joint gene identification project but outside this work, it was shown that SLC39A14 mutations lead to neurodegeneration through manganese accumulation in the brain.

In six selected DNA samples, one male individual was identified with a hemizygous X-linked dominant pathogenic de novo WDR45 mutation, namely {c.[19dupC], p.[Arg7Profs*64]}. The individual had shown delayed and impaired psychomotor development from early infancy on. He had never learned to speak and had shown cognitive deficits already as a child.

He clinically deteriorated rapidly at the age of 28 years and a worsening of psychomotor functions was observed. He showed parkinsonian features, dystonia, spastic tetraparesis and lost the ability to ambulate within six months. The mother of the subject had wild type alleles in both her X chromosomes. The results of this male affected individual contributed to define the clinical phenotype of beta-propeller protein-associated neurodegeneration or BPAN as a subtype of NBIA.

X-inactivation patterns were investigated in four female individuals with BPAN. Two of these individuals showed random X-inactivation patterns (ratio of 50:50 to 75:25) and two demonstrated extremely skewed X-inactivation patterns (ratio of > 90:10) in peripheral blood cells. The ratios for extremely skewed X-inactivation are consistent with investigations done by other researchers. The results strongly suggest that skewed X-inactivation is a relevant disease mechanism in BPAN.

7 Zusammenfassung

Neurodegeneration mit Eisenablagerung im Gehirn (NBIA) ist eine Gruppe seltener monogener Erkrankungen, welche durch einen progressiv neurodegenerativen Krankheitsprozess und eine Akkumulation von Eisen im Gehirn gekennzeichnet sind. Dabei ist die Ablagerung von Eisen in den Basalganglien des Gehirns charakteristisch. Derzeit sind zehn NBIA Subtypen bekannt. Trotz großer Fortschritte in der Identifizierung von mit NBIA assoziierten Genen konnte bei etwa 30% der Patienten noch kein genetischer Defekt diagnostiziert werden.

Die vorliegende Untersuchung war Teil eines Genidentifikationsprojekts. Das Ziel dieser Arbeit war die Suche nach Mutationen in zwei vordefinierten NBIA-Kandidatengenen, SLC39A14 und WDR45. Beide Gene wurden vor Beginn dieser Arbeit als Kandidatengene identifiziert. Im Fall von SLC39A14 hatte eine kooperierende Forschungsgruppe zwei Indexpatienten mit homozygoten Mutationen identifiziert. Im Fall von WDR45 waren vor Beginn dieser Arbeit 13 Indexpatienten mit WDR45-Mutationen in Zusammenarbeit mit einer US-Forschungsgruppe gefunden worden.

In der vorliegenden Arbeit wurden 251 DNA-Proben mit idiopathischer NBIA auf Mutationen im SLC39A14-Gen untersucht. Sechs ausgewählte DNA-Proben, die zu einer klinisch definierten NBIA-Subgruppe gehörten, wurden auf WDR45-Mutationen untersucht. Die Mutationsanalysen wurden mittels Sangersequenzierung durchgeführt. Darüber hinaus wurden in vier Patienten mit genetisch nachgewiesenen WDR45-Mutationen Untersuchungen zur X-Inaktivierung gemacht, um mögliche Abweichungen im X-Inaktivierungsverhalten zu erforschen.

In den 251 analysierten DNA-Proben wurden im Gen SLC39A14 verschiedene homozygote und heterozygote Varianten gefunden. Allerdings wurden alle diese Varianten als nicht-pathogen interpretiert. Das Fehlen von pathogenen SLC39A14-Mutationen in der untersuchten Kohorte bedeutet, dass SLC39A14 als NBIA-Kandidatengen nicht bestätigt werden konnte. Wie weitere im Rahmen des gemeinsamen Genidentifikationsprojekts, aber außerhalb dieser Arbeit, durchgeführte Untersuchungen zeigen konnten, führen SLC39A14-Mutationen zu einer Neurodegeneration durch die Ablagerung von Mangan im Gehirn.

In sechs ausgewählten DNA-Proben wurde ein männlicher Patient mit einer hemizygoten X-chromosomal dominanten pathogenen de novo WDR45-Mutation {c.[19dupC], p.[Arg7Profs*64]} identifiziert. Der Patient hatte von früher Kindheit an eine verzögerte und eingeschränkte psychomotorische Entwicklung gezeigt. Er hatte nie sprechen gelernt und hatte schon als Kind kognitive Defizite gehabt. Im Alter von 28 Jahren kam es zu einer schnellen klinischen Verschlechterung. Neben einer Verschlechterung der psychomotorischen Funktionen zeigte der Patient parkinsonoide Merkmale, ferner eine Dystonie und eine spastische Tetraparese. Infolgedessen kam es innerhalb von sechs Monaten zur Immobilität des Patienten. Die Mutter des Patienten zeigte in beiden X-Chromosomen Wildtyp-Allele. Die Ergebnisse zu dem männlichen Individuum leisteten einen Beitrag zur Beschreibung des klinischen Phänotyps von Beta-Propeller Protein-assoziierter Neurodegeneration (BPAN) als einem Subtyp von NBIA.

Bei vier weiblichen Individuen mit BPAN wurde das X-Inaktivierungsmuster analysiert. Zwei der Individuen zeigten in Blutzellen ein zufälliges X-Inaktivierungsmuster (Verhältnis von 50:50 bis 75:25) und zwei zeigten ein extrem einseitiges X-Inaktivierungsmuster (Verhältnis von > 90:10). Die Zahlenverhältnisse für extrem einseitige X-Inaktivierung sind vereinbar mit Untersuchungen, die andere Forscher gemacht haben. Die Ergebnisse sprechen stark dafür, dass X-Inaktivierung ein relevanter Krankheitsmechanismus bei BPAN ist.

8 Table of figures

9 Table of tables

10 References

1. Ackermann, E.J.; Kempner, E.S.; Dennis, E.A. (1994): Ca(2+)-independent cytosolic phospholipase A2 from macrophage-like P388D1 cells. Isolation and characterization. In *J. Biol. Chem.* 269 (12), pp. 9227-9233.

2. Aicardi, J.; Castelein, P. (1979): Infantile neuroaxonal dystrophy. In *Brain* 102 (4), pp. 727-748.

3. Alazami, A.M.; Al-Saif, A.; Al-Semari, A.; Bohlega, S.; Zlitni, S.; Alzahrani, F.; Bavi, P.; Kaya, N.; Colak, D.; Khalak, H.; Baltus, A.; Peterlin, B.; Danda, S.; Bhatia, K.P.; Schneider, S.A.; Sakati, N.; Walsh, C.A.; Al-Mohanna, F.; Meyer, B.; Alkuraya, F.S. (2008): Mutations in C2orf37, encoding a nucleolar protein, cause hypogonadism, alopecia, diabetes mellitus, mental retardation, and extrapyramidal syndrome. In *Am. J. Hum. Genet.* 83 (6), pp. 684-691.

4. Alderson, N.L.; Rembiesa, B.M.; Walla, M.D.; Bielawska, A.; Bielawski, J.; Hama, H. (2004): The human FA2H gene encodes a fatty acid 2-hydroxylase. In *J. Biol. Chem.* 279 (47), pp. 48562-48568.

5. Allen, R.C.; Zoghbi, H.Y.; Moseley, A.B.; Rosenblatt, H.M.; Belmont, J.W. (1992): Methylation of HpaII and HhaI sites near the polymorphic CAG repeat in the human androgen-receptor gene correlates with X chromosome inactivation. In *Am. J. Hum. Genet.* 51 (6), pp. 1229-1239.

6. Al-Semari, A.; Bohlega, S. (2007): Autosomal-recessive syndrome with alopecia, hypogonadism, progressive extra-pyramidal disorder, white matter disease, sensory neural deafness, diabetes mellitus, and low IGF1. In *Am. J. Med. Genet. A* 143 (2), pp. 149-160.

7. Amir, R.E.; van den Veyver, I.B.; Wan, M.; Tran, C.Q.; Francke, U.; Zoghbi, H.Y. (1999): Rett syndrome is caused by mutations in X-linked MECP2, encoding methyl-CpG-binding protein 2. In *Nat. Genet.* 23 (2), pp. 185-188.

8. Andreini, C.; Banci, L.; Bertini, I.; Rosato, A. (2006): Counting the zinc-proteins encoded in the human genome. In *J. Proteome Res.* 5 (1), pp. 196-201.

9. Angelini, L.; Nardocci, N.; Rumi, V.; Zorzi, C.; Strada, L.; Savoiardo, M. (1992): Hallervorden-Spatz disease: clinical and MRI study of 11 cases diagnosed in life. In *J. Neurol.* 239 (8), pp. 417-425.

10. Ariani, F.; Hayek, G.; Rondinella, D.; Artuso, R.; Mencarelli, M.A.; Spanhol-Rosseto, A.; Pollazzon, M.; Buoni, S.; Spiga, O.; Ricciardi, S.; Meloni, I.; Longo, I.; Mari, F.; Broccoli, V.; Zappella, M.; Renieri, A. (2008): FOXG1 is responsible for the congenital variant of Rett syndrome. In *Am. J. Hum. Genet.* 83 (1), pp. 89-93.

11. Barth, H.; Meiling-Wesse, K.; Epple, U.D.; Thumm, M. (2001): Autophagy and the cytoplasm to vacuole targeting pathway both require Aut10p. In *FEBS Lett.* 508 (1), pp. 23-28.

12. Basler, K.; Oesch, B.; Scott, M.; Westaway, D.; Wälchli, M.; Groth, D.F.; McKinley, M.P.; Prusiner, S.B.; Weissmann, C. (1986): Scrapie and cellular PrP isoforms are encoded by the same chromosomal gene. In *Cell* 46 (3), pp. 417-428.

13. Baumeister, F.A.M.; Auer, D.P.; Hörtnagel, K.; Freisinger, P.; Meitinger, T. (2005): The eye-of-the-tiger sign is not a reliable disease marker for Hallervorden-Spatz syndrome. In *Neuropediatrics* 36 (3), pp. 221-222.

14. Begum, N.A.; Kobayashi, M.; Moriwaki, Y.; Matsumoto, M.; Toyoshima, K.; Seya, T. (2002): Mycobacterium bovis BCG cell wall and lipopolysaccharide induce a novel gene, BIGM103, encoding a 7-TM protein: identification of a new protein family having Zn-transporter and Zn-metalloprotease signatures. In *Genomics* 80 (6), pp. 630-645.

15. Behrends, C.; Sowa, M.E.; Gygi, S.P.; Harper, J.W. (2010): Network organization of the human autophagy system. In *Nature* 466 (7302), pp. 68-76.

16. Behrens, M.I.; Brüggemann, N.; Chana, P.; Venegas, P.; Kägi, M.; Parrao, T.; Orellana, P.; Garrido, C.; Rojas, C.V.; Hauke, J.; Hahnen, E.; González, R.; Seleme, N.; Fernández, V.; Schmidt, A.; Binkofski, F.; Kömpf, D.; Kubisch, C.; Hagenah, J.; Klein, C.; Ramirez, A. (2010): Clinical spectrum of Kufor-Rakeb syndrome in the Chilean kindred with ATP13A2 mutations. In *Mov. Disord.* 25 (12), pp. 1929-1937.

17. Bin, B.-H.; Fukada, T.; Hosaka, T.; Yamasaki, S.; Ohashi, W.; Hojyo, S.; Miyai, T.; Nishida, K.; Yokoyama, S.; Hirano, T. (2011): Biochemical characterization of human ZIP13 protein: a homo-dimerized zinc transporter involved in the spondylocheiro dysplastic Ehlers-Danlos syndrome. In *J. Biol. Chem.* 286 (46), pp. 40255-40265.

18. Bosgraaf, L.; van Haastert, P.J.M. (2003): Roc, a Ras/GTPase domain in complex proteins. In *Biochim. Biophys. Acta* 1643 (1-3), pp. 5-10.

19. Bower, M.A.; Bushara, K.; Dempsey, M.A.; Das, S.; Tuite, P.J. (2011): Novel mutations in siblings with later-onset PLA2G6-associated neurodegeneration (PLAN). In *Mov. Disord.* 26 (9), pp. 1768-1769.

20. Brown, D.R.; Qin, K.; Herms, J.W.; Madlung, A.; Manson, J.; Strome, R.; Fraser, P.E.; Kruck, T.; Bohlen, A. von; Schulz-Schaeffer, W.; Giese, A.; Westaway, D.; Kretzschmar, H. (1997): The cellular prion protein binds copper in vivo. In *Nature* 390 (6661), pp. 684-687.

21. Carrilho, I.; Santos, M.; Guimarães, A.; Teixeira, J.; Chorão, R.; Martins, M.; Dias, C.; Gregory, A.; Westaway, S.; Nguyen, T.; Hayflick, S.; Barbot, C. (2008): Infantile neuroaxonal dystrophy: what's most important for the diagnosis? In *Eur. J. Paediatr. Neurol.* 12 (6), pp. 491-500.

22. Caughey, B.; Raymond, G.J. (1991): The scrapie-associated form of PrP is made from a cell surface precursor that is both protease- and phospholipase-sensitive. In *J. Biol. Chem.* 266 (27), pp. 18217-18223.

23. Chang, M.-H.; Hung, W.-L.; Liao, Y.-C.; Lee, Y.-C.; Hsieh, P.F. (2009): Eye of the tiger-like MRI in parkinsonian variant of multiple system atrophy. In *J Neural Transm* 116 (7), pp. 861-866.

24. Chinnery, P.F.; Crompton, D.E.; Birchall, D.; Jackson, M.J.; Coulthard, A.; Lombès, A.; Quinn, N.; Wills, A.; Fletcher, N.; Mottershead, J.P.; Cooper, P.; Kellett, M.; Bates, D.; Burn, J. (2007): Clinical features and natural history of neuroferritinopathy caused by the FTL1 460InsA mutation. In *Brain* 130 (Pt 1), pp. 110-119.

25. Clayton-Smith, J.; Watson, P.; Ramsden, S.; Black, G.C. (2000): Somatic mutation in MECP2 as a non-fatal neurodevelopmental disorder in males. In *Lancet* 356 (9232), pp. 830-832.

26. Conley, M.E.; Brown, P.; Pickard, A.R.; Buckley, R.H.; Miller, D.S.; Raskind, W.H.; Singer, J.W.; Fialkow, P.J. (1986): Expression of the gene defect in X-linked agammaglobulinemia. In *N. Engl. J. Med.* 315 (9), pp. 564-567.

27. Cossu, G.; Abbruzzese, G.; Matta, G.; Murgia, D.; Melis, M.; Ricchi, V.; Galanello, R.; Barella, S.; Origa, R.; Balocco, M.; Pelosin, E.; Marchese, R.; Ruffinengo, U.; Forni, G.L. (2014): Efficacy and safety of deferiprone for the treatment of pantothenate kinase-associated neurodegeneration (PKAN) and neurodegeneration with brain iron accumulation (NBIA): results from a four years follow-up. In *Parkinsonism Relat. Disord.* 20 (6), pp. 651-654.

28. Curtis, A.R.; Fey, C.; Morris, C.M.; Bindoff, L.A.; Ince, P.G.; Chinnery, P.F.; Coulthard, A.; Jackson, M.J.; Jackson, A.P.; McHale, D.P.; Hay, D.; Barker, W.A.; Markham, A.F.; Bates, D.; Curtis, A.; Burn, J. (2001): Mutation in the gene encoding ferritin light polypeptide causes dominant adult-onset basal ganglia disease. In *Nat. Genet.* 28 (4), pp. 350-354.

29. Danbolt, N.; Closs, K. (1942): Akrodermatitis enteropathica. In *Acta Derm. Venereol.* 23, pp. 127-169.

30. Dehay, B.; Ramirez, A.; Martinez-Vicente, M.; Perier, C.; Canron, M.-H.; Doudnikoff, E.; Vital, A.; Vila, M.; Klein, C.; Bezard, E. (2012): Loss of P-type ATPase ATP13A2/PARK9 function induces general lysosomal deficiency and leads to Parkinson disease neurodegeneration. In *Proc. Natl. Acad. Sci. U.S.A.* 109 (24), pp. 9611-9616.

31. Deschauer, M.; Gaul, C.; Behrmann, C.; Prokisch, H.; Zierz, S.; Haack, T.B. (2012): C19orf12 mutations in neurodegeneration with brain iron accumulation mimicking juvenile amyotrophic lateral sclerosis. In *Journal of neurology*, pp. 2434-2439.

32. Di Fonzo, A.; Wu-Chou, Y.-H.; Lu, C.-S.; van Doeselaar, M.; Simons, E.J.; Rohé, C.F.; Chang, H.-C.; Chen, R.-S.; Weng, Y.-H.; Vanacore, N.; Breedveld, G.J.; Oostra, B.A.; Bonifati, V. (2006): A common missense variant in the LRRK2 gene, Gly2385Arg, associated with Parkinson's disease risk in Taiwan. In *Neurogenetics* 7 (3), pp. 133-138.

33. Dick, K.J.; Eckhardt, M.; Paisán-Ruíz, C.; Alshehhi, A.A.; Proukakis, C.; Sibtain, N.A.; Maier, H.; Sharifi, R.; Patton, M.A.; Bashir, W.; Koul, R.; Raeburn, S.; Gieselmann, V.; Houlden, H.; Crosby, A.H. (2010): Mutation of FA2H underlies a complicated form of hereditary spastic paraplegia (SPG35). In *Hum. Mutat.* 31 (4), pp. E1251-60.

34. Dobyns, W.B.; Filauro, A.; Tomson, B.N.; Chan, A.S.; Ho, A.W.; Ting, N.T.; Oosterwijk, J.C.; Ober, C. (2004): Inheritance of most X-linked traits is not dominant or recessive, just X-linked. In *Am. J. Med. Genet. A* 129 (2), pp. 136-143.

35. Dusi, S.; Valletta, L.; Haack, T.B.; Tsuchiya, Y.; Venco, P.; Pasqualato, S.; Goffrini, P.; Tigano, M.; Demchenko, N.; Wieland, T.; Schwarzmayr, T.; Strom, T.M.; Invernizzi, F.; Garavaglia, B.; Gregory, A.; Sanford, L.; Hamada, J.; Bettencourt, C.; Houlden, H.; Chiapparini, L.; Zorzi, G.; Kurian, M.A.; Nardocci, N.; Prokisch, H.; Hayflick, S.; Gout, I.; Tiranti, V. (2014): Exome sequence reveals mutations in CoA synthase as a cause of neurodegeneration with brain iron accumulation. In *Am. J. Hum. Genet.* 94 (1), pp. 11-22.

36. Eckhardt, M.; Yaghootfam, A.; Fewou, S.N.; Zöller, I.; Gieselmann, V. (2005): A mammalian fatty acid hydroxylase responsible for the formation of alpha-hydroxylated galactosylceramide in myelin. In *Biochem. J.* 388 (Pt 1), pp. 245-254.

37. Edvardson, S.; Hama, H.; Shaag, A.; Gomori, J.M.; Berger, I.; Soffer, D.; Korman, S.H.; Taustein, I.; Saada, A.; Elpeleg, O. (2008): Mutations in the fatty acid 2-hydroxylase gene are associated with leukodystrophy with spastic paraparesis and dystonia. In *Am. J. Hum. Genet.* 83 (5), pp. 643-648.

38. Ehsani, S.; Huo, H.; Salehzadeh, A.; Pocanschi, C.L.; Watts, J.C.; Wille, H.; Westaway, D.; Rogaeva, E.; St George-Hyslop, P.H.; Schmitt-Ulms, G. (2011): Family reunion--the ZIP/prion gene family. In *Prog. Neurobiol.* 93 (3), pp. 405-420.

39. Ehsani, S.; Mehrabian, M.; Pocanschi, C.L.; Schmitt-Ulms, G. (2012a): The ZIP-prion connection. In *Prion* 6 (4), pp. 317-321.

40. Ehsani, S.; Salehzadeh, A.; Huo, H.; Reginold, W.; Pocanschi, C.L.; Ren, H.; Wang, H.; So, K.; Sato, C.; Mehrabian, M.; Strome, R.; Trimble, W.S.; Hazrati, L.-N.; Rogaeva, E.; Westaway, D.; Carlson, G.A.; Schmitt-Ulms, G. (2012b): LIV-1 ZIP Ectodomain Shedding in Prion-Infected Mice Resembles Cellular Response to Transition Metal Starvation. In *J. Mol. Biol.* 422 (4), pp. 556-574.

41. Eiberg, H.; Hansen, L.; Korbo, L.; Nielsen, I.M.; Svenstrup, K.; Bech, S.; Pinborg, L.H.; Friberg, L.; Hjermind, L.E.; Olsen, O.R.; Nielsen, J.E. (2012): Novel mutation in ATP13A2 widens the spectrum of Kufor-Rakeb syndrome (PARK9). In *Clin. Genet.* 82 (3), pp. 256-263.

42. Eide, D.; Broderius, M.; Fett, J.; Guerinot, M.L. (1996): A novel iron-regulated metal transporter from plants identified by functional expression in yeast. In *Proc. Natl. Acad. Sci. U.S.A.* 93 (11), pp. 5624-5628.

43. Exome Aggregation Consortium (2015): ExAC Browser Beta. Cambridge, Massachusetts, USA. [23.02.2015 accessed]. Available online at http://exac.broadinstitute.org.

44. Farrer, M.J.; Stone, J.T.; Lin, C.-H.; Dächsel, J.C.; Hulihan, M.M.; Haugarvoll, K.; Ross, O.A.; Wu, R.-M. (2007): Lrrk2 G2385R is an ancestral risk factor for Parkinson's disease in Asia. In *Parkinsonism Relat. Disord.* 13 (2), pp. 89-92.

45. Fearon, E.R.; Kohn, D.B.; Winkelstein, J.A.; Vogelstein, B.; Blaese, R.M. (1988): Carrier detection in the Wiskott Aldrich syndrome. In *Blood* 72 (5), pp. 1735-1739.

46. Fong, H.K.; Hurley, J.B.; Hopkins, R.S.; Miake-Lye, R.; Johnson, M.S.; Doolittle, R.F.; Simon, M.I. (1986): Repetitive segmental structure of the transducin beta subunit: homology with the CDC4 gene and identification of related mRNAs. In *Proc. Natl. Acad. Sci. U.S.A.* 83 (7), pp. 2162-2166.

47. Fukada, T.; Civic, N.; Furuichi, T.; Shimoda, S.; Mishima, K.; Higashiyama, H.; Idaira, Y.; Asada, Y.; Kitamura, H.; Yamasaki, S.; Hojyo, S.; Nakayama, M.; Ohara, O.; Koseki, H.; Dos Santos, H.G.; Bonafe, L.; Ha-Vinh, R.; Zankl, A.; Unger, S.; Kraenzlin, M.E.; Beckmann, J.S.; Saito, I.; Rivolta, C.; Ikegawa, S.; Superti-Furga, A.; Hirano, T. (2008): The zinc transporter SLC39A13/ZIP13 is required for connective tissue development; its involvement in BMP/TGF-beta signaling pathways. In *PLoS ONE* 3 (11), pp. e3642: 1-13.

48. Funayama, M.; Hasegawa, K.; Kowa, H.; Saito, M.; Tsuji, S.; Obata, F. (2002): A new locus for Parkinson's disease (PARK8) maps to chromosome 12p11.2-q13.1. In *Ann. Neurol.* 51 (3), pp. 296-301.

49. Gálvez-Peralta, M.; He, L.; Jorge-Nebert, L.F.; Wang, B.; Miller, M.L.; Eppert, B.L.; Afton, S.; Nebert, D.W. (2012): ZIP8 zinc transporter: indispensable role for both multiple-organ organogenesis and hematopoiesis in utero. In *PLoS ONE* 7 (5), pp. e36055, 1-15.

50. Garcia, M.; Leonardi, R.; Zhang, Y.-M.; Rehg, J.E.; Jackowski, S. (2012): Germline deletion of pantothenate kinases 1 and 2 reveals the key roles for CoA in postnatal metabolism. In *PLoS ONE* 7 (7), pp. e40871: 1-13.

51. Garone, C.; Pippucci, T.; Cordelli, D.M.; Zuntini, R.; Castegnaro, G.; Marconi, C.; Graziano, C.; Marchiani, V.; Verrotti, A.; Seri, M.; Franzoni, E. (2011): FA2H-related disorders: a novel c.270+3AT splice-site mutation leads to a complex neurodegenerative phenotype. In *Dev Med Child Neurol* 53 (10), pp. 958-961.

52. Girijashanker, K.; He, L.; Soleimani, M.; Reed, J.M.; Li, H.; Liu, Z.; Wang, B.; Dalton, T.P.; Nebert, D.W. (2008): Slc39a14 gene encodes ZIP14, a metal/bicarbonate symporter: similarities to the ZIP8 transporter. In *Mol. Pharmacol.* 73 (5), pp. 1413-1423.

53. Giunta, C.; Elçioglu, N.H.; Albrecht, B.; Eich, G.; Chambaz, C.; Janecke, A.R.; Yeowell, H.; Weis, M.; Eyre, D.R.; Kraenzlin, M.; Steinmann, B. (2008): Spondylocheiro dysplastic form of the Ehlers-Danlos syndrome--an autosomal-recessive entity caused by mutations in the zinc transporter gene SLC39A13. In *Am. J. Hum. Genet.* 82 (6), pp. 1290-1305.

54. Gómez-Suaga, P.; Luzón-Toro, B.; Churamani, D.; Zhang, L.; Bloor-Young, D.; Patel, S.; Woodman, P.G.; Churchill, G.C.; Hilfiker, S. (2012): Leucine-rich repeat kinase 2 regulates autophagy through a calcium-dependent pathway involving NAADP. In *Hum. Mol. Genet.* 21 (3), pp. 511-525.

55. Gregory, A.; Hayflick, S.J. (2005): Neurodegeneration with brain iron accumulation. In *Folia Neuropathol* 43 (4), pp. 286-296.

56. Gregory, A.; Westaway, S.K.; Holm, I.E.; Kotzbauer, P.T.; Hogarth, P.; Sonek, S.; Coryell, J.C.; Nguyen, T.M.; Nardocci, N.; Zorzi, G.; Rodriguez, D.; Desguerre, I.; Bertini, E.; Simonati, A.; Levinson, B.; Dias, C.; Barbot, C.; Carrilho, I.; Santos, M.; Malik, I.; Gitschier, J.; Hayflick, S.J. (2008): Neurodegeneration associated with genetic defects in phospholipase A(2). In *Neurology* 71 (18), pp. 1402-1409.

57. Griffith, J.S. (1967): Self-replication and scrapie. In *Nature* 215 (5105), pp. 1043-1044.

58. Grotz, N.; Fox, T.; Connolly, E.; Park, W.; Guerinot, M.L.; Eide, D. (1998): Identification of a family of zinc transporter genes from Arabidopsis that respond to zinc deficiency. In *Proc. Natl. Acad. Sci. U.S.A.* 95 (12), pp. 7220-7224.

59. Guan, J.; Stromhaug, P.E.; George, M.D.; Habibzadegah-Tari, P.; Bevan, A.; Dunn, W.A.; Klionsky, D.J. (2001): Cvt18/Gsa12 is required for cytoplasm-to-vacuole transport, pexophagy, and autophagy in Saccharomyces cerevisiae and Pichia pastoris. In *Mol. Biol. Cell* 12 (12), pp. 3821-3838.

60. Haack, T.B.; Hogarth, P.; Kruer, M.C.; Gregory, A.; Wieland, T.; Schwarzmayr, T.; Graf, E.; Sanford, L.; Meyer, E.; Kara, E.; Cuno, S.M.; Harik, S.I.; Dandu, V.H.; Nardocci, N.; Zorzi, G.; Dunaway, T.; Tarnopolsky, M.; Skinner, S.; Frucht, S.; Hanspal, E.; Schrander-Stumpel, C.; Héron, D.; Mignot, C.; Garavaglia, B.; Bhatia, K.; Hardy, J.; Strom, T.M.; Boddaert, N.; Houlden, H.H.; Kurian, M.A.; Meitinger, T.; Prokisch, H.; Hayflick, S.J. (2012): Exome Sequencing Reveals De Novo WDR45 Mutations Causing a Phenotypically Distinct, X-Linked Dominant Form of NBIA. In *Am. J. Hum. Genet.* 91 (6), pp. 1144-1149.

61. Haemers, I.; Kono, S.; Goldman, S.; Gitlin, J.D.; Pandolfo, M. (2004): Clinical, molecular, and PET study of a case of aceruloplasminaemia presenting with focal cranial dyskinesia. In *J. Neurol. Neurosurg. Psychiatr.* 75 (2), pp. 334-337.

62. Hagberg, B. (1985): Rett's syndrome: prevalence and impact on progressive severe mental retardation in girls. In *Acta Paediatr Scand* 74 (3), pp. 405-408.

63. Hagberg, B.; Aicardi, J.; Dias, K.; Ramos, O. (1983): A progressive syndrome of autism, dementia, ataxia, and loss of purposeful hand use in girls: Rett's syndrome: report of 35 cases. In *Ann. Neurol.* 14 (4), pp. 471-479.

64. Hallervorden, J.; Spatz, H. (1922): Eigenartige Erkrankung im extrapyramidalen System mit besonderer Beteiligung des Globus pallidus und der Substantia nigra. Ein Beitrag zu den Beziehungen zwischen diesen beiden Zentren. In *Gesamte Neurol Psychiatr* (79), pp. 254-302.

65. Hampshire, D.J.; Roberts, E.; Crow, Y.; Bond, J.; Mubaidin, A.; Wriekat, A.L.; Al-Din, A.; Woods, C.G. (2001): Kufor-Rakeb syndrome, pallido-pyramidal degeneration with supranuclear upgaze paresis and dementia, maps to 1p36. In *J. Med. Genet.* 38 (10), pp. 680-682.

66. Harris, Z.L.; Takahashi, Y.; Miyajima, H.; Serizawa, M.; MacGillivray, R.T.; Gitlin, J.D. (1995): Aceruloplasminemia: molecular characterization of this disorder of iron metabolism. In *Proc. Natl. Acad. Sci. U.S.A.* 92 (7), pp. 2539-2543.

67. Hartig, M.B.; Hörtnagel, K.; Garavaglia, B.; Zorzi, G.; Kmiec, T.; Klopstock, T.; Rostasy, K.; Svetel, M.; Kostic, V.S.; Schuelke, M.; Botz, E.; Weindl, A.; Novakovic, I.; Nardocci, N.; Prokisch, H.; Meitinger, T. (2006): Genotypic and phenotypic spectrum of PANK2 mutations in patients with neurodegeneration with brain iron accumulation. In *Ann. Neurol.* 59 (2), pp. 248-256.

68. Hartig, M.B.; Iuso, A.; Haack, T.; Kmiec, T.; Jurkiewicz, E.; Heim, K.; Roeber, S.; Tarabin, V.; Dusi, S.; Krajewska-Walasek, M.; Jozwiak, S.; Hempel, M.; Winkelmann, J.; Elstner, M.; Oexle, K.; Klopstock, T.; Mueller-Felber, W.; Gasser, T.; Trenkwalder, C.; Tiranti, V.; Kretzschmar, H.; Schmitz, G.; Strom, T.M.; Meitinger, T.; Prokisch, H. (2011): Absence of an orphan mitochondrial protein, c19orf12, causes a distinct clinical subtype of neurodegeneration with brain iron accumulation. In *Am. J. Hum. Genet.* 89 (4), pp. 543-550.

69. Hayflick, S.J. (2003): Pantothenate kinase-associated neurodegeneration (formerly Hallervorden-Spatz syndrome). In *J. Neurol. Sci.* 207 (1-2), pp. 106-107.

70. Hayflick, S.J.; Kruer, M.C.; Gregory, A.; Haack, T.B.; Kurian, M.A.; Houlden, H.H.; Anderson, J.; Boddaert, N.; Sanford, L.; Harik, S.I.; Dandu, V.H.; Nardocci, N.; Zorzi, G.; Dunaway, T.; Tarnopolsky, M.; Skinner, S.; Holden, K.R.; Frucht, S.; Hanspal, E.; Schrander-Stumpel, C.; Mignot, C.; Héron, D.; Saunders, D.E.; Kaminska, M.; Lin, J.-P.; Lascelles, K.; Cuno, S.M.; Meyer, E.; Garavaglia, B.; Bhatia, K.; Silva, R. de; Crisp, S.; Lunt, P.; Carey, M.; Hardy, J.; Meitinger, T.; Prokisch, H.; Hogarth, P. (2013): β-Propeller protein-associated neurodegeneration: a new X-linked dominant disorder with brain iron accumulation. In *Brain* 136 (Pt 6), pp. 1708-1717.

71. Hayflick, S.J.; Westaway, S.K.; Levinson, B.; Zhou, B.; Johnson, M.A.; Ching, K.H.L.; Gitschier, J. (2003): Genetic, clinical, and radiographic delineation of Hallervorden-Spatz syndrome. In *N. Engl. J. Med.* 348 (1), pp. 33-40.

72. Head, M.W.; Ironside, J.W. (2012): Review: Creutzfeldt-Jakob disease: prion protein type, disease phenotype and agent strain. In *Neuropathol. Appl. Neurobiol.* 38 (4), pp. 296-310.

73. Hojyo, S.; Fukada, T.; Shimoda, S.; Ohashi, W.; Bin, B.-H.; Koseki, H.; Hirano, T. (2011): The zinc transporter SLC39A14/ZIP14 controls G-protein coupled receptor-mediated signaling required for systemic growth. In *PLoS ONE* 6 (3), pp. e18059, 1-15.

74. Holmberg, C.G.; Laurell, C.B. (1948): Investigations in serum copper; isolation of the copper containing protein, and a description of some of its properties. In *Acta Chem Scand* 2, pp. 550-556.

75. Holmberg, C.G.; Laurell, C.B. (1951): Investigations in serum copper; coeruloplasmin as an enzyme. In *Acta Chem Scand* 5, pp. 476-480.

76. Hörtnagel, K.; Prokisch, H.; Meitinger, T. (2003): An isoform of hPANK2, deficient in pantothenate kinase-associated neurodegeneration, localizes to mitochondria. In *Hum. Mol. Genet.* 12 (3), pp. 321-327.

77. Horvath, R.; Holinski-Feder, E.; Neeve, V.C.M.; Pyle, A.; Griffin, H.; Ashok, D.; Foley, C.; Hudson, G.; Rautenstrauss, B.; Nürnberg, G.; Nürnberg, P.; Kortler, J.;

Neitzel, B.; Bässmann, I.; Rahman, T.; Keavney, B.; Loughlin, J.; Hambleton, S.; Schoser, B.; Lochmüller, H.; Santibanez-Koref, M.; Chinnery, P.F. (2012): A new phenotype of brain iron accumulation with dystonia, optic atrophy, and peripheral neuropathy. In *Mov. Disord.* 27 (6), pp. 789-793.

78. Jackowski, S.; Rock, C.O. (1981): Regulation of coenzyme A biosynthesis. In *J. Bacteriol.* 148 (3), pp. 926-932.

79. Jenkitkasemwong, S.; Wang, C.-Y.; Mackenzie, B.; Knutson, M.D. (2012): Physiologic implications of metal-ion transport by ZIP14 and ZIP8. In *Biometals* 25 (4), pp. 643-655.

80. Jeong, J.; Eide, D.J. (2013): The SLC39 family of zinc transporters. In *Mol. Aspects Med.* 34 (2-3), pp. 612-619.

81. Jongeneel, C.V.; Bouvier, J.; Bairoch, A. (1989): A unique signature identifies a family of zinc-dependent metallopeptidases. In *FEBS Lett.* 242 (2), pp. 211-214.

82. Jorgensen, N.D.; Peng, Y.; Ho, C.C.-Y.; Rideout, H.J.; Petrey, D.; Liu, P.; Dauer, W.T. (2009): The WD40 domain is required for LRRK2 neurotoxicity. In *PLoS ONE* 4 (12), pp. e8463, 1-8.

83. Jung, A.G.; Mathony, U.A.; Behre, B.; Küry, S.; Schmitt, S.; Zouboulis, C.C.; Lippert, U. (2011): Acrodermatitis enteropathica: an uncommon differential diagnosis in childhood - first description of a new sequence variant. In *J Dtsch Dermatol Ges* 9 (12), pp. 999-1002.

84. Kalman, B.; Lautenschlaeger, R.; Kohlmayer, F.; Büchner, B.; Kmiec, T.; Klopstock, T.; Kuhn, K. (2012): An international registry for neurodegeneration with brain iron accumulation. In *Orphanet J Rare Dis* 7 (1), pp. 66: 1-5.

85. Kalscheuer, V.M.; Tao, J.; Donnelly, A.; Hollway, G.; Schwinger, E.; Kübart, S.; Menzel, C.; Hoeltzenbein, M.; Tommerup, N.; Eyre, H.; Harbord, M.; Haan, E.; Sutherland, G.R.; Ropers, H.-H.; Gécz, J. (2003): Disruption of the serine/threonine kinase 9 gene causes severe X-linked infantile spasms and mental retardation. In *Am. J. Hum. Genet.* 72 (6), pp. 1401-1411.

86. Keogh, M.J.; Jonas, P.; Coulthard, A.; Chinnery, P.F.; Burn, J. (2012): Neuroferritinopathy: a new inborn error of iron metabolism. In *Neurogenetics* 13 (1), pp. 93-96.

87. Kocisko, D.A.; Come, J.H.; Priola, S.A.; Chesebro, B.; Raymond, G.J.; Lansbury, P.T.; Caughey, B. (1994): Cell-free formation of protease-resistant prion protein. In *Nature* 370 (6489), pp. 471-474.

88. Kotzbauer, P.T.; Truax, A.C.; Trojanowski, J.Q.; Lee, V.M.-Y. (2005): Altered neuronal mitochondrial coenzyme A synthesis in neurodegeneration with brain iron accumulation caused by abnormal processing, stability, and catalytic activity of mutant pantothenate kinase 2. In *J. Neurosci.* 25 (3), pp. 689-698.

89. Kruer, M.C.; Boddaert, N.; Schneider, S.A.; Houlden, H.; Bhatia, K.P.; Gregory, A.; Anderson, J.C.; Rooney, W.D.; Hogarth, P.; Hayflick, S.J. (2012): Neuroimaging

features of neurodegeneration with brain iron accumulation. In *AJNR Am J Neuroradiol* 33 (3), pp. 407-414.

90. Kruer, M.C.; Paisán-Ruíz, C.; Boddaert, N.; Yoon, M.Y.; Hama, H.; Gregory, A.; Malandrini, A.; Woltjer, R.L.; Munnich, A.; Gobin, S.; Polster, B.J.; Palmeri, S.; Edvardson, S.; Hardy, J.; Houlden, H.; Hayflick, S.J. (2010): Defective FA2H leads to a novel form of neurodegeneration with brain iron accumulation (NBIA). In *Ann. Neurol.* 68 (5), pp. 611-618.

91. Kuhn, J.; Bewermeyer, H.; Miyajima, H.; Takahashi, Y.; Kuhn, K.F.; Hoogenraad, T.U. (2007): Treatment of symptomatic heterozygous aceruloplasminemia with oral zinc sulphate. In *Brain Dev.* 29 (7), pp. 450-453.

92. Kuo, Y.-M.; Duncan, J.L.; Westaway, S.K.; Yang, H.; Nune, G.; Xu, E.Y.; Hayflick, S.J.; Gitschier, J. (2005): Deficiency of pantothenate kinase 2 (Pank2) in mice leads to retinal degeneration and azoospermia. In *Hum. Mol. Genet.* 14 (1), pp. 49-57.

93. Kurian, M.A.; McNeill, A.; Lin, J.-P.; Maher, E.R. (2011): Childhood disorders of neurodegeneration with brain iron accumulation (NBIA). In *Developmental Medicine & Child Neurology* 53 (5), pp. 394-404.

94. Kurian, M.A.; Morgan, N.V.; MacPherson, L.; Foster, K.; Peake, D.; Gupta, R.; Philip, S.G.; Hendriksz, C.; Morton, J.E.V.; Kingston, H.M.; Rosser, E.M.; Wassmer, E.; Gissen, P.; Maher, E.R. (2008): Phenotypic spectrum of neurodegeneration associated with mutations in the PLA2G6 gene (PLAN). In *Neurology* 70 (18), pp. 1623-1629.

95. Küry, S.; Dréno, B.; Bézieau, S.; Giraudet, S.; Kharfi, M.; Kamoun, R.; Moisan, J.-P. (2002): Identification of SLC39A4, a gene involved in acrodermatitis enteropathica. In *Nat. Genet.* 31 (3), pp. 239-240.

96. Kwiatkowski, A.; Ryckewaert, G.; Jissendi Tchofo, P.; Moreau, C.; Vuillaume, I.; Chinnery, P.F.; Destée, A.; Defebvre, L.; Devos, D. (2012): Long-term improvement under deferiprone in a case of neurodegeneration with brain iron accumulation. In *Parkinsonism Relat. Disord.* 18 (1), pp. 110-112.

97. Li, D.; Roberts, R. (2001): WD-repeat proteins: structure characteristics, biological function, and their involvement in human diseases. In *Cell. Mol. Life Sci.* 58 (14), pp. 2085-2097.

98. Liuzzi, J.P.; Aydemir, F.; Nam, H.; Knutson, M.D.; Cousins, R.J. (2006): Zip14 (Slc39a14) mediates non-transferrin-bound iron uptake into cells. In *Proc. Natl. Acad. Sci. U.S.A.* 103 (37), pp. 13612-13617.

99. Lyon, M.F. (1962): Sex chromatin and gene action in the mammalian X-chromosome. In *Am. J. Hum. Genet.* 14, pp. 135-148.

100. Mallucci, G.; Dickinson, A.; Linehan, J.; Klöhn, P.-C.; Brandner, S.; Collinge, J. (2003): Depleting neuronal PrP in prion infection prevents disease and reverses spongiosis. In *Science* 302 (5646), pp. 871-874.

101. Mata, I.F.; Kachergus, J.M.; Taylor, J.P.; Lincoln, S.; Aasly, J.; Lynch, T.; Hulihan, M.M.; Cobb, S.A.; Wu, R.-M.; Lu, C.-S.; Lahoz, C.; Wszolek, Z.K.; Farrer, M.J.

(2005): Lrrk2 pathogenic substitutions in Parkinson's disease. In *Neurogenetics* 6 (4), pp. 171-177.

102. Mata, I.F.; Wedemeyer, W.J.; Farrer, M.J.; Taylor, J.P.; Gallo, K.A. (2006): LRRK2 in Parkinson's disease: protein domains and functional insights. In *Trends Neurosci.* 29 (5), pp. 286-293.

103. Mayo, K.E. (1992): Molecular cloning and expression of a pituitary-specific receptor for growth hormone-releasing hormone. In *Mol. Endocrinol.* 6 (10), pp. 1734-1744.

104. McNeill, A.; Birchall, D.; Hayflick, S.J.; Gregory, A.; Schenk, J.F.; Zimmerman, E.A.; Shang, H.; Miyajima, H.; Chinnery, P.F. (2008a): T2* and FSE MRI distinguishes four subtypes of neurodegeneration with brain iron accumulation. In *Neurology* 70 (18), pp. 1614-1619.

105. McNeill, A.; Pandolfo, M.; Kuhn, J.; Shang, H.; Miyajima, H. (2008b): The neurological presentation of ceruloplasmin gene mutations. In *Eur. Neurol.* 60 (4), pp. 200-205.

106. Migeon, B.R.; Moser, H.W.; Moser, A.B.; Axelman, J.; Sillence, D.; Norum, R.A. (1981): Adrenoleukodystrophy: evidence for X linkage, inactivation, and selection favoring the mutant allele in heterozygous cells. In *Proc. Natl. Acad. Sci. U.S.A.* 78 (8), pp. 5066-5070.

107. Miyajima, H.; Takahashi, Y.; Kamata, T.; Shimizu, H.; Sakai, N.; Gitlin, J.D. (1997): Use of desferrioxamine in the treatment of aceruloplasminemia. In *Ann. Neurol.* 41 (3), pp. 404-407.

108. Morgan, N.V.; Westaway, S.K.; Morton, J.E.V.; Gregory, A.; Gissen, P.; Sonek, S.; Cangul, H.; Coryell, J.; Canham, N.; Nardocci, N.; Zorzi, G.; Pasha, S.; Rodriguez, D.; Desguerre, I.; Mubaidin, A.; Bertini, E.; Trembath, R.C.; Simonati, A.; Schanen, C.; Johnson, C.A.; Levinson, B.; Woods, C.G.; Wilmot, B.; Kramer, P.; Gitschier, J.; Maher, E.R.; Hayflick, S.J. (2006): PLA2G6, encoding a phospholipase A2, is mutated in neurodegenerative disorders with high brain iron. In *Nat. Genet.* 38 (7), pp. 752-754.

109. Moynahan, E.J. (1974): Letter: Acrodermatitis enteropathica: a lethal inherited human zinc-deficiency disorder. In *Lancet* 2 (7877), pp. 399-400.

110. Moynahan, E.J.; Barnes, P.M. (1973): Zinc deficiency and a synthetic diet for lactose intolerance. In *Lancet* 1 (7804), pp. 676-677.

111. Murakami, J.W.; Courchesne, E.; Haas, R.H.; Press, G.A.; Yeung-Courchesne, R. (1992): Cerebellar and cerebral abnormalities in Rett syndrome: a quantitative MR analysis. In *AJR Am J Roentgenol* 159 (1), pp. 177-183.

112. Mutoh, K.; Okuno, T.; Ito, M.; Nakano, S.; Mikawa, H.; Fujisawa, I.; Asato, R. (1988): MR imaging of a group I case of Hallervorden-Spatz disease. In *J Comput Assist Tomogr* 12 (5), pp. 851-853.

113. Najim al-Din, A.S.; Wriekat, A.; Mubaidin, A.; Dasouki, M.; Hiari, M. (1994): Pallido-pyramidal degeneration, supranuclear upgaze paresis and dementia: Kufor-Rakeb syndrome. In *Acta Neurol. Scand.* 89 (5), pp. 347-352.

114. National Center for Biotechnology Information of United States National Library of Medicine (2014): RefSeq: NCBI Reference Sequence Database. A comprehensive, integrated, non-redundant, well-annotated set of reference sequences including genomic, transcript, and protein. Bethesda, Maryland, USA. [12.09.2014 accessed]. Available online at http://www.ncbi.nlm.nih.gov/refseq.

115. National Center for Biotechnology Information of United States National Library of Medicine (2015): dbSNP. Database of single nucleotide polymorphisms (SNPs) and multiple small-scale variations that include insertions/deletions, microsatellites, and non-polymorphic variants. Bethesda, Maryland, USA. [23.02.2015 accessed]. Available online at http://www.ncbi.nlm.nih.gov/snp.

116. Neer, E.J.; Schmidt, C.J.; Nambudripad, R.; Smith, T.F. (1994): The ancient regulatory-protein family of WD-repeat proteins. In *Nature* 371 (6495), pp. 297-300.

117. Nelson, E.D.; Bal, M.; Kavalali, E.T.; Monteggia, L.M. (2011): Selective impact of MeCP2 and associated histone deacetylases on the dynamics of evoked excitatory neurotransmission. In *J. Neurophysiol.* 106 (1), pp. 193-201.

118. Osaki, S.; Johnson, D.A.; Frieden, E. (1966): The possible significance of the ferrous oxidase activity of ceruloplasmin in normal human serum. In *J. Biol. Chem.* 241 (12), pp. 2746-2751.

119. Paisán-Ruíz, C.; Bhatia, K.P.; Li, A.; Hernandez, D.; Davis, M.; Wood, N.W.; Hardy, J.; Houlden, H.; Singleton, A.; Schneider, S.A. (2009): Characterization of PLA2G6 as a locus for dystonia-parkinsonism. In *Ann. Neurol.* 65 (1), pp. 19-23.

120. Paisán-Ruíz, C.; Jain, S.; Evans, E.W.; Gilks, W.P.; Simón, J.; van der Brug, M.; López de Munain, A.; Aparicio, S.; Gil, A.M.; Khan, N.; Johnson, J.; Martinez, J.R.; Nicholl, D.; Carrera, I.M.; Pena, A.S.; Silva, R. de; Lees, A.; Martí-Massó, J.F.; Pérez-Tur, J.; Wood, N.W.; Singleton, A.B. (2004): Cloning of the gene containing mutations that cause PARK8-linked Parkinson's disease. In *Neuron* 44 (4), pp. 595-600.

121. Paisán-Ruíz, C.; Li, A.; Schneider, S.A.; Holton, J.L.; Johnson, R.; Kidd, D.; Chataway, J.; Bhatia, K.P.; Lees, A.J.; Hardy, J.; Revesz, T.; Houlden, H. (2012): Widespread Lewy body and tau accumulation in childhood and adult onset dystonia-parkinsonism cases with PLA2G6 mutations. In *Neurobiol. Aging* 33 (4), pp. 814-823.

122. Paisán-Ruíz, C.; Nath, P.; Washecka, N.; Gibbs, J.R.; Singleton, A.B. (2008): Comprehensive analysis of LRRK2 in publicly available Parkinson's disease cases and neurologically normal controls. In *Hum. Mutat.* 29 (4), pp. 485-490.

123. Panteghini, C.; Zorzi, G.; Venco, P.; Dusi, S.; Reale, C.; Brunetti, D.; Chiapparini, L.; Zibordi, F.; Siegel, B.; Garavaglia, B.; Simonati, A.; Bertini, E.; Nardocci, N.; Tiranti, V. (2012): C19orf12 and FA2H mutations are rare in Italian patients with neurodegeneration with brain iron accumulation. In *Semin Pediatr Neurol* 19 (2), pp. 75-81.

124. Pauly, P.C.; Harris, D.A. (1998): Copper stimulates endocytosis of the prion protein. In *J. Biol. Chem.* 273 (50), pp. 33107-33110.

125. Perera, W.S.; Hooper, N.M. (2001): Ablation of the metal ion-induced endocytosis of the prion protein by disease-associated mutation of the octarepeat region. In *Curr. Biol.* 11 (7), pp. 519-523.

126. Pinilla-Tenas, J.J.; Sparkman, B.K.; Shawki, A.; Illing, A.C.; Mitchell, C.J.; Zhao, N.; Liuzzi, J.P.; Cousins, R.J.; Knutson, M.D.; Mackenzie, B. (2011): Zip14 is a complex broad-scope metal-ion transporter whose functional properties support roles in the cellular uptake of zinc and nontransferrin-bound iron. In *Am. J. Physiol., Cell Physiol.* 301 (4), pp. C862-71.

127. Proikas-Cezanne, T.; Waddell, S.; Gaugel, A.; Frickey, T.; Lupas, A.; Nordheim, A. (2004): WIPI-1alpha (WIPI49), a member of the novel 7-bladed WIPI protein family, is aberrantly expressed in human cancer and is linked to starvation-induced autophagy. In *Oncogene* 23 (58), pp. 9314-9325.

128. Prusiner, S.B. (1982): Novel proteinaceous infectious particles cause scrapie. In *Science* 216 (4542), pp. 136-144.

129. Puck, J.M.; Stewart, C.C.; Nussbaum, R.L. (1992): Maximum-likelihood analysis of human T-cell X chromosome inactivation patterns: normal women versus carriers of X-linked severe combined immunodeficiency. In *Am. J. Hum. Genet.* 50 (4), pp. 742-748.

130. Puistola, U.; Turpeenniemi-Hujanen, T.M.; Myllylä, R.; Kivirikko, K.I. (1980): Studies on the lysyl hydroxylase reaction. II. Inhibition kinetics and the reaction mechanism. In *Biochim. Biophys. Acta* 611 (1), pp. 51-60.

131. Quadri, M.; Federico, A.; Zhao, T.; Breedveld, G.J.; Battisti, C.; Delnooz, C.; Severijnen, L.-A.; Di Toro Mammarella, L.; Mignarri, A.; Monti, L.; Sanna, A.; Lu, P.; Punzo, F.; Cossu, G.; Willemsen, R.; Rasi, F.; Oostra, B.A.; van de Warrenburg, B.P.; Bonifati, V. (2012): Mutations in SLC30A10 cause parkinsonism and dystonia with hypermanganesemia, polycythemia, and chronic liver disease. In *Am. J. Hum. Genet.* 90 (3), pp. 467-477.

132. Ramirez, A.; Heimbach, A.; Gründemann, J.; Stiller, B.; Hampshire, D.; Cid, L.P.; Goebel, I.; Mubaidin, A.F.; Wriekat, A.-L.; Roeper, J.; Al-Din, A.; Hillmer, A.M.; Karsak, M.; Liss, B.; Woods, C.G.; Behrens, M.I.; Kubisch, C. (2006): Hereditary parkinsonism with dementia is caused by mutations in ATP13A2, encoding a lysosomal type 5 P-type ATPase. In *Nat. Genet.* 38 (10), pp. 1184-1191.

133. Rett, A. (1966): Über ein eigenartiges hirnatrophisches Syndrom bei Hyperammonämie im Kindersalter. In *Wien Med Wochenschr* 116 (37), pp. 723-726.

134. Rock, C.O.; Calder, R.B.; Karim, M.A.; Jackowski, S. (2000): Pantothenate kinase regulation of the intracellular concentration of coenzyme A. In *J. Biol. Chem.* 275 (2), pp. 1377-1383.

135. Saitsu, H.; Nishimura, T.; Muramatsu, K.; Kodera, H.; Kumada, S.; Sugai, K.; Kasai-Yoshida, E.; Sawaura, N.; Nishida, H.; Hoshino, A.; Ryujin, F.; Yoshioka, S.; Nishiyama, K.; Kondo, Y.; Tsurusaki, Y.; Nakashima, M.; Miyake, N.; Arakawa, H.; Kato, M.; Mizushima, N.; Matsumoto, N. (2013): De novo mutations in the autophagy

gene WDR45 cause static encephalopathy of childhood with neurodegeneration in adulthood. In *Nat. Genet.* 45 (4), pp. 445-449.

136. Sanger, F.; Nicklen, S.; Coulson, A.R. (1977): DNA sequencing with chain-terminating inhibitors. In *Proc. Natl. Acad. Sci. U.S.A.* 74 (12), pp. 5463-5467.

137. Schanen, N.C.; Dahle, E.J.; Capozzoli, F.; Holm, V.A.; Zoghbi, H.Y.; Francke, U. (1997): A new Rett syndrome family consistent with X-linked inheritance expands the X chromosome exclusion map. In *Am. J. Hum. Genet.* 61 (3), pp. 634-641.

138. Schmitt-Ulms, G.; Ehsani, S.; Watts, J.C.; Westaway, D.; Wille, H. (2009): Evolutionary descent of prion genes from the ZIP family of metal ion transporters. In *PLoS ONE* 4 (9), pp. e7208, 1-13.

139. Schneider, S.A.; Paisán-Ruíz, C.; Quinn, N.P.; Lees, A.J.; Houlden, H.; Hardy, J.; Bhatia, K.P. (2010): ATP13A2 mutations (PARK9) cause neurodegeneration with brain iron accumulation. In *Mov. Disord.* 25 (8), pp. 979-984.

140. Schuelke, M.; Schwarz, J.M.; Seelow, D. (2015): mutation t@sting. Department of Neuropaediatrics, Charité Berlin. Berlin, Germany. [17.06.2015 accessed]. Available online at http://www.mutationtaster.org.

141. Schwartzman, J.S.; Zatz, M.; dos Reis Vasquez, L.; Ribeiro Gomes, R.; Koiffmann, C.P.; Fridman, C.; Guimarães Otto, P. (1999): Rett syndrome in a boy with a 47, XXY karyotype. In *Am. J. Hum. Genet.* 64 (6), pp. 1781-1785.

142. Schwarz, J.M.; Cooper, D.N.; Schuelke, M.; Seelow, D. (2014): MutationTaster2: mutation prediction for the deep-sequencing age. In *Nat. Methods* 11 (4), pp. 361-362.

143. Sethi, K.D.; Adams, R.J.; Loring, D.W.; el Gammal, T. (1988): Hallervorden-Spatz syndrome: clinical and magnetic resonance imaging correlations. In *Ann. Neurol.* 24 (5), pp. 692-694.

144. Sharp, A.; Robinson, D.; Jacobs, P. (2000): Age- and tissue-specific variation of X chromosome inactivation ratios in normal women. In *Hum. Genet.* 107 (4), pp. 343-349.

145. Sheng, D.; Qu, D.; Kwok, K.H.H.; Ng, S.S.; Lim, A.Y.M.; Aw, S.S.; Lee, C.W.H.; Sung, W.K.; Tan, E.K.; Lufkin, T.; Jesuthasan, S.; Sinnakaruppan, M.; Liu, J. (2010): Deletion of the WD40 domain of LRRK2 in Zebrafish causes Parkinsonism-like loss of neurons and locomotive defect. In *PLoS Genet.* 6 (4), pp. e1000914, 1-11.

146. Shevell, M. (1992): Racial hygiene, active euthanasia, and Julius Hallervorden. In *Neurology* 42 (11), pp. 2214-2219.

147. Shi, C.-h.; Tang, B.-s.; Wang, L.; Lv, Z.-y.; Wang, J.; Luo, L.-z.; Shen, L.; Jiang, H.; Yan, X.-x.; Pan, Q.; Xia, K.; Guo, J.-f. (2011): PLA2G6 gene mutation in autosomal recessive early-onset parkinsonism in a Chinese cohort. In *Neurology* 77 (1), pp. 75-81.

148. Sina, F.; Shojaee, S.; Elahi, E.; Paisán-Ruíz, C. (2009): R632W mutation in PLA2G6 segregates with dystonia-parkinsonism in a consanguineous Iranian family. In *Eur. J. Neurol.* 16 (1), pp. 101-104.

149. Singh, A.; Haldar, S.; Horback, K.; Tom, C.; Zhou, L.; Meyerson, H.; Singh, N. (2013): Prion protein regulates iron transport by functioning as a ferrireductase. In *J. Alzheimers Dis.* 35 (3), pp. 541-552.

150. Singh, A.; Mohan, M.L.; Isaac, A.O.; Luo, X.; Petrak, J.; Vyoral, D.; Singh, N. (2009): Prion protein modulates cellular iron uptake: a novel function with implications for prion disease pathogenesis. In *PLoS ONE* 4 (2), pp. e4468, 1-16.

151. Skidmore, F.M.; Drago, V.; Foster, P.; Schmalfuss, I.M.; Heilman, K.M.; Streiff, R.R. (2008): Aceruloplasminaemia with progressive atrophy without brain iron overload: treatment with oral chelation. In *J. Neurol. Neurosurg. Psychiatr.* 79 (4), pp. 467-470.

152. Stamelou, M.; Tuschl, K.; Chong, W.K.; Burroughs, A.K.; Mills, P.B.; Bhatia, K.P.; Clayton, P.T. (2012): Dystonia with brain manganese accumulation resulting from SLC30A10 mutations: a new treatable disorder. In *Mov. Disord.* 27 (10), pp. 1317-1322.

153. Tanida, I. (2011): Autophagosome formation and molecular mechanism of autophagy. In *Antioxid. Redox Signal.* 14 (11), pp. 2201-2214.

154. Tao, J.; van Esch, H.; Hagedorn-Greiwe, M.; Hoffmann, K.; Moser, B.; Raynaud, M.; Sperner, J.; Fryns, J.-P.; Schwinger, E.; Gécz, J.; Ropers, H.-H.; Kalscheuer, V.M. (2004): Mutations in the X-linked cyclin-dependent kinase-like 5 (CDKL5/STK9) gene are associated with severe neurodevelopmental retardation. In *Am. J. Hum. Genet.* 75 (6), pp. 1149-1154.

155. Taylor, K.M. (2000): LIV-1 breast cancer protein belongs to new family of histidine-rich membrane proteins with potential to control intracellular Zn2+ homeostasis. In *IUBMB Life* 49 (4), pp. 249-253.

156. Taylor, K.M.; Morgan, H.E.; Johnson, A.; Nicholson, R.I. (2005): Structure-function analysis of a novel member of the LIV-1 subfamily of zinc transporters, ZIP14. In *FEBS Lett.* 579 (2), pp. 427-432.

157. Tuderman, L.; Myllylä, R.; Kivirikko, K.I. (1977): Mechanism of the prolyl hydroxylase reaction. 1. Role of co-substrates. In *Eur. J. Biochem.* 80 (2), pp. 341-348.

158. Turpeenniemi-Hujanen, T.; Myllylä, R. (1984): Concomitant hydroxylation of proline and lysine residues in collagen using purified enzymes in vitro. In *Biochim. Biophys. Acta* 800 (1), pp. 59-65.

159. Tuschl, K.; Clayton, P.T.; Gospe, S.M.; Gulab, S.; Ibrahim, S.; Singhi, P.; Aulakh, R.; Ribeiro, R.T.; Barsottini, O.G.; Zaki, M.S.; Del Rosario, M.L.; Dyack, S.; Price, V.; Rideout, A.; Gordon, K.; Wevers, R.A.; Chong, W.K.K.; Mills, P.B. (2012): Syndrome of hepatic cirrhosis, dystonia, polycythemia, and hypermanganesemia caused by mutations in SLC30A10, a manganese transporter in man. In *Am. J. Hum. Genet.* 90 (3), pp. 457-466.

160. University of California Santa Cruz (2012): UCSC Genome Bioinformatics. Santa Cruz, California, USA. [25.05.2012 accessed for SLC39A14, 30.07.2012 accessed for WDR45]. Available online at https://www.genome.ucsc.edu.

161. Usenovic, M.; Tresse, E.; Mazzulli, J.R.; Taylor, J.P.; Krainc, D. (2012): Deficiency of ATP13A2 leads to lysosomal dysfunction, α-synuclein accumulation, and neurotoxicity. In *J. Neurosci.* 32 (12), pp. 4240-4246.

162. van den Veyver, I.B. (2001): Skewed X inactivation in X-linked disorders. In *Semin. Reprod. Med.* 19 (2), pp. 183-191.

163. Vidal, R.; Ghetti, B.; Takao, M.; Brefel-Courbon, C.; Uro-Coste, E.; Glazier, B.S.; Siani, V.; Benson, M.D.; Calvas, P.; Miravalle, L.; Rascol, O.; Delisle, M.B. (2004): Intracellular ferritin accumulation in neural and extraneural tissue characterizes a neurodegenerative disease associated with a mutation in the ferritin light polypeptide gene. In *J. Neuropathol. Exp. Neurol.* 63 (4), pp. 363-380.

164. Wall, M.A.; Coleman, D.E.; Lee, E.; Iñiguez-Lluhi, J.A.; Posner, B.A.; Gilman, A.G.; Sprang, S.R. (1995): The structure of the G protein heterotrimer Gi alpha 1 beta 1 gamma 2. In *Cell* 83 (6), pp. 1047-1058.

165. Wang, C.-Y.; Jenkitkasemwong, S.; Duarte, S.; Sparkman, B.K.; Shawki, A.; Mackenzie, B.; Knutson, M.D. (2012): ZIP8 Is an Iron and Zinc Transporter Whose Cell-surface Expression Is Up-regulated by Cellular Iron Loading. In *Journal of Biological Chemistry* 287 (41), pp. 34032-34043.

166. Wang, K.; Zhou, B.; Kuo, Y.-M.; Zemansky, J.; Gitschier, J. (2002): A novel member of a zinc transporter family is defective in acrodermatitis enteropathica. In *Am. J. Hum. Genet.* 71 (1), pp. 66-73.

167. Watt, N.T.; Griffiths, H.H.; Hooper, N.M. (2013): Neuronal zinc regulation and the prion protein. In *Prion* 7 (3), pp. 203-208.

168. Will, R.G.; Ironside, J.W.; Zeidler, M.; Cousens, S.N.; Estibeiro, K.; Alperovitch, A.; Poser, S.; Pocchiari, M.; Hofman, A.; Smith, P.G. (1996): A new variant of Creutzfeldt-Jakob disease in the UK. In *Lancet* 347 (9006), pp. 921-925.

169. Woodhouse, N.J.; Sakati, N.A. (1983): A syndrome of hypogonadism, alopecia, diabetes mellitus, mental retardation, deafness, and ECG abnormalities. In *J. Med. Genet.* 20 (3), pp. 216-219.

170. Yang, F.; Naylor, S.L.; Lum, J.B.; Cutshaw, S.; McCombs, J.L.; Naberhaus, K.H.; McGill, J.R.; Adrian, G.S.; Moore, C.M.; Barnett, D.R. (1986): Characterization, mapping, and expression of the human ceruloplasmin gene. In *Proc. Natl. Acad. Sci. U.S.A.* 83 (10), pp. 3257-3261.

171. Yoshida, K.; Furihata, K.; Takeda, S.; Nakamura, A.; Yamamoto, K.; Morita, H.; Hiyamuta, S.; Ikeda, S.; Shimizu, N.; Yanagisawa, N. (1995): A mutation in the ceruloplasmin gene is associated with systemic hemosiderosis in humans. In *Nat. Genet.* 9 (3), pp. 267-272.

172. Yoshino, H.; Tomiyama, H.; Tachibana, N.; Ogaki, K.; Li, Y.; Funayama, M.; Hashimoto, T.; Takashima, S.; Hattori, N. (2010): Phenotypic spectrum of patients with PLA2G6 mutation and PARK14-linked parkinsonism. In *Neurology* 75 (15), pp. 1356-1361.

173. Zhao, H.; Eide, D. (1996): The yeast ZRT1 gene encodes the zinc transporter protein of a high-affinity uptake system induced by zinc limitation. In *Proc. Natl. Acad. Sci. U.S.A.* 93 (6), pp. 2454-2458.

174. Zhou, B.; Westaway, S.K.; Levinson, B.; Johnson, M.A.; Gitschier, J.; Hayflick, S.J. (2001): A novel pantothenate kinase gene (PANK2) is defective in Hallervorden-Spatz syndrome. In *Nat. Genet.* 28 (4), pp. 345-349.

175. Zimprich, A.; Biskup, S.; Leitner, P.; Lichtner, P.; Farrer, M.; Lincoln, S.; Kachergus, J.; Hulihan, M.; Uitti, R.J.; Calne, D.B.; Stoessl, A.J.; Pfeiffer, R.F.; Patenge, N.; Carbajal, I.C.; Vieregge, P.; Asmus, F.; Müller-Myhsok, B.; Dickson, D.W.; Meitinger, T.; Strom, T.M.; Wszolek, Z.K.; Gasser, T. (2004): Mutations in LRRK2 cause autosomal-dominant parkinsonism with pleomorphic pathology. In *Neuron* 44 (4), pp. 601-607.

176. Zöller, I.; Meixner, M.; Hartmann, D.; Büssow, H.; Meyer, R.; Gieselmann, V.; Eckhardt, M. (2008): Absence of 2-hydroxylated sphingolipids is compatible with normal neural development but causes late-onset axon and myelin sheath degeneration. In *J. Neurosci.* 28 (39), pp. 9741-9754.

11 Supplementary Materials

Table 15 – List of primers that were used

Gene	Exon and direction	Primer sequence	Primer size (bp)	Product size (bp)
SLC39A14	2_Forward	5'-TCAAGAAGGAGCAGAGAAGCA-3'	21	480
	2_Reverse	5’-AGACAGGGAACCCTGAGAGG-3'	20	
SLC39A14	3_Forward	5’-TCCTCTGGGAAGGCTGAGTA-3'	20	371
	3_Reverse	5’-CATTCAGTGAGGAGCAGCAG-3'	20	
SLC39A14	4_Forward	5’-GGCATGTGCCTTCTCTCC-3'	18	300
	4_Reverse	5’-CCTTCTATCCAAACGGAGGTC-3'	21	
SLC39A14	4b_Forward	5’-GAGTGTCCCCACCCTCAGT-3'	19	298
	4b_Reverse	5’-GTAGGGGAGGAGGGGATTG-3'	19	
SLC39A14	5_Forward	5’-AGGGGGATCAGTAAAGATGCT-3'	21	242
	5_Reverse	5’-TGTTTGAGATGGGTGTTTTCC-3'	21	
SLC39A14	6_Forward	5’-AGCAGGTGCTCAATCAGGTT-3'	20	328
	6_Reverse	5’-ACCATGTGCCCTCAAGGTAA-3'	20	
SLC39A14	7_Forward	5’-GGCTTACCTTGAGGGCACAT-3'	20	377
	7_Reverse	5’-GCACTGTGAAGACAGGGAGA-3'	20	
SLC39A14	8_Forward	5’-CCATGCCCATCTTACTCTTCC-3'	21	299
	8_Reverse	5’-ACCTAACATCCATCCCCTTAG-3'	21	
SLC39A14	9_Forward	5’-TTGCCCTGGACTTACAAGATG-3'	21	297
	9_Reverse	5’-GTGGTGCATTGTGGATGGT-3'	19	
SLC39A14	9b_Forward	5’-CGGCCATGTTTATGTTTTTG-3'	20	299
	9b_Reverse	5’-CATCATGCAGTTAGGAAATACCA-3'	23	
WDR45	3+4_Forward	5'-CGACGTTGTAAAACGACGGCCAGT GAGGAAATCAGGTGAGGCAG-3'	44	427
	3+4_Reverse	5'-CAGGAAACAGCTATGACC CAGGGTGTCAGTGGAGGTG-3'	37	
WDR45	5_Forward	5’-CGACGTTGTAAAACGACGGCCAGT CAATGGGCAGAAGAGCTGG -3’	43	220
	5_Reverse	5’-CAGGAAACAGCTATGACC GCCAGGAATCCGAGAAATC-3’	37	

WDR45	6+7_Forward	5’-CGACGTTGTAAAACGACGGCCAGT GCTGCCCCTTACCCTAAACC-3’	44	449
	6+7_Reverse	5’-CAGGAAACAGCTATGACC TTCTTTCCTCATCTCTGCCC-3’	38	
WDR45	8_Forward	5’-CGACGTTGTAAAACGACGGCCAGT GCTCTGTCCATTCTGAGATGC-3’	45	205
	8_Reverse	5’-CAGGAAACAGCTATGACC AGTCCACAAGGAAGCCAGTC-3’	38	
WDR45	9+10_Forward	5’-CGACGTTGTAAAACGACGGCCAGT CCCTTCCCTCCATACCACC-3’	43	503
	9+10_Reverse	5’-CAGGAAACAGCTATGACC AAGCCCAGGTATGGTAAATGG-3’	39	
WDR45	11_Forward	5’-CGACGTTGTAAAACGACGGCCAGT ACCCTACCGTGTCCCTGTC-3’	43	268
	11_Reverse	5’-CAGGAAACAGCTATGACC AACCTGCAGGCCTTTGC-3’	35	
WDR45	12_Forward	5’-CGACGTTGTAAAACGACGGCCAGT GATGCCTGAGAGGACTGGAG-3’	44	561
	12_Reverse	5’-CAGGAAACAGCTATGACC GCCCCTGAGGTCAAGCC-3’	35	
androgen receptor	1_Forward	5‘-CCGAGGAGCTTTCCAGAATC-3‘	20	248
	1_Reverse	5’-TACGATGGGCTTGGGGAGAA-3’	20	

12 Acknowledgements

First of all, I would like to sincerely thank my dissertation advisor Prof. Dr. Thomas Meitinger for the opportunity to perform this work at his institute. I am very grateful for all his help and support in the past years.

My very special thanks also go to Dr. Holger Prokisch for intensely supervising, supporting and helping me throughout this whole research work. I am thankful for every advice and suggestion.

For introducing me into the genetic methods and all technical support, I am very grateful to Eveline Botz and Rosi Hellinger.

I also want to thank Dr. Tobias Haack and the whole research group at the Institute of Human Genetics for all fruitful discussions.

Most of all, I am very thankful to my parents and family for all their support and encouragement.